PREFACE

The mechanism of the thermal decomposition of hydrocarbons has been a subject of controversy for almost forty years. The earliest workers considered that the decomposition was a simple molecular split into an olefin and a smaller saturated hydrocarbon. Then, almost thirty years ago, F.O. Rice and his co-workers detected free radicals in systems of decomposing hydrocarbons and proposed that the reaction proceeded entirely by a free-radical chain mechanism.

The early work of C.N. Hinshelwood indicated that the uninhibited reaction was a mixture of both free-radical and molecular reactions, but that, when enough nitric oxide was added, the chains were suppressed leaving the molecular reaction. It soon became apparent that, if the maximally inhibited reaction were molecular, it would have become necessary to abandon the conventional theories of unimolecular reactions. However, over the past twenty years evidence has accumulated to indicate that the maximally inhibited reaction is, in fact, non-molecular.

Although it was generally realized that at least part of the maximally inhibited reaction was non-molecular, early attempts to explain the experimental facts by a free-radical mechanism were unsuccessful. Then, in 1960, a new type of mechanism was proposed by workers in this laboratory

and was successfully applied to the pyrolysis of ethane. It then became apparent that, in order to establish the generality of this mechanism, further work would have to be done on more complicated compounds, and this thesis presents results obtained with propane and n-butane. Mechanisms for the inhibited and uninhibited decompositions of both propane and n-butane are proposed, and experimental facts and theoretical arguments are adduced in support of them.

The author is indebted to Professor K.J. Laidler under whose expert guidance this work was carried out, and wishes to express his gratitude for Professor Laidler's expert direction and infinite patience. He also wishes to thank Drs. B.W. Wojciechowski and Margaret H. Back for their many profitable suggestions and Messrs. Othman bin M. Nor, Paul Northover and Erazio Berolo for performing many of the calculations. Finally he wishes to thank his wife for her support during the period of this investigation.

The assistance of the National Research Council of Canada in the form of three studentships is hereby gratefully acknowledged.

TABLE OF CONTENTS

LIST OF TABLES

LIST OF FIGURES

Page No.

Page No.

LIST OF PLATES

ABSTRACTS

Uninhibited Decomposition of Propane

The pyrolysis of propane was investigated from 530 to 670°C and at pressures up to 600 mm. In an unpacked vessel, the reaction was first-order at lower temperatures and higher pressures and became 3/2-order at higher temperatures and lower pressures. The rates were somewhat reduced in a packed vessel and an apparent order of 1.2 was obtained. The activation energy of the reaction in its first-order region was 67.1 kcal. per mole, and in its 3/2-order region was 54.5 kcal. per mole. Added carbon dioxide had no effect on the rates, either in the first-order or 3/2-order regions.

It is concluded that the reaction is largely homogeneous and occurs by a free-radical mechanism. The initiation reaction is considered to be the dissociation of propane into a methyl and an ethyl radical, this reaction being in its second-order low-pressure region under the conditions of the experiments. The termination reaction when the over-all order is unity is concluded to be the recombination of a methyl and a propyl radical in the presence of a third body. In the 3/2-order region the termination reaction is believed to be the recombination of two methyl radicals, also in the third-order region. These mechanisms are shown to give a satisfactory interpretation of the over-

all behavior.

Nitric Oxide Inhibited Decomposition of Propane

The kinetics of the pyrolysis of propane inhibited by nitric oxide were studied from 640 to 560°C and at partial pressures of propane from 25 to 550 mm. The pressure-time curves were found to be S-shaped and the induction periods were lengthened considerably as the propane pressure was lowered. Complete inhibition was obtained with about 12% nitric oxide. The initial rates were proportional to the 3/2-power of the pressure at most temperatures and to a slightly lower power at the highest temperatures. The orders of the inflexion-point rates were close to unity at the highest temperatures, and increased steadily as the temperature was lowered. The activation energy calculated from the inflexion point rates was 69.4 kcal. per mole. The rates decreased with an increase in the surface to volume ratio, but the addition of a large excess of carbon dioxide had no effect on the fully inhibited rates. The results are shown to be consistent with a mechanism involving initiation by the abstraction of a hydrogen atom from propane by nitric oxide and termination by the reaction of HNO and a propyl radical.

Uninhibited Decomposition of n-Butane

The kinetics of the thermal decomposition of n-

butane have been studied at temperatures from 520 to 590°C and at pressures from 30 to 600 mm.; the rate was followed from pressure changes and by gas chromatography. The reaction was 3/2-order at all temperatures, with an activation energy of 59.9 kcal. per mole. The reaction was very sensitive to surface; packing the vessel and 'conditioning' it usually led to a decrease in rate and increase in activation energy. The reaction is concluded to be largely homogeneous and to occur almost entirely by a free-radical mechanism. The initiation is believed to be the dissociation of a butane molecule into two ethyl radicals, in the first-order region, and termination is believed to be the second-order combination of ethyl radicals. The surface effect is attributed to a certain amount of initiation by abstraction of a hydrogen atom from a butane molecule by the surface, and to surface catalysis of the recombination of ethyl radicals.

Nitric Oxide Inhibited Decomposition of n-Butane

The kinetics of the pyrolysis of n-butane, when maximally inhibited by nitric oxide, were studied from 540 to 610°C and from 30 to 500 mm. partial pressure of butane. The reaction had a short induction period and was accurately of the three-halves order with an activation energy of 65.9 kcal. per mole. The reaction was somewhat less inhibited by surface than was the uninhibited reaction. An excess

of carbon dioxide had no effect on the rate. These results are explained in terms of a free-radical mechanism for the maximally inhibited decomposition. It is proposed that the initiating step in the inhibited decomposition is mainly $C_4H_{10} + NO \longrightarrow C_4H_9 + HNO$. This is followed by the ordinary chain propagating reactions, and equilibria such as $C_2H_5 + NO \rightleftharpoons C_2H_5NO$ are established. The main chain terminating step, of the type $\beta + \beta NO$, is concluded to be $C_2H_5 + C_2H_5NO \longrightarrow C_4H_{10} + NO$ or $C_2H_6 + C_2H_4 + NO$. This scheme leads to 3/2-order kinetics, and provides a satisfactory quantitative interpretation of the experimental behavior.

Part I

THE UNINHIBITED PYROLYSIS OF PROPANE

INTRODUCTION

Although the thermal decomposition of hydrocarbons has been a subject of investigation for almost forty years, not too much can be said with certainty about the mechanisms of such decompositions. Interest in this subject has revived in recent years, and a very thorough investigation of the thermal decomposition of ethane has been carried out in this laboratory. It therefore seemed appropriate to make a thorough re-investigation of the pyrolysis of the next higher homologue, propane. In addition, propane is an industrially important fuel gas, and is an important constituent of refinery 'light ends'. Therefore, a knowledge of its behavior on pyrolysis may have practical uses as well as being of academic interest.

Review of Earlier Work

Early work by Pease (1), Frey and Smith (2) and others (3), (4), (5) established that the reaction was mainly homogeneous, close to first-order, and could be represented by:

$$C_3H_8 \longrightarrow C_3H_6 + H_2$$

$$C_3H_8 \longrightarrow C_2H_4 + CH_4$$

Small amounts of ethane and butane were also detected.

Marek and McCluer (6) were among the first workers to obtain accurate kinetic data. Correcting for back reaction, they obtained a first-order rate constant

$$k = 2.76 \times 10^{13} e^{-62,100/RT} \text{ sec}^{-1}$$

A little later, Paul and Marek (7) obtained

$$k = 4.0 \times 10^{16} e^{-74,850/RT} \text{ sec}^{-1}$$

Although the discrepancy between the two activation energies is quite large, it should be pointed out that the absolute rates are in much better agreement. Pray and Kepp (8), working at 575°C, obtained a rate in agreement with the above workers, and made very thorough analyses of the reaction products. They found about equal amounts of all four main products listed above. All this early work was done in flow systems, and therefore any individual rate constants are subject to considerable error.

Dintses and Frost (9) (10) (11) investigated the thermal decomposition of propane in a static system. They found that, between 1 and 78 mm. and at temperatures from 619 to 666°C, the first-order rate constants dropped off sharply with time, and that the rate constant for any given run was

$$k = \frac{1}{t} \left(\ln \frac{1}{1-X} - 0.921 X \right) \text{ sec}^{-1}$$

where X is the fraction of propane reacted after t seconds. They concluded that, because of the complexity of the reaction, free radicals were probably involved.

A detailed investigation of the thermal decomposition of propane was made by Steacie and Puddington (12). They investigated the reaction in a static system from 551 to 602°C, and at pressures of 50 to 600 mm. It was found that the first-order rate constants at infinite pressure could be given by:

$$k = 2.9 \times 10^{13} e^{-63,300/RT} \text{ sec}^{-1}$$

However, it has since been shown that free radicals are involved in the pyrolysis of propane, and the validity of this extrapolation to high pressures is questionable. Analyses showed that the reaction products were H_2, CH_4, C_2H_4 and C_3H_6, all in equal quantities and with little or no dependence on initial pressure or temperature.

While the above work was proceeding on the over-all reaction, other workers were showing that free radicals are important in the pyrolysis of propane. Using the Paneth technique, Rice, Johnston and Evering (13) detected free radicals and Rice and Johnston (14) found the activation energy for the split into free radicals to be 71.5 kcal. per mole. Until very recently this was considered impossibly low for the breaking of a C-C bond, but if the initial split

is in its second-order region, this value is quite reasonable. Rice (15) (16) suggested an over-all mechanism for the pyrolysis similar to the Rice-Herzfeld (17) mechanism for the thermal decomposition of ethane:

$$C_3H_8 \longrightarrow CH_3 + C_2H_5$$

$$R + C_3H_8 \longrightarrow RH + CH_3CH_2CH_2$$

$$CH_3CH_2CH_2 \longrightarrow CH_3 + C_2H_4$$

$$R + C_3H_6 \longrightarrow RH + CH_3CHCH_3$$

$$CH_3CHCH_3 \longrightarrow C_3H_6 + H$$

$$R + C_3H_7 \longrightarrow \text{Products}$$

where R represents either H or CH_3.
From this, making the assumption that secondary hydrogen atoms are twice as reactive as primary ones, they predicted that the products should be 60% ($C_2H_4 + CH_4$) and 40% ($C_3H_6 + H_2$). This mechanism also yields the result that the reaction should be first-order over all, with an activation energy of 60 to 65 kcal. per mole. However the values chosen by Rice for the activation energies of the individual reactions have since been shown to be considerably in error.

Belchetz and Rideal (18) investigated the decomposition of propane on a carbon filament at low pressures and proposed a reaction mechanism involving methylene radicals. They found the activation energy of the primary split to be

94.2 kcal. per mole, vastly different from the value obtained by other workers. However, as the authors point out themselves, the presence of the carbon filament may make their results incompatible with those of other workers.

Lossing, Ingold and Henderson (19) have detected methyl radicals in the pyrolysis of propane, using a mass spectrometric technique. Patat (20) found H atoms in the system, using the ortho-para hydrogen conversion as a test for them. However, he found that they were present in too small a quantity to explain a Rice-Herzfeld type mechanism.

There is a great deal of evidence to show that certain substances can sensitize the decomposition of propane at a temperature where ordinary thermal decomposition is negligible. Echols and Pease (21) showed that ethylene oxide could start chain reactions in propane at 425°C, although the average chain length was very short. This is to be expected if one of the chain propagating steps has a fairly high activation energy. Sickman and Rice (22) found that methyl radicals from the decomposition of azomethane could also sensitize the decomposition of propane. This particular sensitising reaction has been re-investigated recently by Stepukhovich and Tatarintsev (23).

Since 1955, a great deal of work on the thermal decomposition of propane has been done by Russian workers. Stepukhovich and his co-workers (24) (25) (26) have inves-

tigated the effects of added acetylene, allene and bivinyl on the rate of reaction. The rate was unaffected by acetylene and bivinyl, and was reduced by allene. He considered this to be evidence that hydrogen atoms are involved in the decomposition of propane. Voevodsky (27) made a fairly thorough study of the effect of surface on the rate of reaction. At pressures below 20 mm. he found that changing the surface to volume ratio had a considerable effect on the rate of reaction, but admitted that, at pressures of 100 mm. or more, the surface may play a smaller part. He postulated that chain initiation and termination are fundamentally surface reactions, with the chain propagating steps taking place in the gas phase. However recent work by Martin, Niclause and Dzierzynski (28) has shown that oxygen may have been present in Voevodsky's system. Voevodsky's work will be discussed in somewhat more detail in Part II of this thesis.

A study of the relation between the yield of products and the extent of decomposition, temperature and pressure has been made recently by Stepukhovich, Kosyreva and Petrosyan (29). They used gas chromatography as their analytical tool and thus obtained much better results than had been previously possible. They found, as earlier workers had, that the initial products were H_2, CH_4, C_3H_6 and C_2H_4 in almost equal quantities. They explained the increasing proportion of CH_4 and C_2H_4 as the reaction proceeds in terms of the isomerization

of isopropyl radicals to n-propyl radicals. However they did not attempt to write any mechanism for the reaction or to deal with the over-all kinetics.

Also, quite recently, Neiman and co-workers (30) (31) (32) studied the thermal decomposition of propane using ^{14}C as a tracer. They concluded that almost all the ethane formed in the reaction resulted from the hydrogenation of ethylene; not from the recombination of methyl radicals and that the reaction proceeded by a free-radical mechanism. The thermal decomposition of 1-^{14}C propane has also been studied by Frey, Danby and Hinshelwood (33). To explain their results, they had to assume that the C_3H_7 radical involved one delocalised H atom and thus that n-propyl and iso-propyl radicals were not separate entities at these temperatures.

Thus it would appear from the above discussion that no attempt has been made in recent years to determine the over-all mechanism of the thermal decomposition of propane. Since, in addition to the work described above, which relates directly to the pyrolysis of propane, a considerable amount of knowledge about the individual reactions of any proposed mechanism has accumulated in recent years, it seemed appropriate to re-investigate the over-all kinetics of the decomposition and to try to fit a mechanism to the data. The experiments described in the following sections are designed to obtain such data, and the attempts to fit an over-all mechanism are

described.

EXPERIMENTAL

Apparatus

A schematic diagram of the all glass apparatus is shown in figure 1, and a photograph of the actual arrangement is shown as plate 1. Three storage bulbs, two of two-litres capacity (V_1 and V_2) and one of five-litres capacity (V_3), were provided. These served to store the hydrocarbon, inhibitor, and inert gas respectively. Each bulb was connected to the vacuum manifold and to a mercury manometer (M_1, M_2 and M_3). The inlet to each bulb was from a tank of pure gas and each bulb had an outlet to a fourth bulb (V_4). This bulb also had a connection to the vacuum manifold and to a mercury manometer (M_4), but in addition was fitted with a Pirani gauge head (G_2). The outlet from this bulb was to the reaction vessel (R) which is described below. The reaction vessel could be evacuated by opening it to the vacuum manifold, or the reaction mixture could be collected for analysis using the Toeppler pump (P_3) to push it into the removable sampling bulb (V_5). Provision was, of course, made for evacuating the sampling system.

The main vacuum pumping system consisted of an Edwards type 203 oil diffusion pump (P_2) backed by a Welsh rotary pump (P_1) which provided a backing pressure of

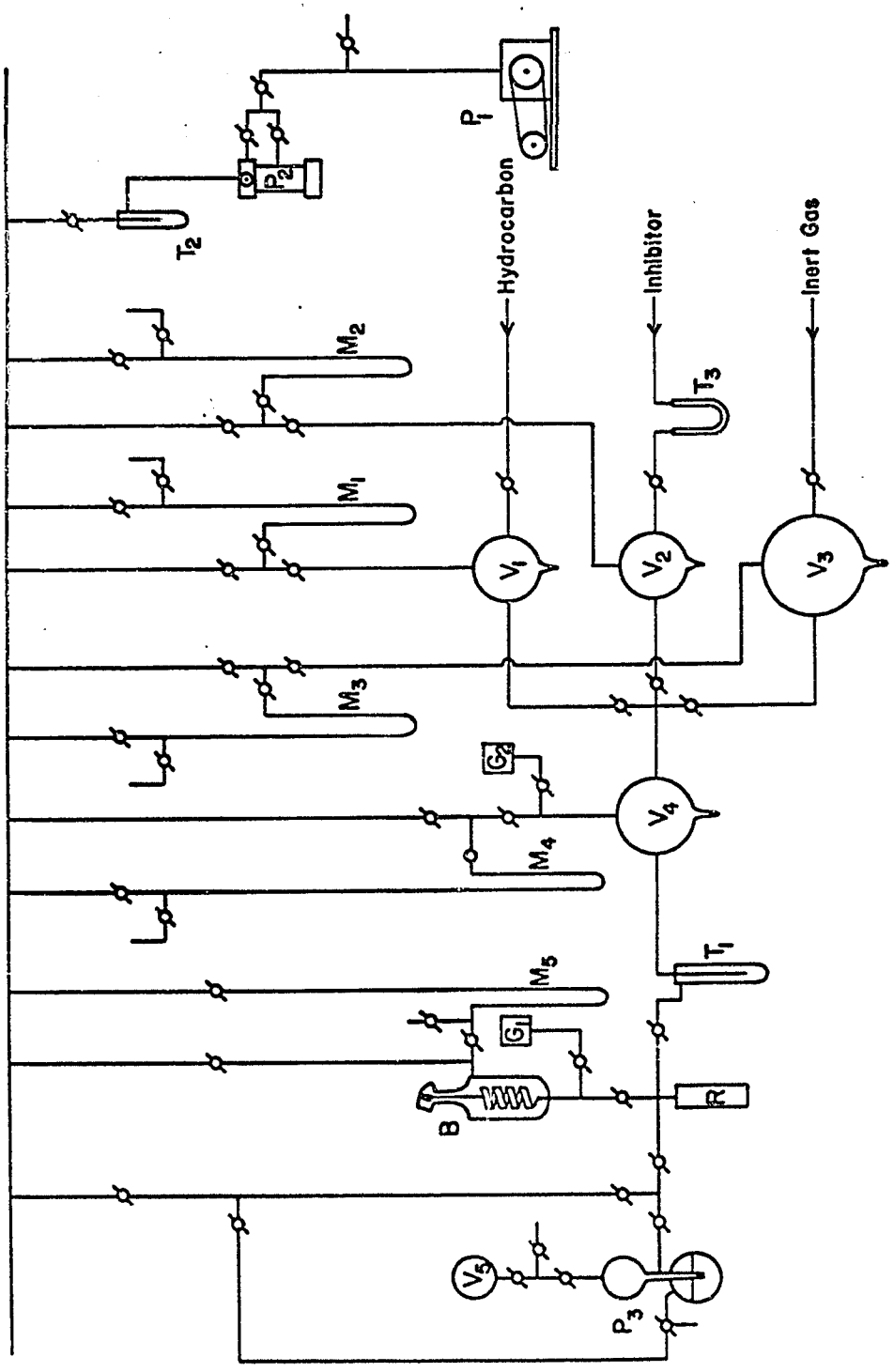

Figure 1 Schematic diagram of the apparatus.

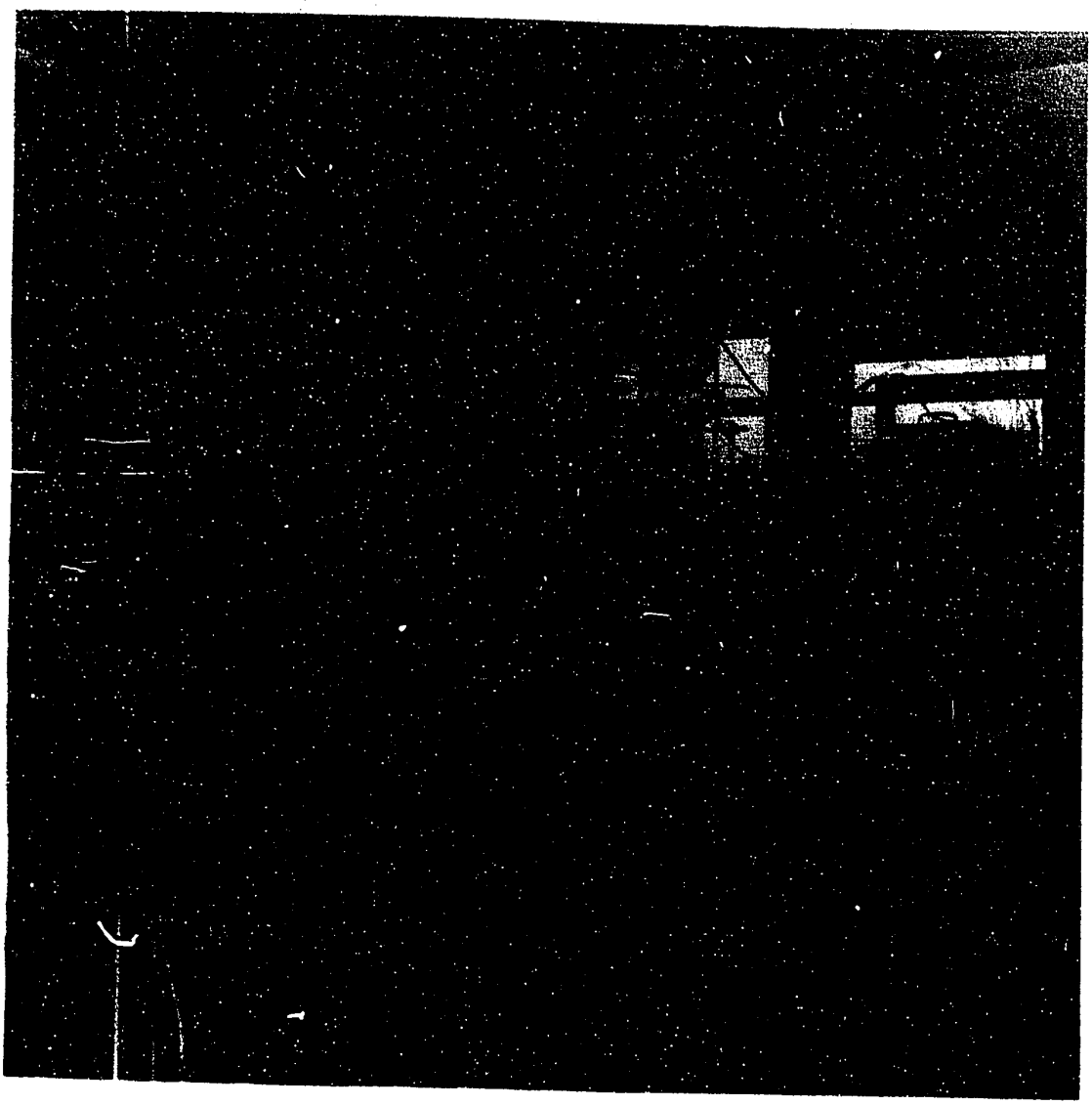

Plate 1 View of the Apparatus.

2×10^{-2} mm. The system was capable of evacuating the apparatus to less than 10^{-5} mm.

As explained below, rates of reaction were followed by measuring rates of pressure increase in the reaction vessel and then correlating the pressure increase with the decrease in propane concentration. The increase in pressure was followed using a quartz spiral Bourdon gauge (B). Details of this gauge and its accessories are shown in figure 2. A small mirror (O) was mounted on the rotating vertical, axial arm of the spiral gauge, and light from a 500 watt bulb (L) fell on this mirror and then passed through a light shield to a Beckman photo-pen recorder (C) some six feet away. This recorder featured two photo-electric cells mounted on its pen carriage. The circuits of the recorder were so arranged that the pen carriage would seek and lock on to the position where a high but equal output was obtained from each photo-tube. Thus the carriage would lock on to the mid-point of the light beam and remain centered on this point while the light beam moved in the horizontal plane. The sensitivity of the arrangement was such that a change of pressure of about 1/4 mm. could easily be detected, and the width of the chart paper (10 in.) spanned a pressure increase of 200 mm. To damp out small oscillations, the coils of the quartz spiral gauge were immersed in silicone oil. To change the range of the pressure recording system, an arrangement was provided

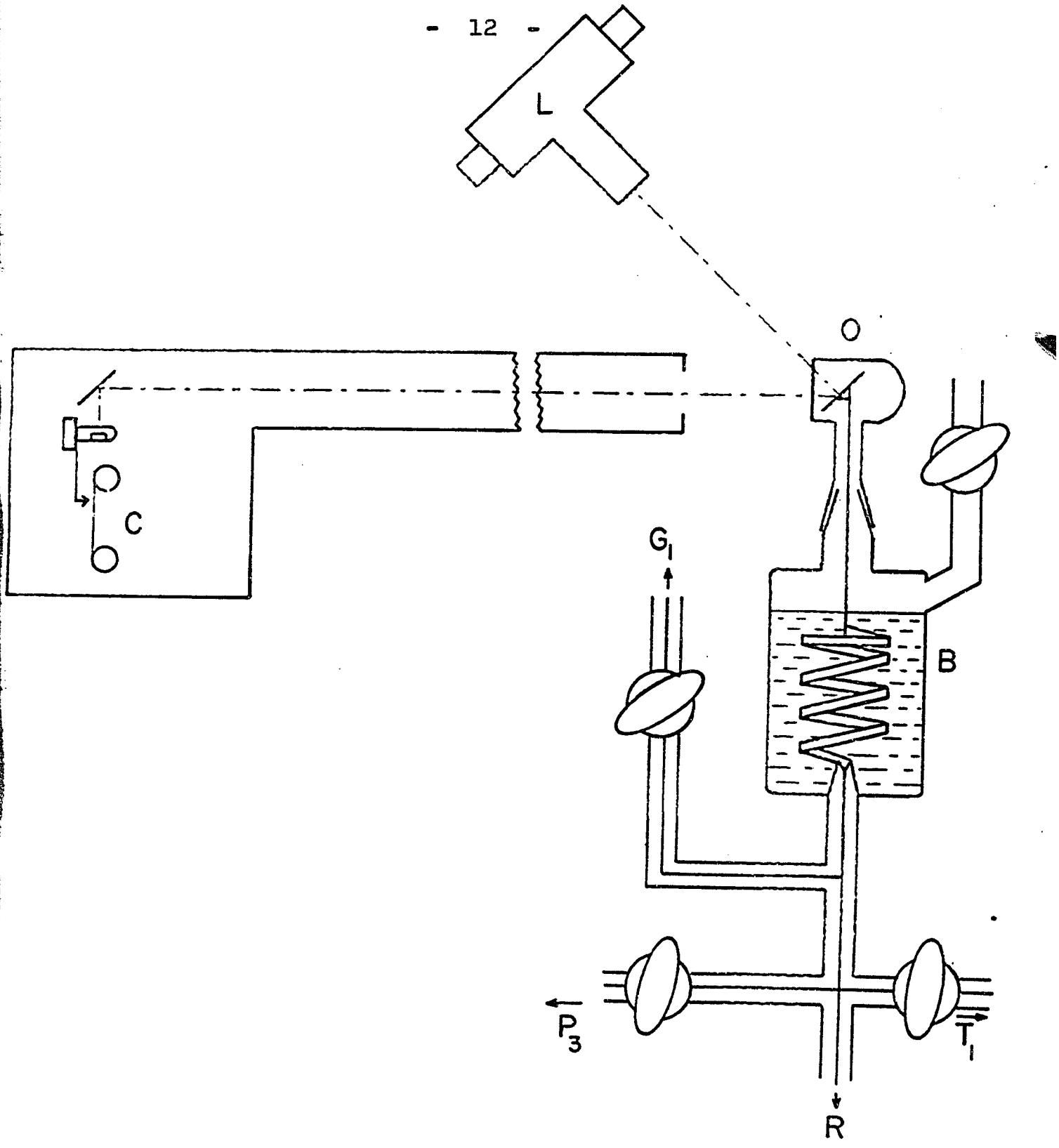

Figure 2 Details of quartz spiral gauge and its accessories.

whereby dry air could be admitted above the silicone oil and its pressure measured on a mercury manometer (M_5). It was also possible to change the speed of the chart and thus to measure a large range of rates. The use of a Beckman photo-pen recorder to measure the rates of gas phase reactions was first described by Laidler and Wojciechowski (34).

Two cylindrical reaction vessels were used. Both were of quartz tubing, 4.4 cm. in diameter and about 20 cm. long. A thermocouple well was fitted to each one, and each was provided with a capillary inlet-outlet tube attached to the quartz through a graded seal, and ending in a ground-glass joint. One of the vessels was packed with quartz tubing to give 11.6 times the surface to volume ratio of the other. The reaction vessel was connected to the quartz spiral gauge with capillary tubing of 1 mm. bore, and all other tubing was capillary from the reaction vessel out to the first stopcock encountered. An Edwards Pirani gauge head (G_1) was mounted between the reaction vessel and spiral gauge to measure the pressure in the vessel while it was being evacuated. Since the gauge had a large dead volume, a stopcock was provided to isolate it from the system while a run was in progress. With these precautions, the 'dead volume' above the reaction vessel was estimated to be about 3 ml.

The reaction vessel was fitted into a hole drilled axially in a stainless steel cylinder 4" in diameter by 10"

long which formed the core of a furnace. Unto this core two insulated concentric coils of Kanthal 1-A resistance wire were wound, and the whole core was surrounded with asbestos insulation. The inner coil, with a resistance of twenty ohms, was regulated with a Variac. The outer coil was regulated with a Variac and controlled with a Thermo-Electric on-off signalling controller. The sensing thermocouple of this controller was placed in a hole drilled in the stainless steel block close to the coils. This position assured the fastest response of the controller to small changes in the temperature of the block. In practice, the temperature of the furnace was adjusted with the inner coil to slightly below that desired. Then the outer coil was turned on and the voltage across it adjusted to give equal times on both halves of the on-off cycle of the controller. This arrangement controlled the temperature of the block to within $\pm$ 0.3°C.

Temperatures were measured with a chromel-alumel thermocouple calibrated at the melting points of zinc, lead and tin. A Thermo-Electric Mini-Mite pyrometer was used as the measuring instrument.

Procedure

The propane used was Matheson Instrument Grade with a stated minimum purity of 99.7%. This gas was introduced directly into the storage vessel (V_1) and small traces of

low-boiling gases were removed by the freeze-thaw technique. The propane was then further purified by bulb to bulb low-temperature fractionation.

Before measuring a set of rates at a given temperature, about 650 mm. of gas, either pure propane or a mixture of propane and inert gas, were condensed in the mixing bulb (V_4). When the reaction vessel was evacuated to 5 microns or less, the stop-cocks to the Pirani gauge and manifold were closed. Gas was admitted to the reaction vessel from the mixing vessel and the stopcock quickly closed. The photopen followed the reaction for several minutes and the reaction vessel was again evacuated to 5 microns. This sequence was then repeated, but at a slightly lower initial pressure. It was established early in the investigation that pumping below 10 microns had no effect on the reaction rate, so that pumping below 5 microns was not done routinely. The entire procedure was repeated at several temperatures until, including duplicates, over six hundred rates were measured in the unpacked vessel and over three hundred in the packed vessel.

To correlate extent of reaction with pressure increase, and to identify reaction products, analyses were made of the products of some fifty pyrolyses. Fixed fractions of the reaction products were analysed by gas chromatography using a Perkin-Elmer Vapor Fractometer. For all quantitative work, a two-meter silica gel column at 35°C was used. Peak

heights were used as a quantitative measure of partial pressure, these being calibrated by standards prepared from Matheson C.P. grade gases.

Results

The pyrolysis of propane was investigated in the temperature range 530 to 670°C. As explained above, a photopen recorder automatically recorded the change in pressure with time and the record of a typical run is shown in figure 3. From this record, the initial rate was calculated from the initial slope of the curve. At first these slopes were measured using a Gerber Derivimeter but later it was found that the slopes could be drawn manually with the same degree of accuracy.

The results of a number of runs in both the packed and unpacked vessels are shown plotted logarithmically in figure 4. From this type of plot the order can easily be obtained. In the unpacked vessel, the reaction was first-order at lower temperatures and higher pressures, and 3/2-order at higher temperatures and lower pressures. The first-order and 3/2-order rate constants obtained are listed in table 1. In the packed vessel an intermediate order was observed which was about 1.3. Since this order is meaningless, rate constants were not calculated, but rates at 200 m.m. are listed in table 2. A comparison of rates of reaction

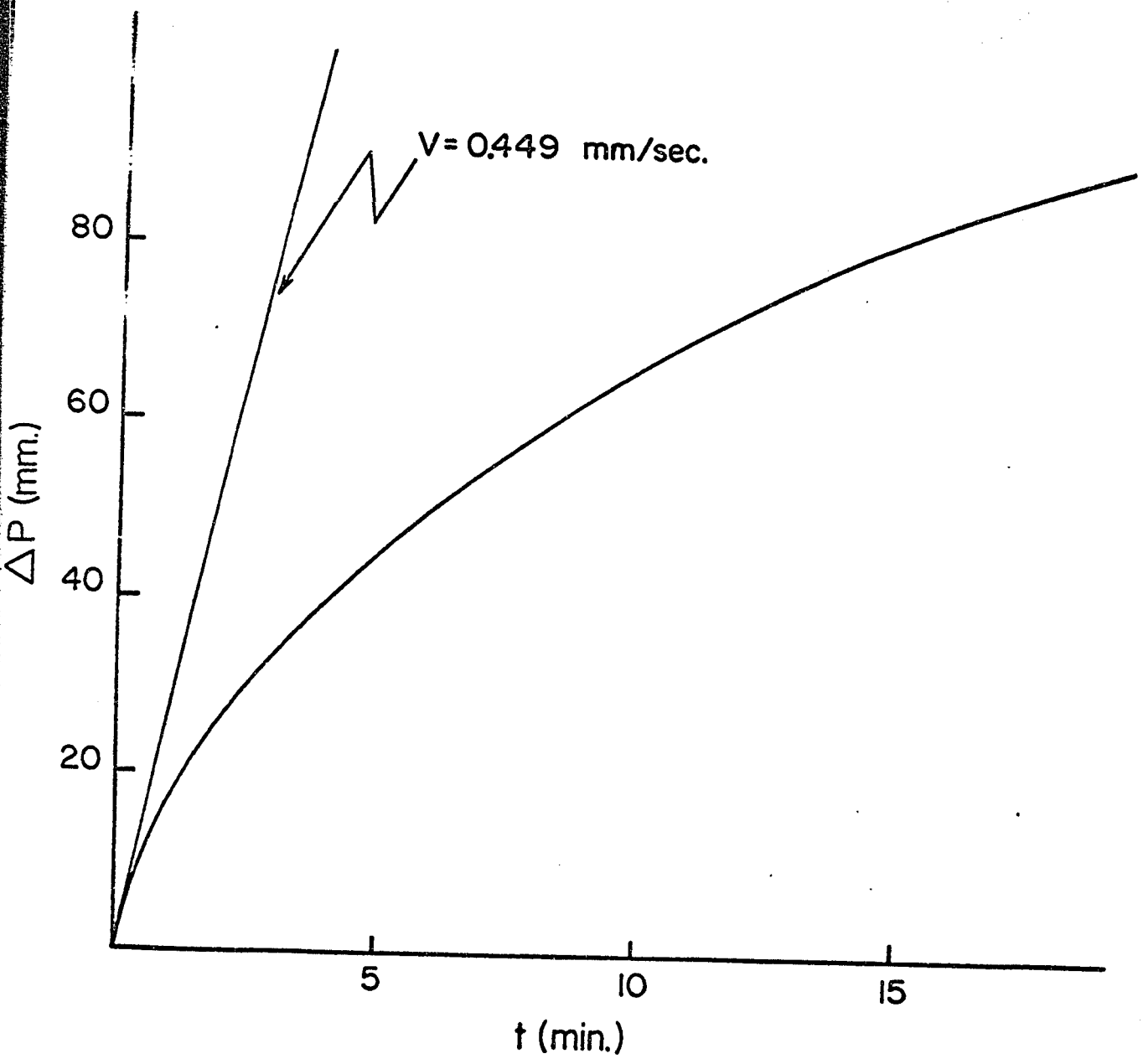

Figure 3 Typical ΔP-time curve for the uninhibited pyrolysis of propane.
Propane pressure = 180 mm.
Temperature = 590°C.

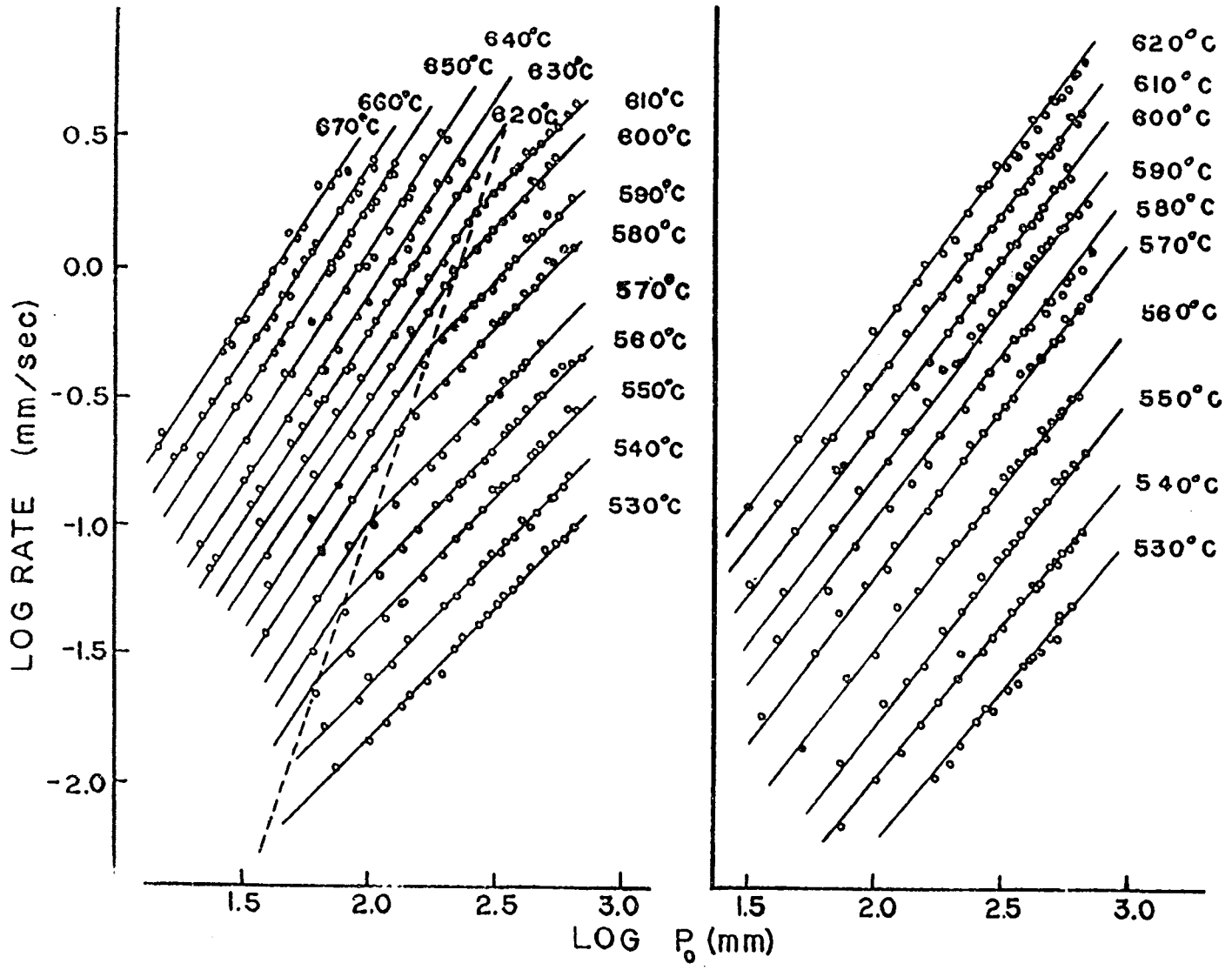

Figure 4 Plot of log rate against log P for the uninhibited pyrolysis of propane. The left hand plot shows rates measured in the unpacked vessel; the right hand plot rates measured in the packed vessel.

Table 1

Rate Constants Obtained in the Unpacked Vessel

T°C	$10^4 k_1 (sec^{-1})$	$10^4 k_{3/2} (mm.^{-1/2} sec^{-1})$
530	1.48	-
540	2.31	-
550	3.89	-
560	6.17	-
570	9.90	0.98
580	18.00	1.46
590	27.45	2.01
600	41.2	2.82
610	60.2	3.71
620	-	5.25
630	-	6.75
640	-	10.47
650	-	15.83
660	-	22.4
670	-	30.2

Table 2

Rates of Reaction in the Packed Vessel at 200 mm. Pressure

T°C	10^2V(mm./sec)	T°C	10^2V(mm./sec)
530	1.27	580	23.4
540	2.34	590	38.0
550	3.98	600	56.3
560	7.75	610	85.3
570	14.95	620	130.2

in the packed and unpacked vessels is given in figure 5.

In figure 6 and 7 the logarithms of the first-order and 3/2-order rate constants are plotted against the reciprocals of the absolute temperatures, and activation energies of 67.1 and 54.5 kcal. per mole respectively were obtained. The results of Steacie and Puddington (12) and Frey and Hepp (8) are included for comparison, as well as two points obtained incidentally by Hobbs and Hinshelwood (35) and Ingold, Stubbs and Hinshelwood (36) while investigating the nitric oxide inhibited pyrolysis of propane. Figure 8 shows a plot of the logarithm of the rate at 200 mm. pressure against 1/T for the packed vessel. The apparent activation energy is not constant but varies from 67 kcal. per mole at highest temperatures to 84 kcal. per mole at the lowest ones.

The effect of adding carbon dioxide is shown in figure 9(a) for 650°C, a temperature well within the 3/2-order region at pressures below 200 mm., and in figure 9(b) for 530°C, a temperature in the first-order region. It is seen that, within the experimental error, there is no marked effect of inert gas on the rate of reaction under either condition.

Analytical results showed that, initially, unit increase in pressure corresponds to unit decrease in the partical pressure of propane over the entire range of temperature and pressure used, as shown in figure 10. Analyses of

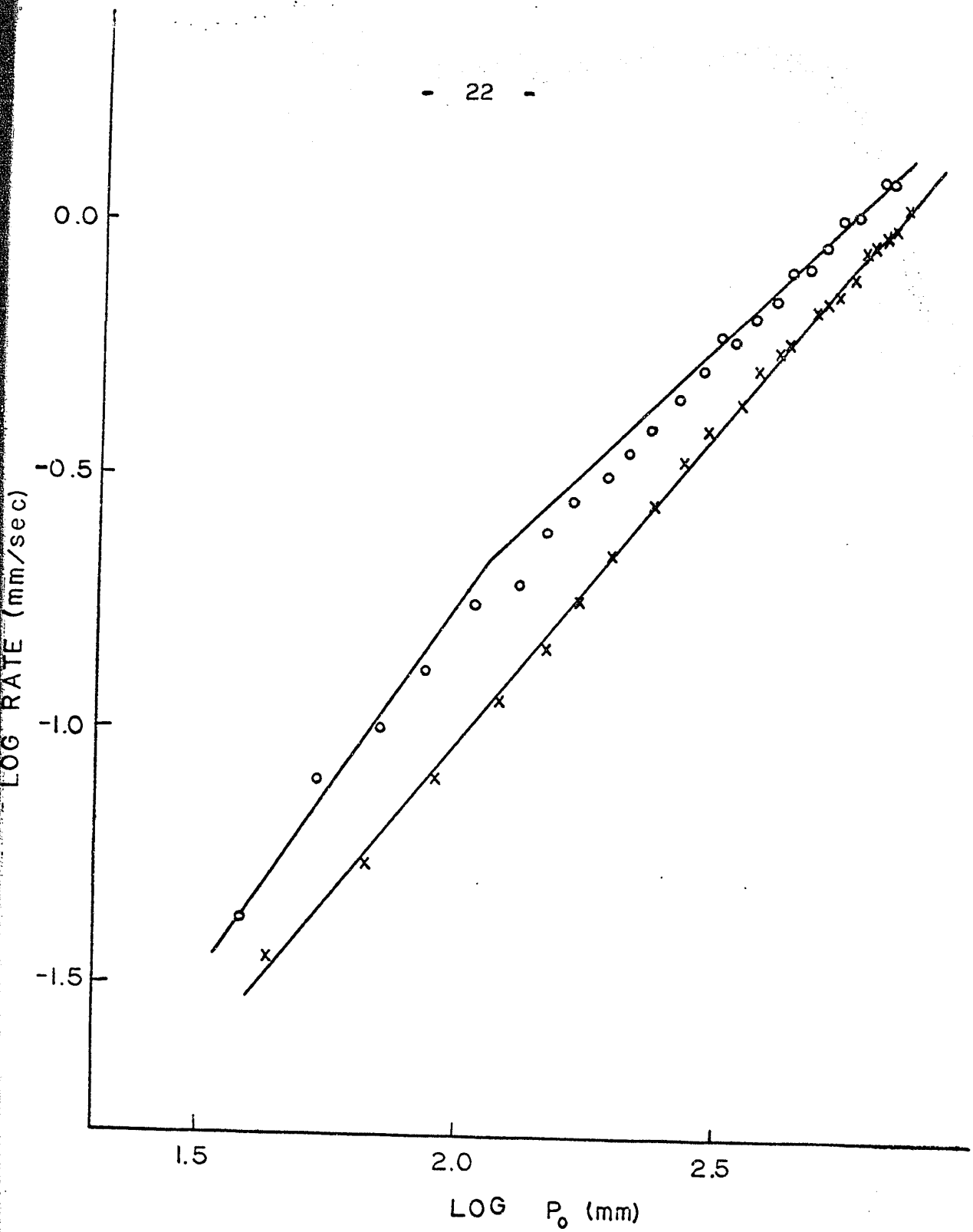

Figure 5 Comparison of rates in the packed and unpacked vessels for the uninhibited pyrolysis of propane. The circles denote rates measured in the unpacked vessel, the crosses those measured in the packed vessel, all at 580°C.

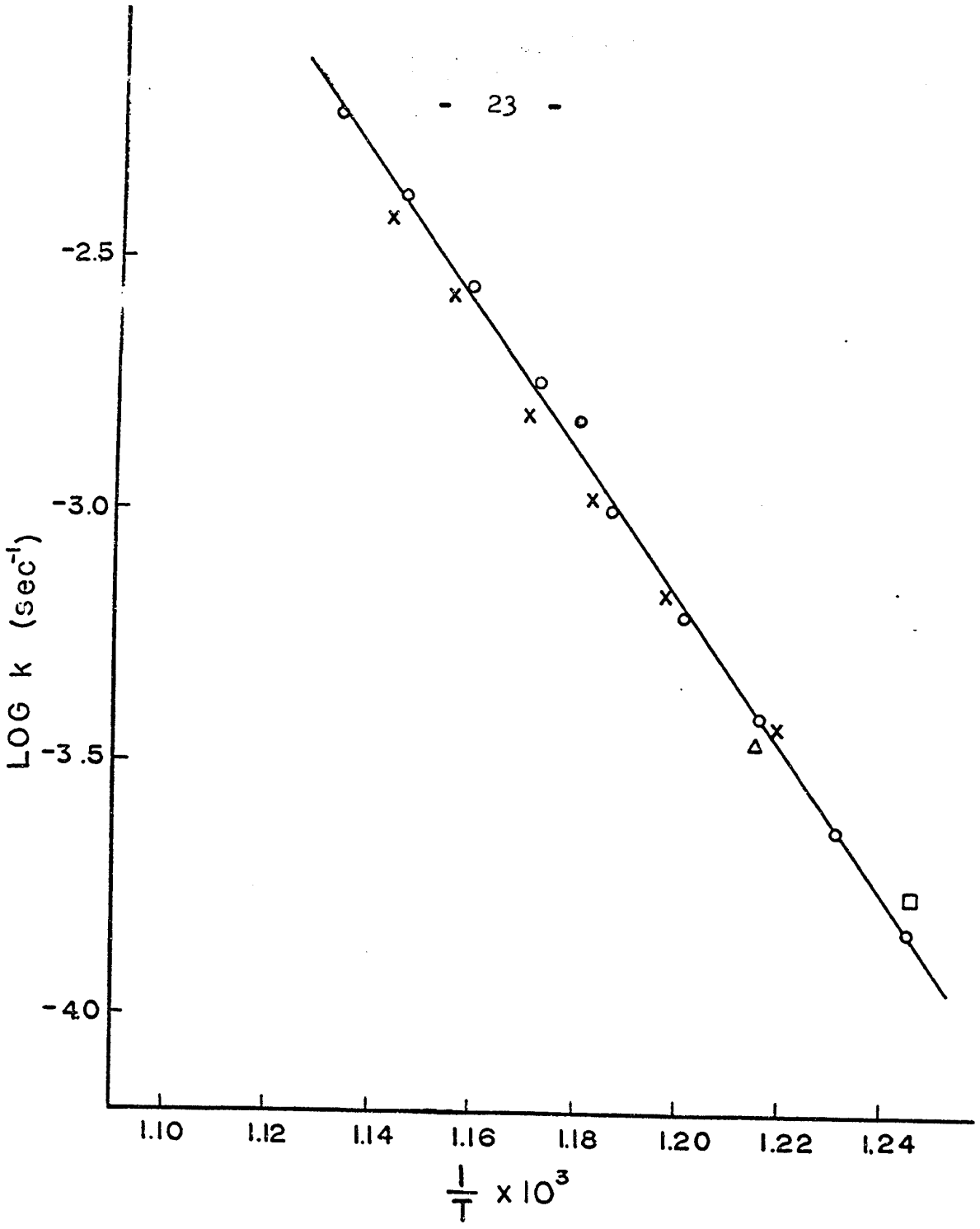

Figure 6 Arrhenius plot of first-order rate constants for the uninhibited pyrolysis of propane. The results of this investigation are shown as O, those of Steacie and Puddington (12) as X, that of Frey and Hepp (8) as ⊙, that of Hobbs and Hinshelwood (35) as Δ, and that of Ingold, Stubbs and Hinshelwood (36) as □.

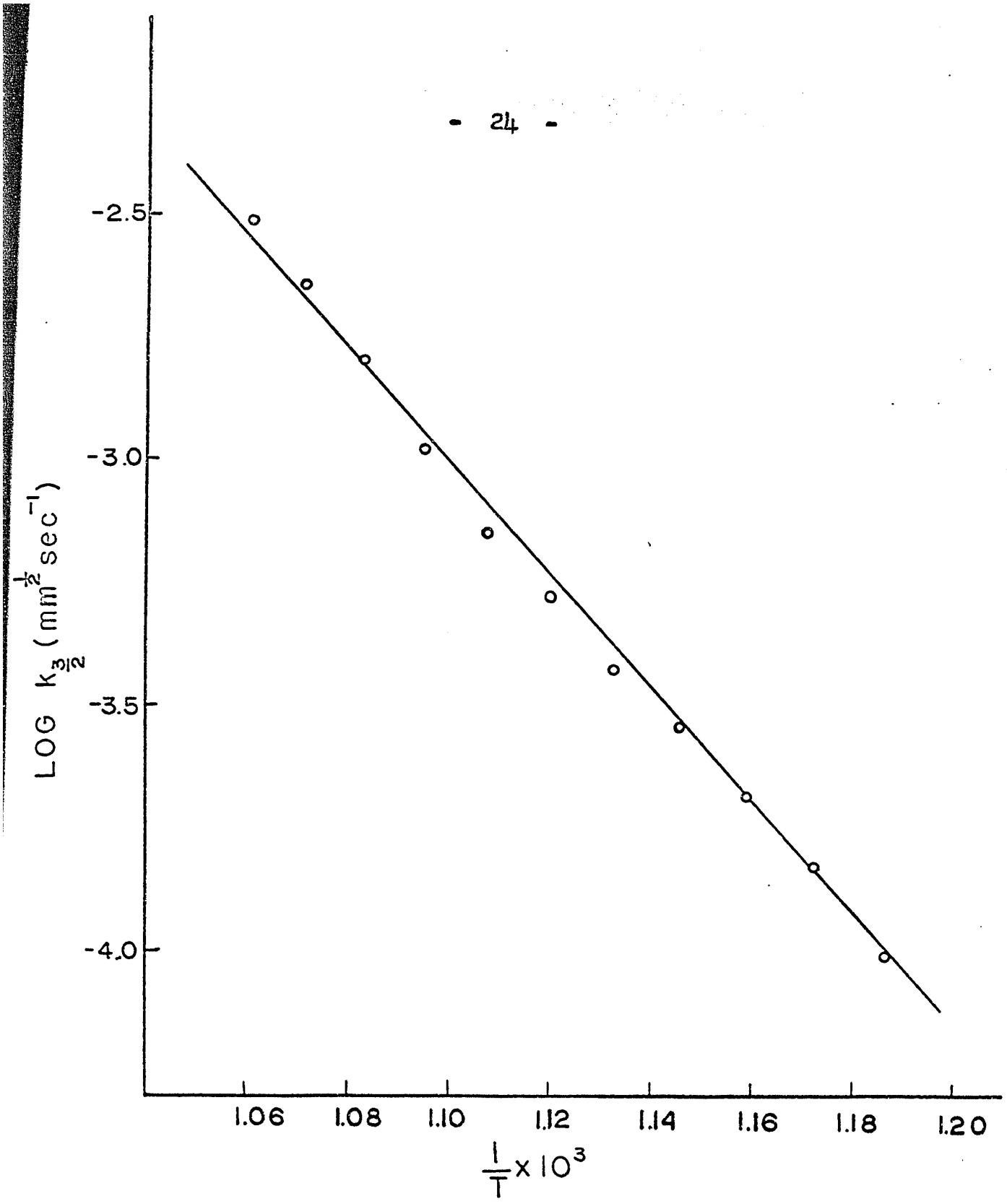

Figure 7 Arrhenius plot of 3/2-order rate constants for the uninhibited pyrolysis of propane.

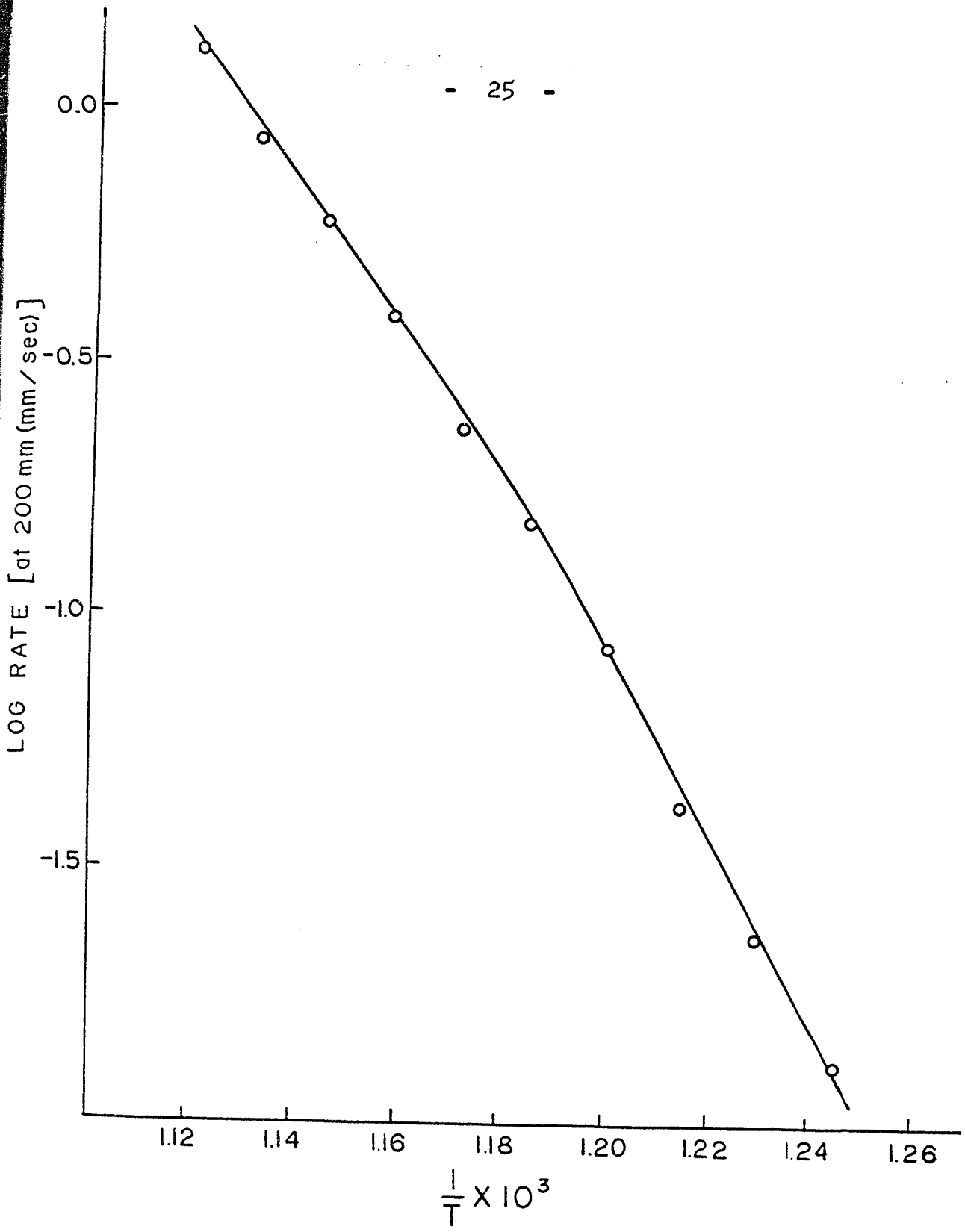

Figure 8 Plot of the logarithm of the rate of the uninhibited pyrolysis of propane at 200 mm in the packed vessel against 1/T.

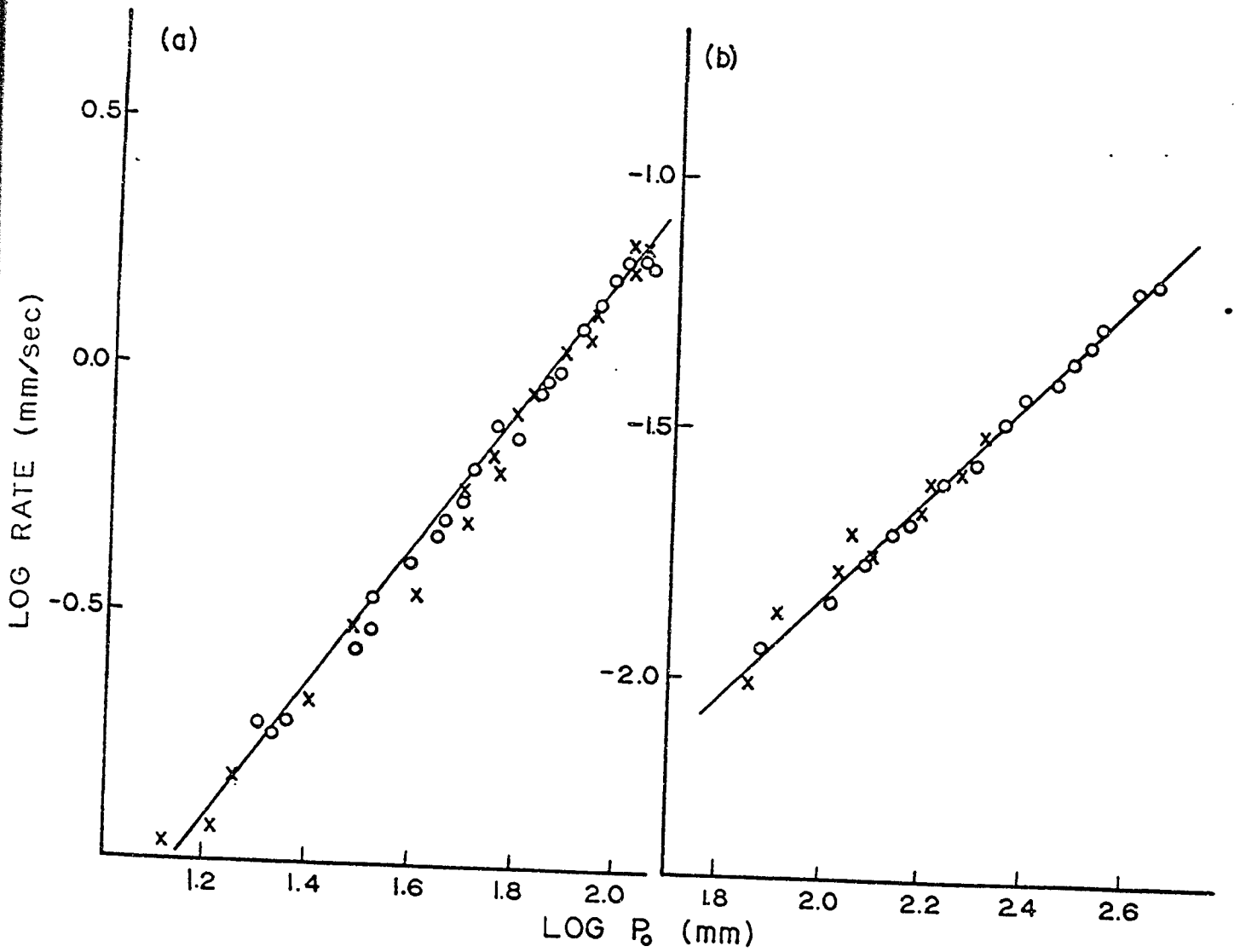

Figure 9 Effect of added carbon dioxide on the uninhibited pyrolysis of propane. The left hand plot (9a) is at 650°C, the right hand (9b) is at 530°C. The circles denote rates measured with no added CO_2. The crosses denote rates with $CO_2/C_3H_8 = 2.5$.

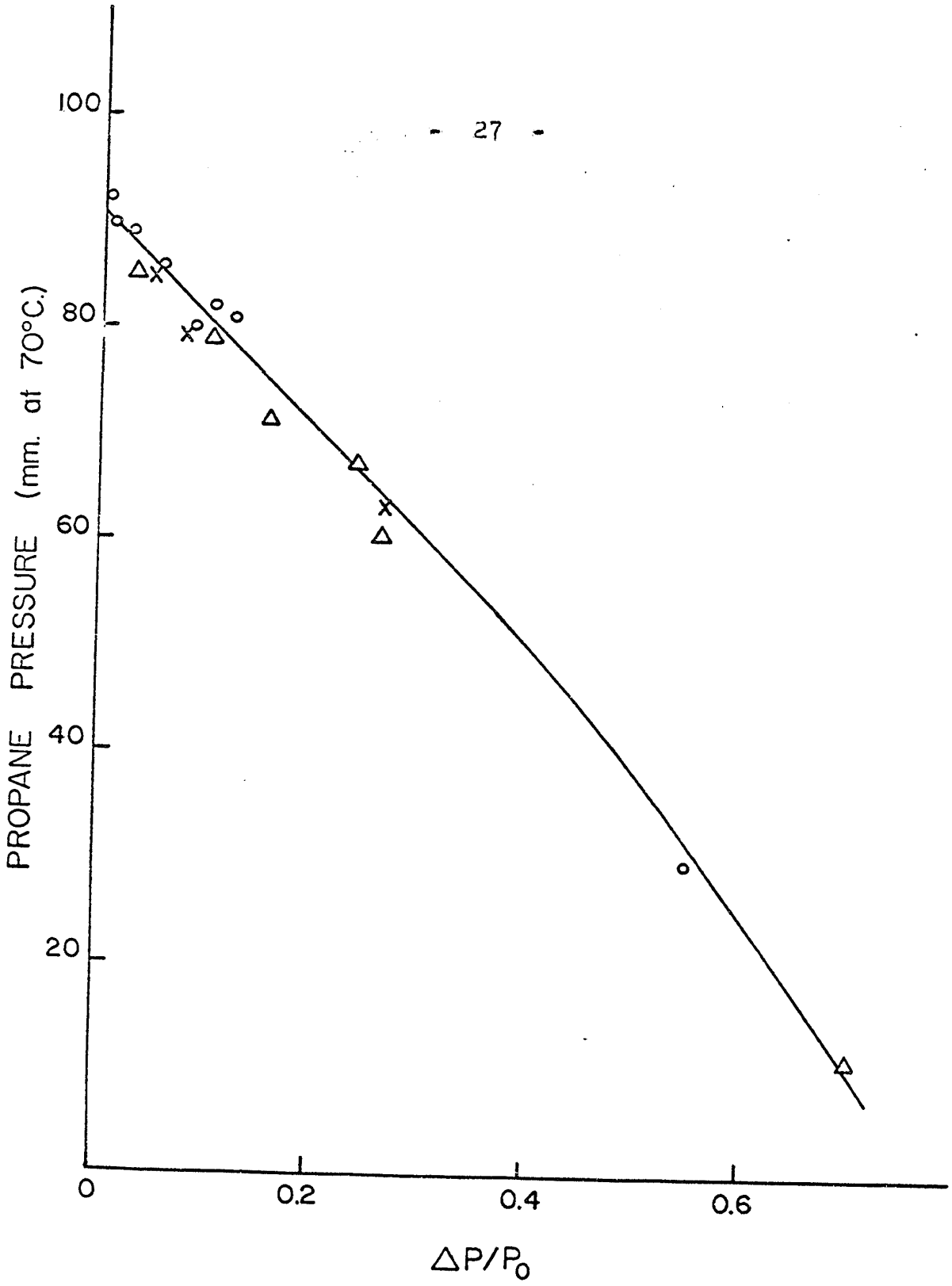

Figure 10 Correlation between the increase in total pressure and decrease in partial pressure of propane. Results obtained at 540°C are shown as O, at 570°C as X and at 600°C as Δ.

the products showed the chief initial products to be H_2, CH_4, C_2H_4 and C_3H_6 in almost equal amounts. Table 3 shows the results of a typical set of analyses done at a temperature of 570°C and an initial pressure of 212 mm.

Using the analytical result that the partial pressure of propane decreases 1 mm. for every mm. of pressure rise, the rate constants in the unpacked vessel become:

$$k_1 = 2.58 \times 10^{14} e^{-67,100/RT} \text{ sec}^{-1}$$

$$k_{3/2} = 8.50 \times 10^{13} e^{-54,500/RT} \text{ ml}^{1/2} \text{ mole}^{-1/2} \text{ sec}^{-1}$$

DISCUSSION

Mechanism of the Reaction

The purpose of this work was to evaluate the original Rice-Herzfeld mechanism and to propose an alternative scheme, if necessary. The original Rice-Herzfeld mechanism, as given by Steacie (37), is:

(1) $C_3H_8 \longrightarrow CH_3 + C_2H_5$

(2) $C_2H_5 \longrightarrow C_2H_4 + H$

(3a) $H + C_3H_8 \longrightarrow H_2 + n\text{-}C_3H_7$

(4a) $CH_3 + C_3H_8 \longrightarrow CH_4 + n\text{-}C_3H_7$

(5a) $n\text{-}C_3H_7 \longrightarrow CH_3 + C_2H_4$

(3b) $H + C_3H_8 \longrightarrow H_2 + i\text{-}C_3H_7$

Table 3

Amount of Products

T = 570°C Pressure = 212 mm.

Compound	Amount (mm. at 70°C)
H_2	12.5
CH_4	19.5
C_2H_6	2.7
C_2H_4	13.6
C_3H_6	12.2
C_3H_8	- 29.0 (used up)

(4b) $CH_3 + C_3H_8 \longrightarrow CH_4 + i\text{-}C_3H_7$

(6a) $i\text{-}C_3H_7 \longrightarrow C_3H_6 + H$

(8) $H + C_3H_7 \longrightarrow H_2 + C_3H_6$ or C_3H_8

(7) $CH_3 + C_3H_7 \longrightarrow CH_4 + C_3H_6$ or C_4H_{10}

Since, in recent years, it has been shown that $n\text{-}C_3H_7$ may produce $C_3H_6 + H$ at a rate almost 10% that of reaction 5a at these temperatures (38), and since isomerization of propyl radicals is possible at these temperatures (33) (29), all propyl radicals are taken as equivalent. Furthermore, it is considered likely that the ethyl radicals produced in reaction 1 have less than the normal 'thermal' energy, and since the only way this energy can be obtained is by collision with other molecules, it is probable that they will abstract before they have acquired enough energy to decompose by reaction 2. A modified Rice mechanism may thus be written as:

(1) $C_3H_8 \longrightarrow CH_3 + C_2H_5$

(9) $C_2H_5 + C_3H_8 \longrightarrow C_2H_6 + C_3H_7$

(3) $H + C_3H_8 \longrightarrow H_2 + C_3H_7$

(4) $CH_3 + C_3H_8 \longrightarrow CH_4 + C_3H_7$

(5) $C_3H_7 \longrightarrow CH_3 + C_2H_4$

(6) $C_3H_7 \longrightarrow H + C_3H_6$

(7) $CH_3 + C_3H_7 \longrightarrow CH_4 + C_3H_6$ or C_4H_{10}

When the steady state treatment is applied to this scheme, the following concentrations of radicals are obtained:

$$[C_2H_5] = \frac{k_1}{k_9}[C_3H_8] \qquad [1]$$

$$[CH_3] = \left(\frac{k_1 k_5}{k_4 k_7}\right)^{1/2} \qquad [2]$$

$$[H] = \frac{k_6}{k_3}\left(\frac{k_1 k_4}{k_5 k_7}\right)^{1/2} \qquad [3]$$

$$[C_3H_7] = \left(\frac{k_1 k_4}{k_5 k_7}\right)^{1/2}[C_3H_8] \qquad [4]$$

The over-all rate is given by

$$V_1 = \left(\frac{k_1 k_4}{k_5 k_7}\right)^{1/2}(k_5 + k_6)[C_3H_8] \qquad [5a]$$

As has been shown, the over-all order of the reaction is first at high pressures and becomes 3/2 at lower pressures for any given temperature. Furthermore inert gas appears to have little or no effect in either the first-order or 3/2-order region. A proposed mechanism in the first-order region is:

(1a) $X + C_3H_8 \longrightarrow CH_3 + C_2H_5 + X$

(9) $C_2H_5 + C_3H_8 \longrightarrow C_2H_6 + C_3H_7$

(3) $H + C_3H_8 \longrightarrow H_2 + C_3H_7$

(4) $CH_3 + C_3H_8 \rightarrow CH_4 + C_3H_7$

(5) $C_3H_7 \rightarrow CH_3 + C_2H_4$

(6) $C_3H_7 \rightarrow H + C_3H_6$

(7a) $X + CH_3 + C_3H_7 \rightarrow CH_4 + C_3H_6 + X$ or $C_4H_{10} + X$

Initially all the X is C_3H_8, so when the steady state treatment is applied, similar radical concentrations are obtained as in the modified Rice scheme, and the rate is given by:

$$V_1 = \left(\frac{k_{1a}k_4}{k_5k_{7a}}\right)^{1/2} (k_5 + k_6)\,[C_3H_8] \qquad [5]$$

When the over-all order becomes 3/2, it is postulated that the initiating step remains the same, and that the termination step becomes

(10) $X + CH_3 + CH_3 \rightarrow C_2H_6 + X$

Thus the over-all mechanism becomes:

(1a) $X + C_3H_8 \rightarrow CH_3 + C_2H_5 + X$

(9) $C_2H_5 + C_3H_8 \rightarrow C_2H_6 + C_3H_7$

(3) $H + C_3H_8 \rightarrow H_2 + C_3H_7$

(4) $CH_3 + C_3H_8 \rightarrow CH_4 + C_3H_7$

(5) $C_3H_7 \rightarrow CH_3 + C_2H_4$

(6) $C_3H_7 \longrightarrow H + C_3H_6$

(10) $X + CH_3 + CH_3 \longrightarrow C_2H_6 + X$

Initially all the X is C_3H_8, so that the following expressions for the radical concentrations are obtained:

$$[C_2H_5] = \frac{k_{1a}}{k_9} [C_3H_8] \qquad [6]$$

$$[CH_3] = \left(\frac{k_{1a}}{k_{10}}\right)^{1/2} [C_3H_8]^{1/2} \qquad [7]$$

$$[H] = \frac{k_4 k_6}{k_3 k_5} \left(\frac{k_{1a}}{k_{10}}\right)^{1/2} [C_3H_8]^{1/2} \qquad [8]$$

$$[C_3H_7] = \frac{k_4}{k_5} \left(\frac{k_{1a}}{k_{10}}\right)^{1/2} [C_3H_8]^{3/2} \qquad [9]$$

The over-all rate is

$$V_{3/2} = \frac{k_4}{k_5} \left(\frac{k_{1a}}{k_{10}}\right)^{1/2} (k_5 + k_6) [C_3H_8]^{3/2} \qquad [10]$$

The reasons for choosing the initiation and termination reactions used are given in the following sections.

Order of the Reaction

The over-all order for any reaction mechanism is determined solely by the initiating and terminating steps. The various possibilities have been worked out some time ago by Goldfinger, Letort and Niclause (39) and are listed below in table 4. In this table β radicals are ones, such as CH_3

Table 4

Over-All Orders of Reaction for Various Types of Initiation and Termination Reactions

First-Order Initiation		Second-Order Initiation		Over-All Order
Simple Termination	Third-Body Termination	Simple Termination	Third-Body Termination	
		$\beta\beta$		2
$\beta\beta$		$\beta\mu$	$\beta\beta M$	3/2
$\beta\mu$	$\beta\beta M$	$\mu\mu$	$\beta\mu M$	1
$\mu\mu$	$\beta\mu M$		$\mu\mu M$	1/2
	$\mu\mu M$			0

or H, which take part in bimolecular reactions, while μ radicals are ones which decompose unimolecularly, such as C_3H_7.

It is readily seen from this table that there are only certain sets of mechanisms by which a reaction which is first-order at higher pressures can become 3/2-order at lower pressures. These are as follows:

I	$^1_{\beta\beta}M_1$	→	$^2_{\beta\beta}M_{3/2}$
II	$^1_{\beta\mu}{}_1$	→	$^2_{\beta\mu}{}_{3/2}$
III	$^2_{\beta\mu}M_1$	→	$^2_{\beta\beta}M_{3/2}$
IV	$^2_{\mu\mu}{}_1$	→	$^2_{\beta\mu}{}_{3/2}$
V	$^1_{\beta\mu}{}_1$	→	$^1_{\beta\beta}{}_{3/2}$

The terminology used is that the initial superscript represents the order of the initiating step and the final subscript the order of the over-all reaction. The symbols such as ββM indicate the nature of the termination step, and the arrows show the transition expected when the pressure is lowered. The five cases listed are those in which only one factor changes at a time; it is very unlikely that two changes would occur in the same pressure region and in a consistent manner over a wide temperature range.

The following sections will show that, out of these five cases, only III is allowable.

Effect of Inert Gas

As shown in figure 9, the addition of inert gas, at partial pressures up to three times that of propane, appears to have no marked effect on the rate of pyrolysis of propane, at least to within the experimental error. This fact has been established at 650°C, a temperature well within the 3/2-order region, and in the first-order region, at 530°C, using CO_2 as an inert gas. Therefore the molecularity of the initiating and terminating steps is the same in both the first and 3/2-order cases provided that no chain propagating reactions are pressure dependent. Thus, of the possible mechanisms considered in the above section, I, II and IV are definitely excluded. It should, perhaps, be stressed that when inert gas effects are noted they are often quite striking. For example Kuchler and Theile (40) noted almost a 65% increase in rate, when pyrolyzing 60 mm. ethane, on adding 4.45 times this amount of CO_2.

The Initiating Step

It has been shown recently by Laidler and Wojciechowski (41), using theoretical calculations by Gill and Laidler (42), that the initiating step in the pyrolysis of ethane

$$C_2H_6 \quad \longrightarrow \quad 2\,CH_3$$

is in its second-order region at 600°C at pressures up to

1800 mm. Unfortunately, for molecules as large as propane it is impossible to show by calculation that the initiation is of the second order.

Assuming the activated complex for the splitting off of a methyl group from a paraffin to take the form

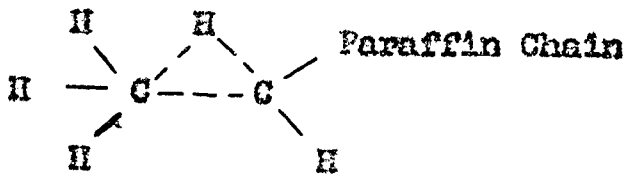

Wojciechowski and Laidler (43) have predicted that the s of the Hinshelwood-Rice-Ramsperger-Kassel (44) (45) theory of unimolecular reaction rates will be about 9 regardless of the length of the paraffin chain. Thus the splitting off of a methyl group will be in its second-order region at the temperature of pyrolysis and conversely, by the principle of microscopic reversibility, the addition of a methyl radical to any other paraffin radical will involve a third body at these temperatures. These considerations preclude the fifth possible mechanism mentioned in the discussion of the over-all order of the reaction.

The high-pressure rate constant for initiation is given by

$$k_1 = \nu e^{-E_o/RT} \qquad [11]$$

where E_o is 82 kcal. per mole. However in the second-order

region, the Hinshelwood-Rice-Ramsperger-Kassel (HRRR) theory gives the rate constant as

$$k_1 = Z \left(\frac{E_o}{RT}\right)^{s-1} \frac{1}{(s-1)!} e^{-E_o/RT} \qquad [12]$$

Z is proportional to $T^{-1/2}$, so that the temperature dependence of the rate constant is given by

$$k_1 \propto \left(\frac{1}{T}\right)^{s-\frac{1}{2}} e^{-E_o/RT} \qquad [13]$$

Therefore the low pressure activation energy is given by

$$E_{1a} = E_o - (s - \tfrac{1}{2}) RT \qquad [14]$$

Assuming that 9 degrees of freedom are used in the Kassel formulation

$$E_{1a} = 82{,}000 - 8.5\ RT \qquad [15]$$

$$= 67.2 \text{ kcal. per mole}$$

at 600°C, as given in table 5.

Chain Propagating Steps

Analytical results have shown that the chief products of the reaction are H_2, CH_4, C_2H_4 and C_3H_6 all in about equal quantities. This implies that

$$V_3 = V_4 = V_5 = V_6$$

Table 5

Kinetic Parameters for Reactions Involved in the Propane Pyrolysis

Reaction	A*	E(kcal/mole)	k_{600}*	Reference
1	4.0×10^{17}	82.0	1.20×10^{-3}	(46)
1(a)	9.0×10^{17}	67.2	13.3	calculated (see text)
2	3.0×10^{14}	39.5	3.96×10^{4}	(47)
3	1.0×10^{12}	8.2	8.85×10^{9}	calc. from (48)
4	1.0×10^{13}	8.5	7.45×10^{10}	calc. from (49)
5	8.0×10^{13}	31	1.39×10^{6}	(38)
6	1.3×10^{14}	37	7.12×10^{4}	(38)
7	1.0×10^{14}	0	1.00×10^{14}	assumed
7(a)		[-16.5]	1.3×10^{19}	calculated
8	1.0×10^{13}	0	1.00×10^{13}	assumed
9	1.0×10^{12}	10.0	3.20×10^{9}	assumed
10		[-14.8]	1.00×10^{16}	(42)
11	1.0×10^{14}	0	1.00×10^{14}	assumed

* Rates and frequency factors in sec^{-1} or $ml.\ mole^{-1}\ sec^{-1}$. Bracketed activation energies are apparent values, equivalent to a temperature-dependent pre-exponential factor.

Also, the temperature dependence of these rates does not seem to vary over the range 530°C to 600°C, implying that

$$E_5 \simeq E_6$$

Until recently, it was thought that E_5 had a value around 20 kcal. per mole and E_6 around 35 kcal. per mole (see Bywater and Steacie (47)). On this basis reaction 6 would be many orders of magnitude slower than reaction 5 if the C_3H_7 was n-propyl, and all the C_3H_6 would have to come from the i-propyl radical. It may now be seen that V_6 is about 5% of V_5 at 600°C, according to the consistent set of reaction parameters quoted in table 5. However, these parameters are at present a matter of some controversy and since the rates are calculated by extrapolating A's and E's obtained below 400°C to 600°C, the actual rates may be considerably in error. A number of estimates of these parameters by different workers is listed in table 6. It may be seen that present knowledge of reaction 5 is unsatisfactory, but it may be assumed that, if C_3H_7 is n-propyl, about 5 to 10% of the reaction goes by reaction 6. If, as postulated by Rice (16) and verified recently by Semenov (54) the C_3H_7 is 40% i-propyl and 60% n-propyl, a 10% production of C_3H_6 from the n-propyl would explain the equal distribution of products assuming that all the i-propyl goes to C_3H_6.

Table 6

Kinetic Parameters and Rates of Reaction 5

A(sec^{-1})	E(kcal/mole)	k_{600}(sec^{-1})	Reference
8.0×10^{13}	31	1.39×10^{6}	Jackson and McNesby (38)
3.39×10^{15}	34.5	7.60×10^{6}	Kerr and Calvert (50)
5.0×10^{11}	25.2	2.46×10^{5}	Kerr and Trotman-Dickenson (51)(52)
6.31×10^{15}	34.9	1.01×10^{7}	Calvert and Sleppy (53)
3.0×10^{9}	20	2.95×10^{4}	Bywater and Steacie (47)

Chain Terminating Steps

The values of k_{7a} and k_{10} were calculated using methods similar to those used to calculate k_{1a}. The value of k_{10} was calculated directly from the third-order rate constant at 200°C, 3×10^{20} moles^{-2} sec^{-1}, calculated by Gill and Laidler (42). They used the results of Dodd and Steacie (55) and employed the HKRR theory with s = 9. This calculation was similar to that done by Laidler and Wojciechowski (41).

The value of k_{7a} was obtained from equation 12, using s = 11, and a collision diameter similar to that calculated for reaction 10.

It may easily be shown, using the values of pre-exponential factors and activation energies listed in table 5, that the termination steps chosen are faster than any other possible steps. For example, assuming second-order initiation, the other possible chain termination to give first order over all is

(11) $C_3H_7 + C_3H_7 \longrightarrow C_6H_{14}$ or $C_3H_6 + C_3H_8$

Using the expressions for CH_3 and C_3H_7 obtained from the steady-state treatment of the Rice mechanism

$$\frac{V_{7a}}{V_{11}} = \frac{k_{7a}[CH_3][C_3H_7]}{k_{11}[C_3H_7][C_3H_7]} = \frac{k_{7a}k_6}{k_{11}k_3} = 2.5 \qquad [16]$$

Other possible terminating steps are found to be even slower in relation to V_{7a}.

The transition between first and 3/2 order should occur when V_{7a} equals V_8, which means that

$$k_{7a}[CH_3][C_3H_7][C_3H_8] = k_8[CH_3]^2[C_3H_8] \qquad [17]$$

If the values for the concentrations of the various radicals are inserted into this equation

$$[C_3H_8] = 1.43 \times 10^{-6} \text{ moles /ml.}$$

$$\approx 76 \text{ mm.}$$

The actual value is somewhat more than this (about 220 mm.) but in view of the approximations made in estimating the rate constants and the uncertainty in some of the kinetic parameters, the agreement is quite satisfactory.

The variation with pressure of the transition point can also be calculated from equation 17. Figure 11 shows a plot of the logarithm of the transition pressure against the reciprocal of the absolute temperature, and leads to an activation energy of 26.2 kcal per mole. The value calculated using equations 17, 2 and 4, and inserting values from table 5 is 24.2 kcal.per mole, in reasonable agreement.

Simple geometric considerations show that this 'break-point activation energy' should bear a relationship

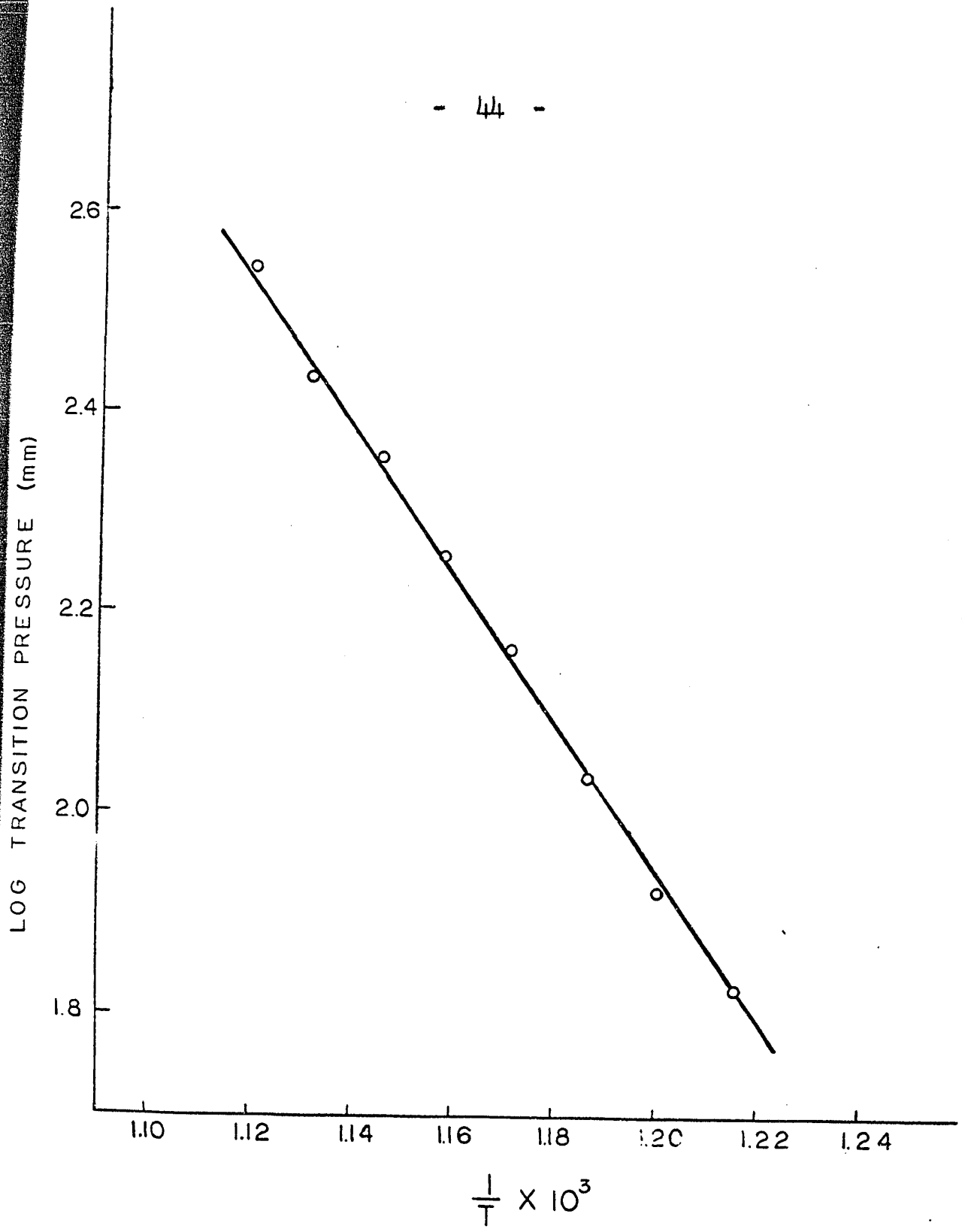

Figure 11 The logarithm of the pressure of the transition of the uninhibited propene pyrolysis from first to 3/2-order kinetics plotted against 1/T.

to the orders and activation energies of the two kinetic descriptions. Figure 12 shows a typical reaction exhibiting n'th order kinetics at high pressures and m'th order at lower ones. E_n can be identified with the vertical distance PB and E_m with PA. Similarly the break-point activation energy,

$$E_p = -R \frac{d \ln P}{d(1/T)} \qquad [18]$$

can be identified with P_2C.

In triangle P_2AC,

$$n = \frac{BC}{P_2C} \quad \text{and} \quad m = \frac{AC}{P_2C} \qquad [19]$$

$$m-n = \frac{AC - BC}{P_2C} = \frac{AB}{P_2C} = \frac{E_n - E_m}{E_p} \qquad [20]$$

Using the first-order and 3/2-order activation energies obtained experimentally, it is found that the predicted E_p is 25.3 kcal. per mole compared to the measured 26.2 kcal. per mole. This discrepancy comes about because E_p was obtained using only a few temperatures in the lower end of the temperature range used for obtaining $E_{3/2}$. The calculated activation energies, given in the next section, are, of course, in exact agreement with equation 20.

Activation Energies and Rate Constants

Using the values given in table 5 the overall activation energy may be calculated for the reaction in

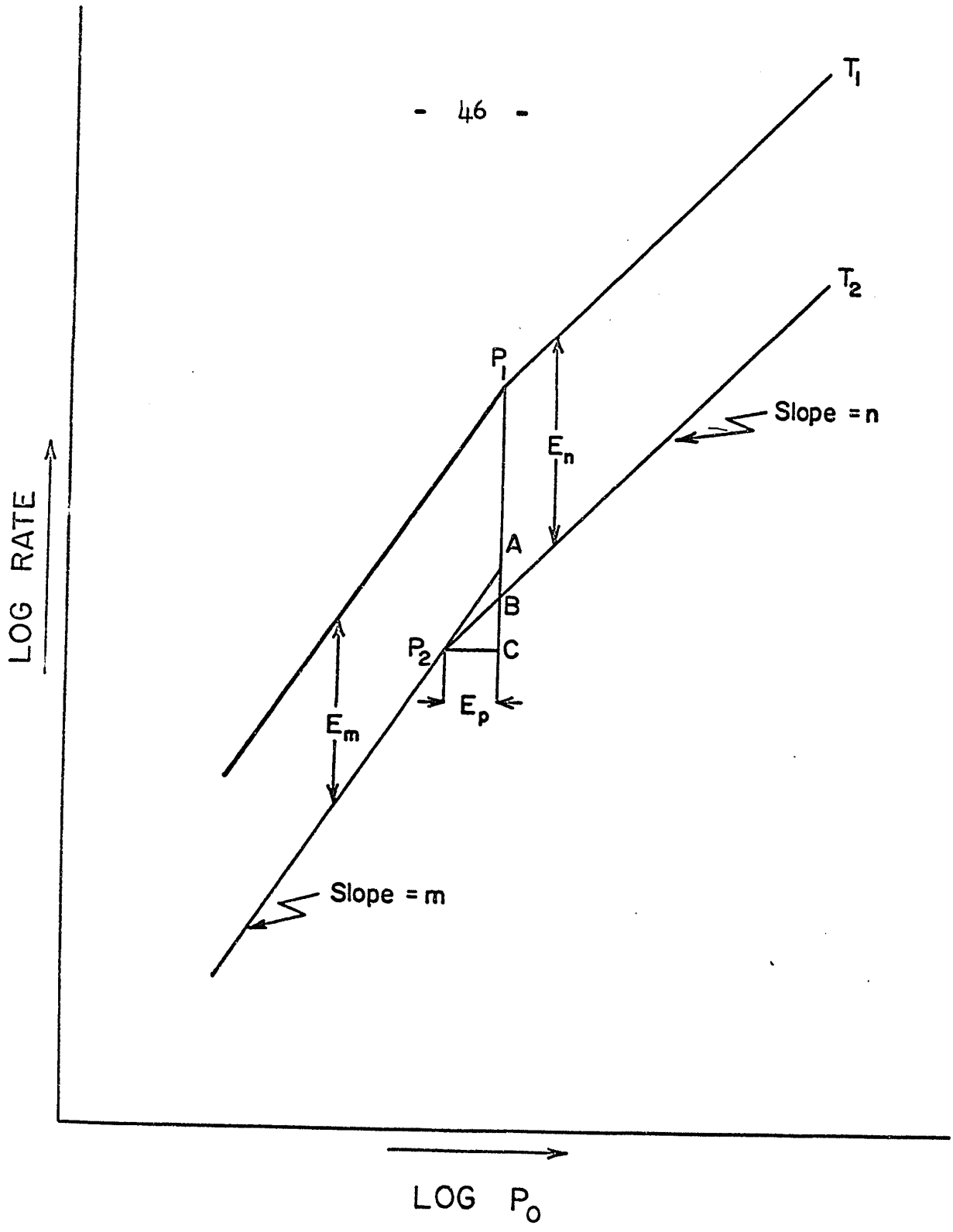

Figure 12 Hypothetical plots of log rate against log pressure for a reaction which changes order with pressure, showing the origin of the 'break-point activation energy'.

the first-order region if a method for estimating the activation energy of $(k_5 + k_6)$ is available. Since the rates of reactions 5 and 6 are about equal, the simplest procedure is to take the arithmetic mean, and therefore from equation 5

$$E_a = \tfrac{1}{2}(E_{1a} + E_4 - E_5 - E_{7a}) + \tfrac{1}{2}(E_5 + E_6) \qquad [21]$$

$$= 64.6 \text{ kcal. per mole}$$

In view of the lack of certainty in some of the experimental values this is in satisfactory agreement with the experimental value of 67.1 kcal. per mole. The frequency factor, calculated on a similar basis is 9.5×10^{12} sec^{-1}, to be compared with 2.58×10^{14} sec^{-1} obtained experimentally. Absolute rate constants agree reasonably well, the experimental rate constant being 4.12×10^{-3} at 600°C, the calculated 6.43×10^{-4}.

The activation energy in the 3/2-order region, using equation 10 and the arithmetic mean of E_5 and E_6 for the activation energy of $(k_5 + k_6)$, becomes:

$$E = E_4 - E_5 + \tfrac{1}{2}(E_{1a} - E_{10}) + \tfrac{1}{2}(E_6 + E_5) \qquad [22]$$

$$= 52.5 \text{ kcal. per mole}$$

in good agreement with the experimental value of 54.5 kcal. per mole.

The frequency factor becomes 1.21×10^{13} $ml^{1/2}$ $mole^{-1/2}$

sec^{-1} in fair agreement with the experimental value of 8.5×10^{13} $ml^{1/2}$ $mole^{-1/2}$ sec^{-1}. Again, rate constants are in better agreement than frequency factors, the experimental being 1.94 $ml^{1/2}$ $mole^{-1/2}$ sec^{-1}, the calculated 8.75×10^{-1} $ml^{1/2}$ $mole^{-1/2}$ sec^{-1}.

Effect of Surface

It may be seen from figure 5 that the rate is lowered some 20% by increasing the surface to volume ratio by a factor of 12. There is also a tendency to smear out the differences between the first and 3/2-order regions, giving a meaningless overall order of 1.2 to 1.3. The decrease in rate is attributed to a partial inhibition of the rate by a mechanism similar to that put forward in the following section to explain the inhibition by nitric oxide. A bare surface site, S, may be equivalent to NO and a hydrogen atom may be abstracted from a propane molecule by this site.

$$C_3H_8 + S \longrightarrow C_3H_7 + SH$$

Termination may be partly the reverse of this mechanism, and so a new reaction scheme may be partly involved.

CONCLUSIONS

It is concluded that the thermal decomposition of propane is largely homogeneous, and is first-order at low

temperatures and high pressures, becoming 3/2-order at higher temperatures and lower pressures. It is thought that a free radical reaction mechanism involving second-order initiation and third-body termination adequately explains the experimental results obtained, as well as those obtained by other workers. Values of individual rate constants and activation energies are calculated or quoted from recent sources, and these are shown to be consistent with the proposed mechanism.

The rate constants in the first-order and 3/2-order over all regions may be given as

$$k_1 = 2.58 \times 10^{14} e^{-67,100/RT} \text{ sec}^{-1}$$

$$k_{3/2} = 8.50 \times 10^{13} e^{-54,500/RT} \text{ ml}^{1/2} \text{ moles}^{-1/2} \text{ sec}^{-1}$$

Part II

PYROLYSIS OF PROPANE INHIBITED BY NITRIC OXIDE

INTRODUCTION

The thermal decomposition of hydrocarbons, in the presence of sufficient nitric oxide to reduce the rate of reaction to a minimum, has been the subject of even more controversy than the uninhibited reaction. Although there has been some agreement that free radicals were involved in the uninhibited reaction, the very nature of the inhibited reaction has been in doubt. The view that the nitric oxide inhibited pyrolysis of ethane is almost completely free radical in nature has been confirmed in this laboratory (56) (57). The present work was carried out to see if the type of free-radical mechanism involved in the pyrolysis of ethane could be applied to that of propane.

Review of Earlier Work

Staveley (58) was the first to notice that the thermal decomposition of hydrocarbons could be inhibited with nitric oxide. He investigated the thermal decomposition of ethane at 600°C and at pressures of 50 to 500 mm., and found that the inhibited rate was 1/5 to 1/15 that of the uninhibited rate, being relatively faster at the higher pressures.

The first workers to investigate the pyrolysis of propane, inhibited by nitric oxide, were Hobbs and Hinshelwood (35). They found that, at 550°C, as more and more NO was added, the rate became smaller and smaller until, with 100 mm. propane, 14.5 mm. partial pressure of NO caused the rate to reach a limit at about 13% its original value. When the partial pressure of NO approached 50 mm. a slight acceleration was noted. They found that the shape of the inhibition curve (i.e. rate vs [NO]) could be described with the same sort of empirical expression used for ethane, for which they made a thorough investigation. On this basis they concluded that, as with ethane, the NO reacted with the radicals which would ordinarily undergo unimolecular decomposition and thus stopped the chains, leaving a residual reaction which was most likely a molecular split of the propane into an olefin and CH_4 and H_2. Later work has cast considerable doubt on the second conclusion, but the first one is still of some interest. If the NO reacted with the abstracting radical, or β radical to use the terminology of Goldfinger et al. (39), the same absolute amount of NO should be necessary to produce a minimum rate at all pressures of substrate, but if the NO reacted with the μ radical a definite proportion of NO should provide a minimum rate at any pressure of substrate. For the mechanisms considered in this thesis, the above analysis still holds.

At about the same time that Hobbs and Hinshelwood were looking at the NO inhibited reaction, Rice and Polly (59) were investigating the propylene inhibited pyrolysis of a number of organic compounds, including propane. They found that propylene inhibited the rate of pyrolysis and proposed a general free-radical mechanism for NO inhibited organic decompositions of the form:

$$M \rightarrow 2R_1$$

$$M + NO \rightarrow R_2 + HNO$$

$$R_1 + M \rightarrow R_1H + R_2$$

$$R_2 \rightarrow R_1 + M_2$$

$$R_1 + NO \rightarrow R_1NO$$

$$2R_1 \rightarrow R_1R_1$$

$$R_2 + NO \rightarrow R_2NO$$

$$R_1 + R_2 \rightarrow R_1R_2$$

where M represents the parent molecule and R_1 and R_2 are, respectively, the β and μ radicals mentioned above. This mechanism was discussed and modified by Goldansky (60), but still requires drastic modifications in order to predict the correct rates and orders. It is interesting to note that the termination and propagation steps of this mechanism are essentially those postulated by Laidler and Wojciechowski

(57) for the NO inhibited pyrolysis of ethane, and here for that of propane.

The NO inhibited pyrolysis of propane was studied by Stubbs, Ingold and Hinshelwood (35) (61) (62) (63) while investigating the inhibited and uninhibited pyrolyses of the homologous series of n-paraffins from propane to n-decane. They concluded that the NO inhibited reaction was first-order at high pressures with an activation energy of about 72 kcal. per mole. They confirmed that a constant percentage of NO was necessary to produce a fully inhibited rate at any initial pressure of propane, and stated that, at 530°C, 6% NO provided this limit. More NO was used at higher temperatures. Orders for the reaction varying from 1 to 2 were quoted but since these are usually inferred from the rate-pressure curve, their validity is somewhat suspect.

Jach and Hinshelwood (64) made a short study of the effect of inert gas on this system. However propane is mentioned only incidentally and the only inert gas used with it was sulphur hexafluoride. Since it will be shown later that SF_6 may decompose appreciably at these temperatures, their conclusion that the inhibited reaction was greatly accelerated by inert gas is open to question.

Some work has been done on the NO inhibited pyrolysis of propane using radioactive carbon as a tracer. Stevenson,

Wagner, Beeck and Otvos (65) pyrolyzed 1-^{13}C propane under these conditions and concluded that isotopic mixing took place just as rapidly when the reaction was completely inhibited as when it was uninhibited. Frey, Danby and Hinshelwood (33) have studied the pyrolysis of 1-^{14}C propane and also found that the distribution of products was the same whether the reaction was uninhibited or maximally inhibited with NO, but they still maintained that these results were consistent with a molecular mechanism for the fully inhibited reaction.

Poltorak and Voedodsky (66) have shown that, when propane and D_2 were pyrolysed together, D appeared in the hydrocarbon fraction at a rate, relative to the rate of decomposition, which was independent of the amount of NO present. NO was present up to a partial pressure 20% that of propane, so there is no question that the reaction was not totally inhibited. This is strong evidence that at least part of the totally inhibited reaction proceeds by a free-radical mechanism.

Voevodsky (27) has recently investigated the inhibited decomposition of propane using vessels coated with different types of surfaces and in vessel with varying surface to volume ratios. He concluded that at pressures of around 20 mm. the surface may have an important effect, but

that at higher pressures this effect will be less. He proposes that initiation reactions are primarily surface reactions, some of which are reversible and some irreversible, and that the latter can be completely suppressed by NO, full inhibition corresponding to complete suppresion of these reversible reactions. However, as pointed out by Laidler and Wojciechowski (57), this suggestion implies that the amount of nitric oxide required to give complete inhibition should be proportional to the surface to volume ratio, and this has not been observed. Also, since induction periods are noticed in the inhibited reaction, implying abnormally small initial rates, Voevodsky's suggestion is open to criticism. Furthermore the results of Martin et al. (28) throw some doubt on Voevodsky's experimental work.

It has been proposed by Wojciechowski and Laidler (56) that, for various hydrocarbons, a free radical mechanism may be postulated involving abstraction of an H atom from the hydrocarbon to give HNO and a radical. This radical then enters into the usual chain propagating processes and it is assumed that termination is the recombination of some radical with HNO. The equilibrium

$$H + NO \rightleftharpoons HNO$$

is also included. If the radical entering into the recombination reaction is μ, first-order kinetics overall are to

be expected; if it is β, 3/2-order kinetics are predicted. They show, quite plausibly, how these mechanisms explain the sigmoidal shape of the ΔP-time curves, the fact that different inhibitors give the same limiting rate, the effect of adding ethylene and hydrogen to the reaction mixture, the effect of adding extra NO while the reaction is in progress and, of course, the reason for deuterium mixing in the fully inhibited reactions.

The purpose of the present work is to see if the ideas of Wojciechowski and Laidler can be applied to the specific case of propane. In the following sections mechanisms are proposed along the lines of their mechanism for ethane, and experimental evidence for these mechanisms is presented.

EXPERIMENTAL

Apparatus and Method

The apparatus used was described in Part I of this thesis, and the general method was the same. Nitric oxide was Matheson C.P. grade, stated to be 99% pure. NO_2 was removed by passing the cylinder gas through a column of silica gel (T_3), and N_2 was removed by rigorous pumping at liquid nitrogen temperature followed by trap to trap distillations before the gas was stored (in V_2). Before starting a run, about 500 mm. of propane were condensed in the mixing bulb (V_4), about 70 mm.

of NO were then condensed on top of this and the stop-cock to trap T_1 closed. The reaction mixture was then warmed up and given time to mix thoroughly. When the entire contents of the bulb had warmed up, the stop-cock to T_1 (250 ml.) was opened up, in the hope that the sudden rush of gases would aid mixing.

Results

Preliminary experiments, carried out at a number of temperatures and pressures, showed that complete inhibition was obtained with 10% NO at lower temperatures and about 12% at higher temperatures. Most of the experiments carried out later were with 15% NO.

The inhibited pyrolysis of propane was investigated in the temperature range 560 to 640°C and at partial pressures of propane from 25 to 550 mm. A typical plot of ΔP against time is shown in figure 13. It is seen that the curve is sigmoidal in shape and that two rates may be calculated from two slopes, one drawn at the initial point of the curve and the other at the inflexion point. The induction period was lengthened considerably as the propane pressure was lowered; it was also shortened somewhat when large excesses of nitric oxide were added.

In figure 14 the logarithms of the initial and inflexion rates in the unpacked vessel are plotted against

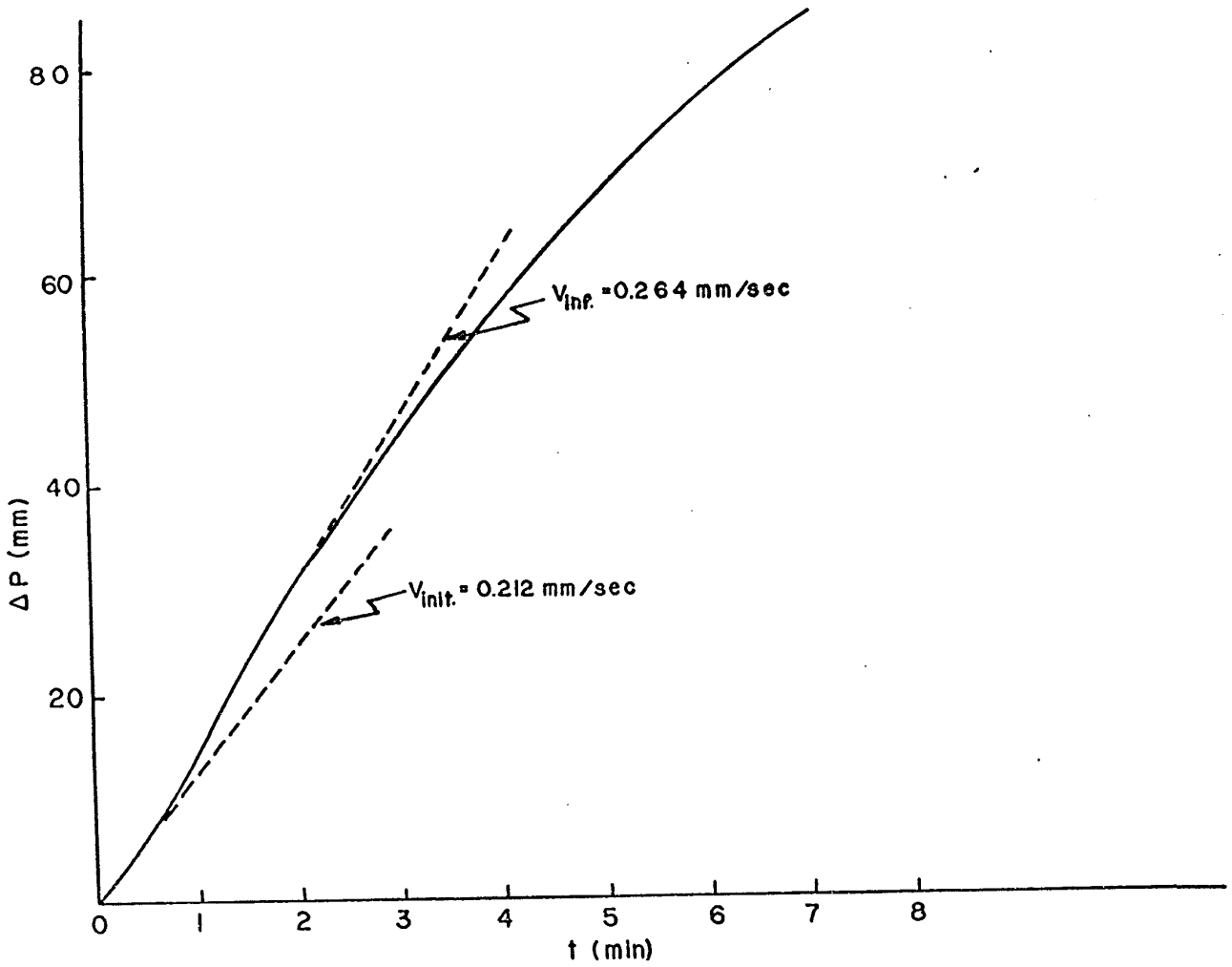

Figure 13 A typical ΔP-time curve for the nitric oxide inhibited pyrolysis of propane. Propane pressure = 282 mm; nitric oxide pressure = 41 mm. Temperature = 600°C.

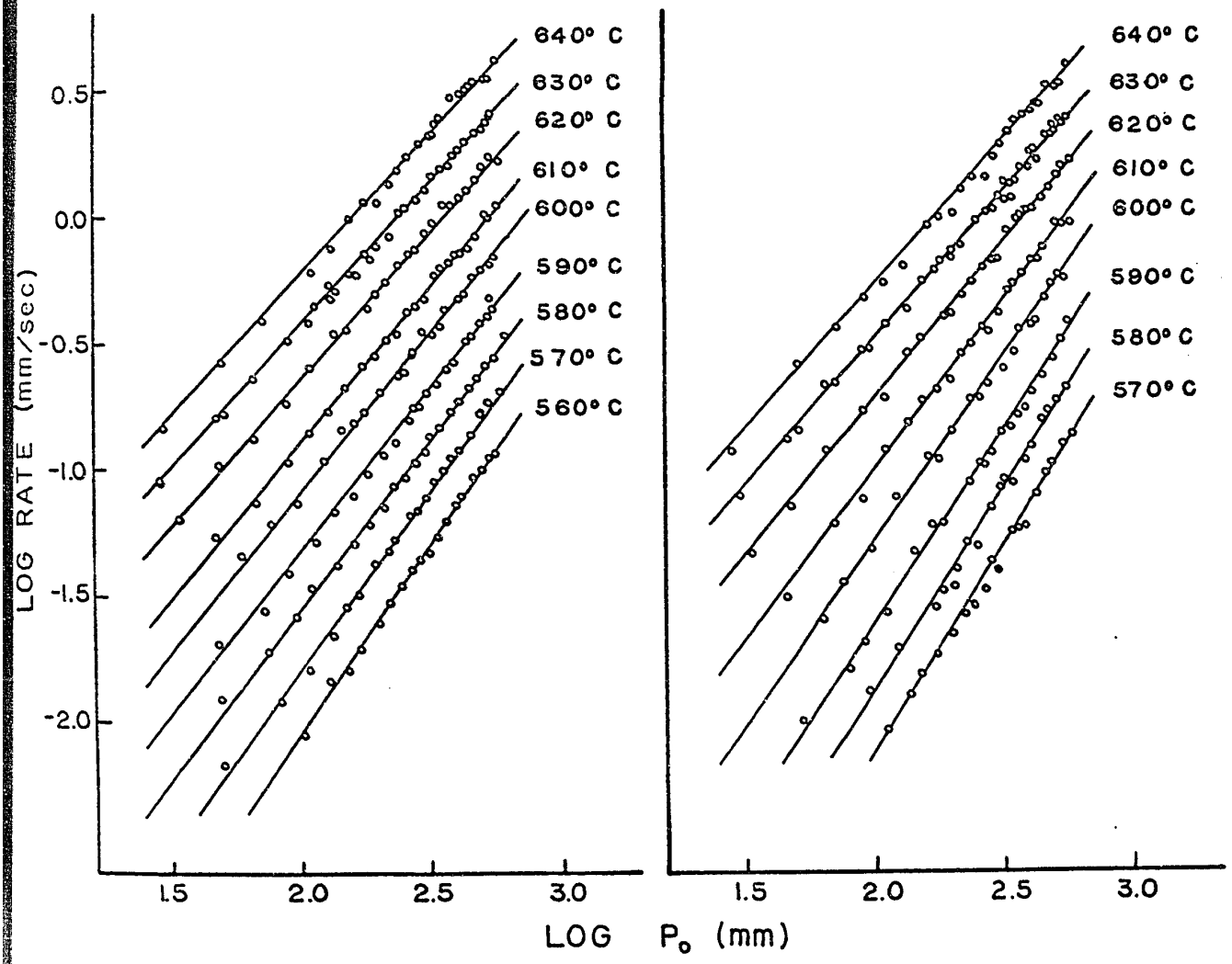

Figure 14 Plot of log rate against log P for the inhibited pyrolysis of propane, rates being those measured in the unpacked vessel. The left hand plot gives initial rates, the right hand plot gives rates measured at the inflexion point.

the logarithm of the pressure. The slopes of such lines give the over-all order for the reaction, and table 7 lists the orders for the inflexion point rates at various temperatures. It is seen that inflexion orders are almost unity at the highest temperatures and increase steadily as the temperature is lowered. The initial rates are 3/2-order at most temperatures and are lowered somewhat at the highest temperatures. In figure 15, the inflexion and initial rates in the unpacked vessel are compared directly at a typical temperature. It is seen that the rates approach each other at the higher pressures, signifying that the induction period has become much shorter. Figure 16 shows a comparison of the uninhibited rate with the inflexion rate of the inhibited reaction. It is easily seen that the order of the inhibited reaction is higher, confirming the fact that the 'chain lengths', or ratios of uninhibited to inhibited rates, increase with decreasing pressure as reported by Hobbs and Hinshelwood (35).

Figure 17 shows the first-order rate constants for the inflexion point rates at 630 mm. plotted against the reciprocal of the absolute temperature to yield Arrhenius parameters. High pressure rate constants of Hobbs and Hinshelwood (35) and of Ingold, Stubbs and Hinshelwood (36) are also included for comparison. The first-order rate constant in the high pressure region may be given as

Table 7

Reaction Order at the Inflexion Point

T°C	Order	T°C	Order
560	1.50	610	1.23
570	1.50	620	1.19
580	1.37	630	1.15
590	1.33	640	1.14
600	1.24		

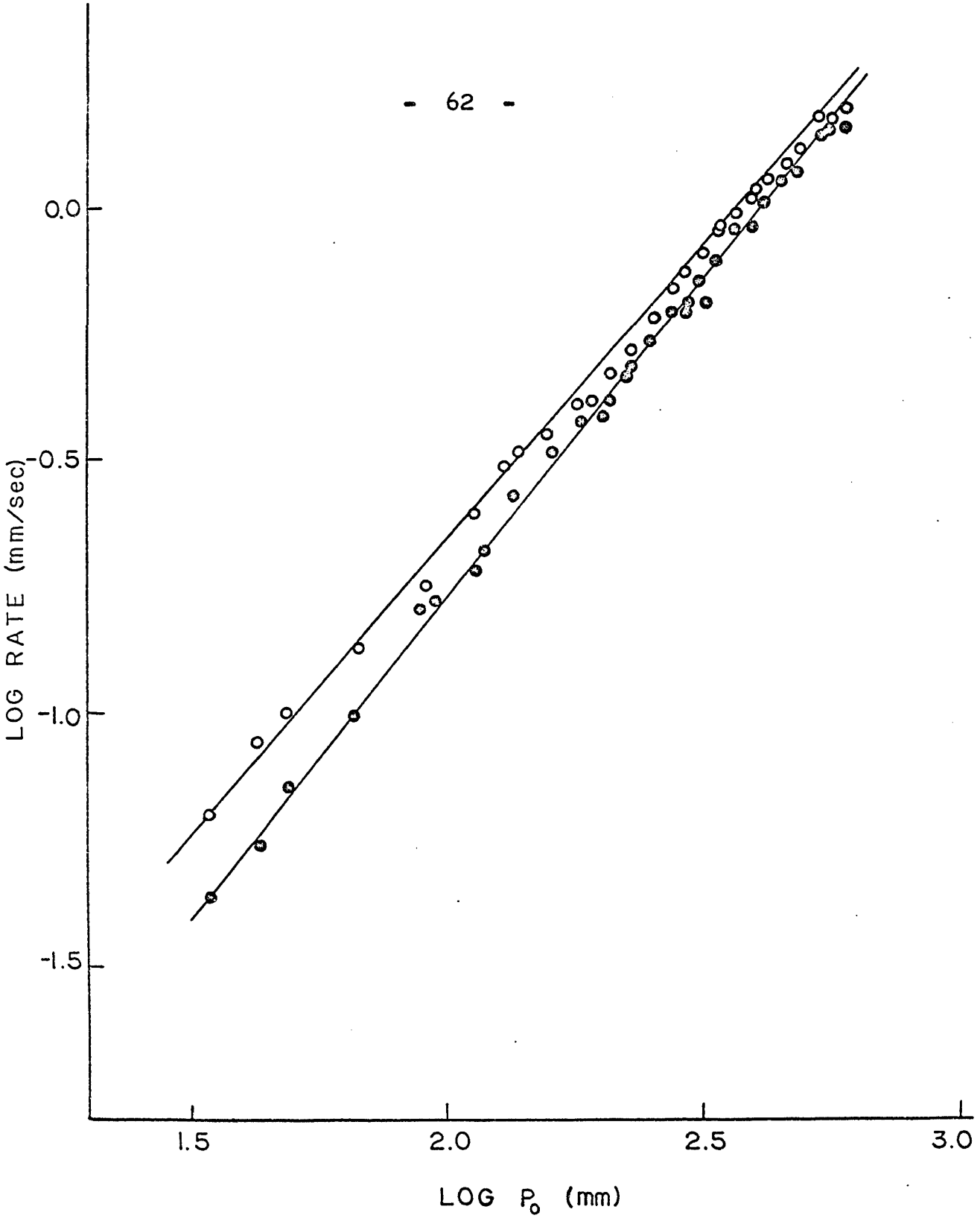

Figure 15 Comparison of initial (o) and inflexion point (0) rates at 620°C for the inhibited pyrolysis of propane.

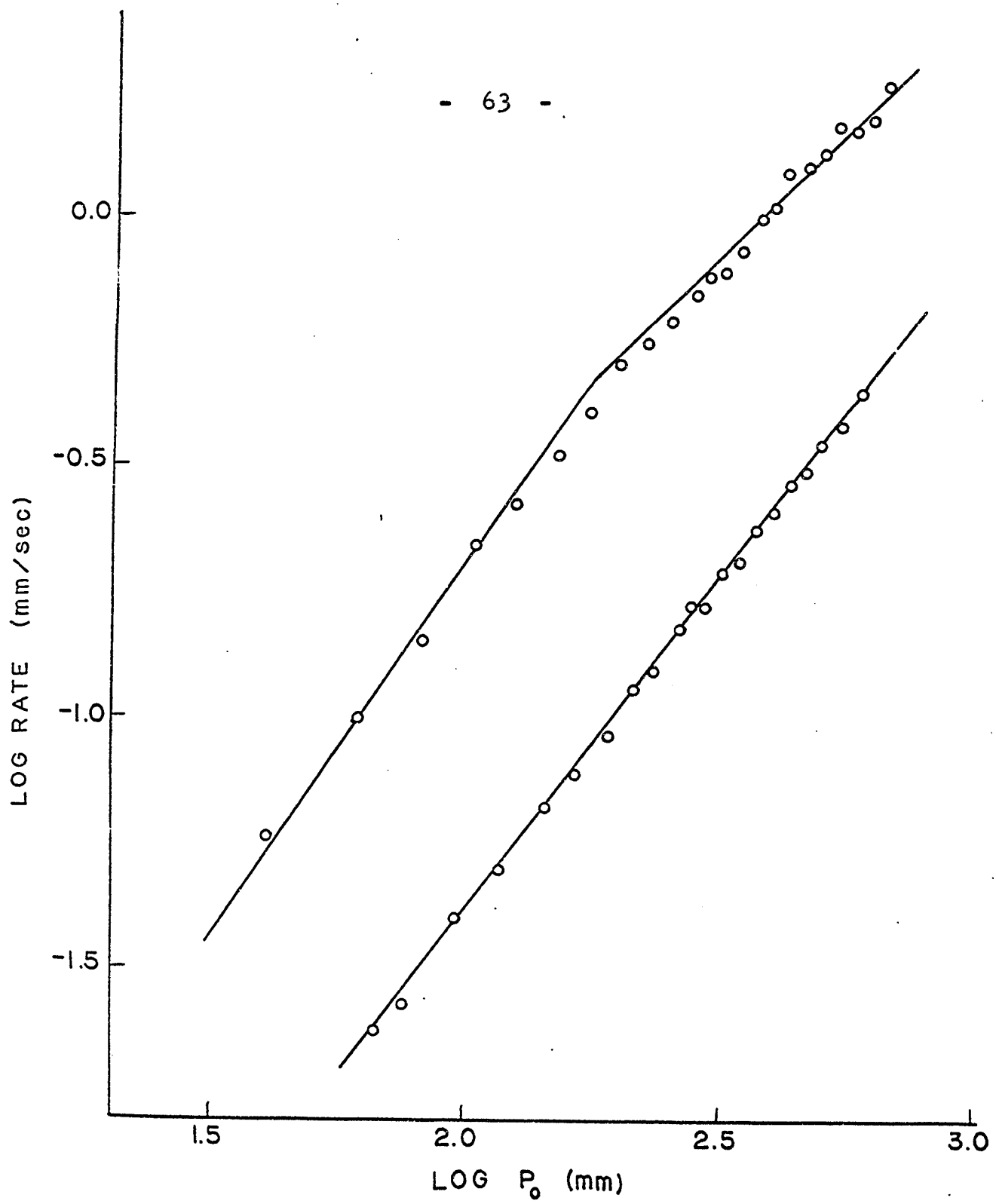

Figure 16 Comparison of uninhibited and inflexion point inhibited rates at 490°C for the pyrolysis of propane. The uninhibited rates are given by the upper set of points, the inhibited by the lower.

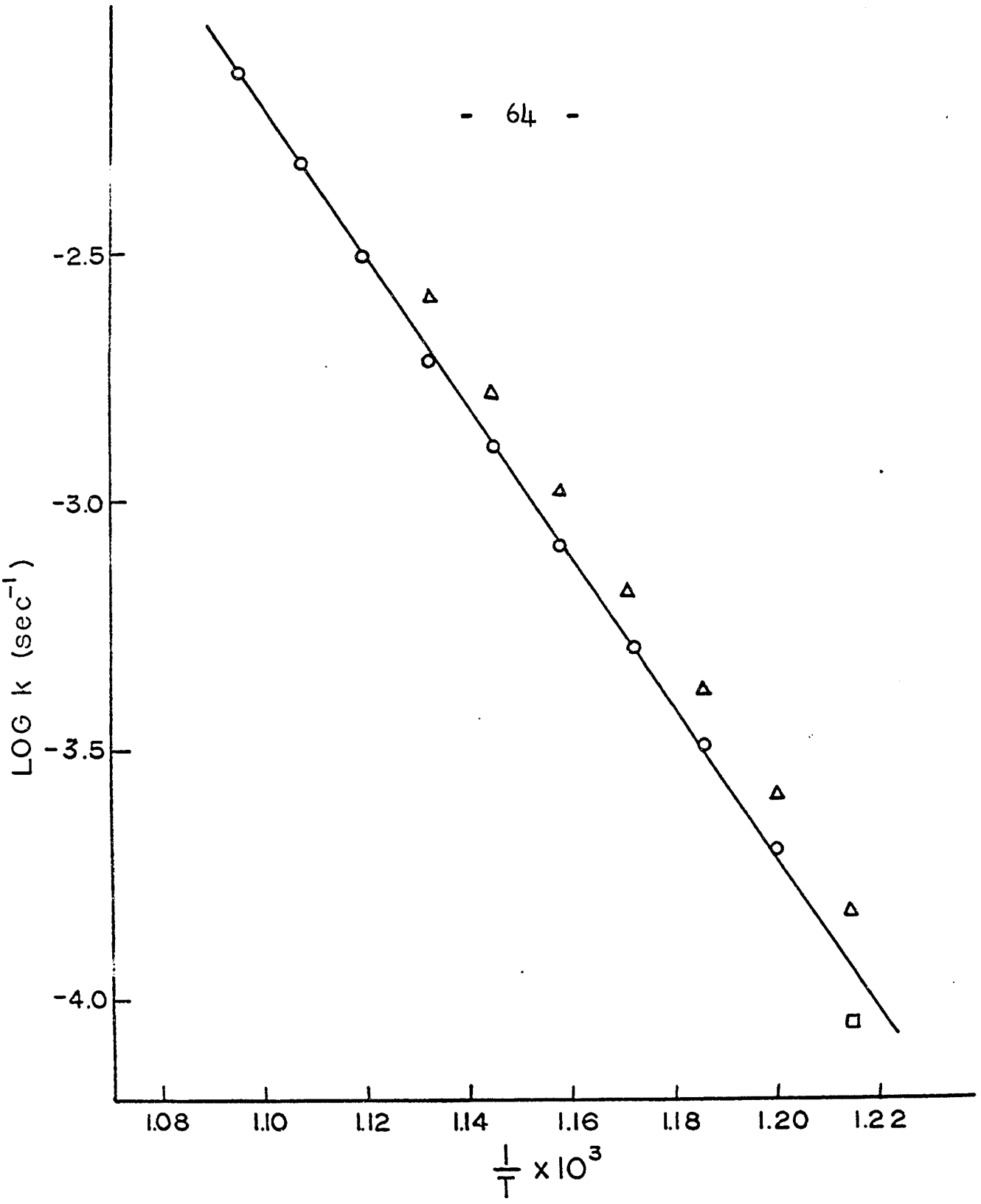

Figure 17 Arrhenius plot for the inhibited pyrolysis of propane, rate constants being those obtained at high pressure. Results of this investigation are shown as O, those of Ingold, Stubbs and Hinshelwood (36) as Δ and that of Hobbs and Hinshelwood (35) as □ .

$$k_1 = 2.99 \times 10^{14} e^{-69,400/RT} \text{ sec}^{-1}$$

Figures 18 and 19 deal with the rate of reaction in the packed vessel. Figure 18 shows a plot of the logarithms of the inflexion point rates against the logarithm of the pressure. As in the unpacked vessel, the order is close to unity at higher temperatures and increases as the temperature is lowered. In the packed vessel initial rates were not too reproducible. Figure 19 gives a comparison of rates in the packed and unpacked vessels, in the form of the logarithm of the rate at 630 mm. plotted against the reciprocal of the absolute temperature. It is seen that the rate in the packed vessel is somewhat lower, but the activation energy is virtually unchanged, being 69.9 kcal. per mole.

The effect of added inert gas (CO_2) is shown in figure 20. It can be seen that, to within the experimental error, CO_2 does not increase the rate of reaction, even when partial pressures 4.4 times those of propane are used. Jach and Hinshelwood (64) have shown that SF_6 can accelerate the inhibited reaction, so an attempt was made to duplicate their work. However, analyses of the products by gas chromatography showed several new unidentified peaks and the reaction reached a very different pressure equilibrium. Therefore the kinetic results using SF_6 as an 'inert gas' were not used. Figure 21 shows the results of analyses of products. It may be seen that

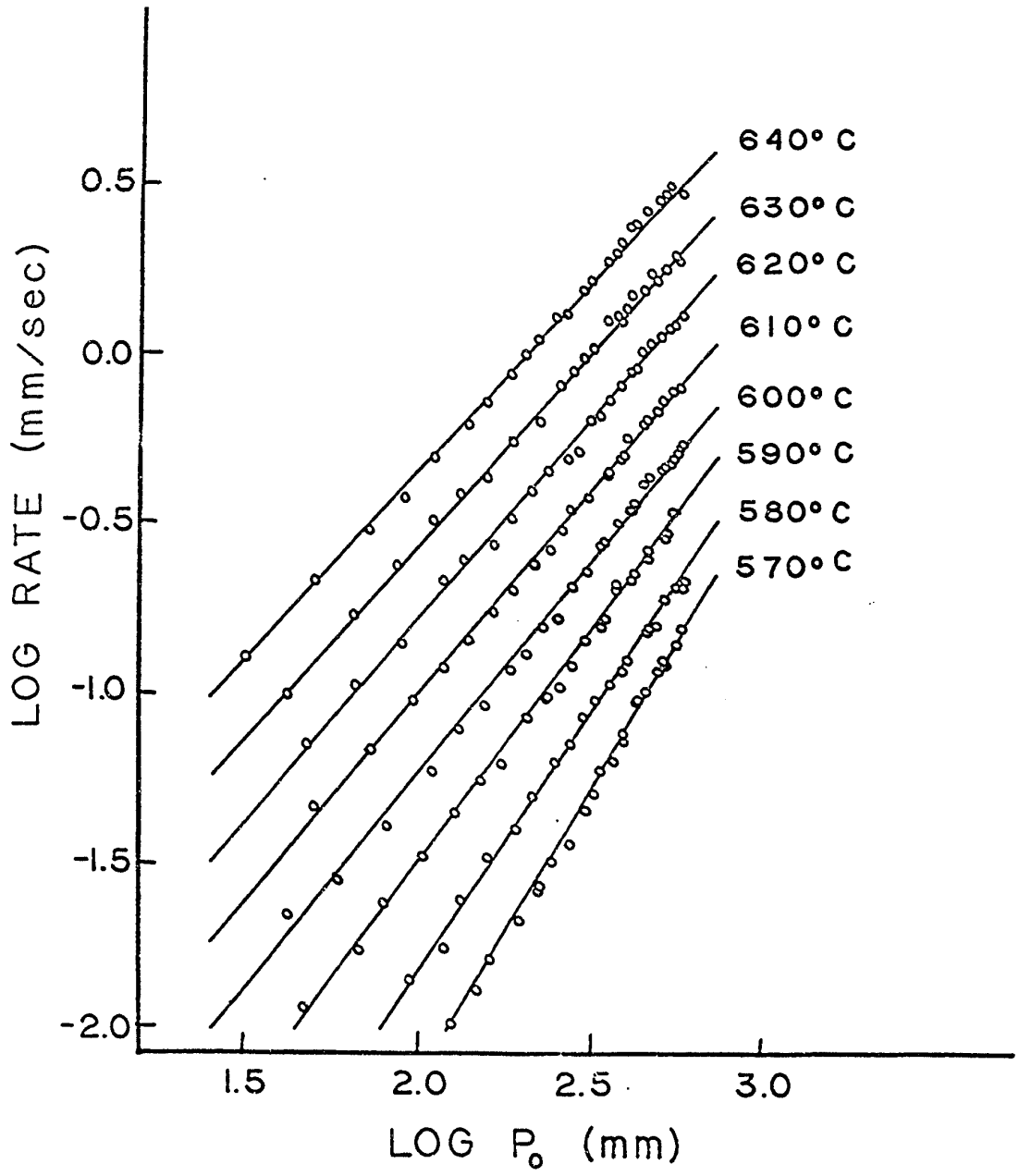

Figure 18 Plots of log rate against log P for the inhibited pyrolysis of propane, rates being those measured in the packed vessel.

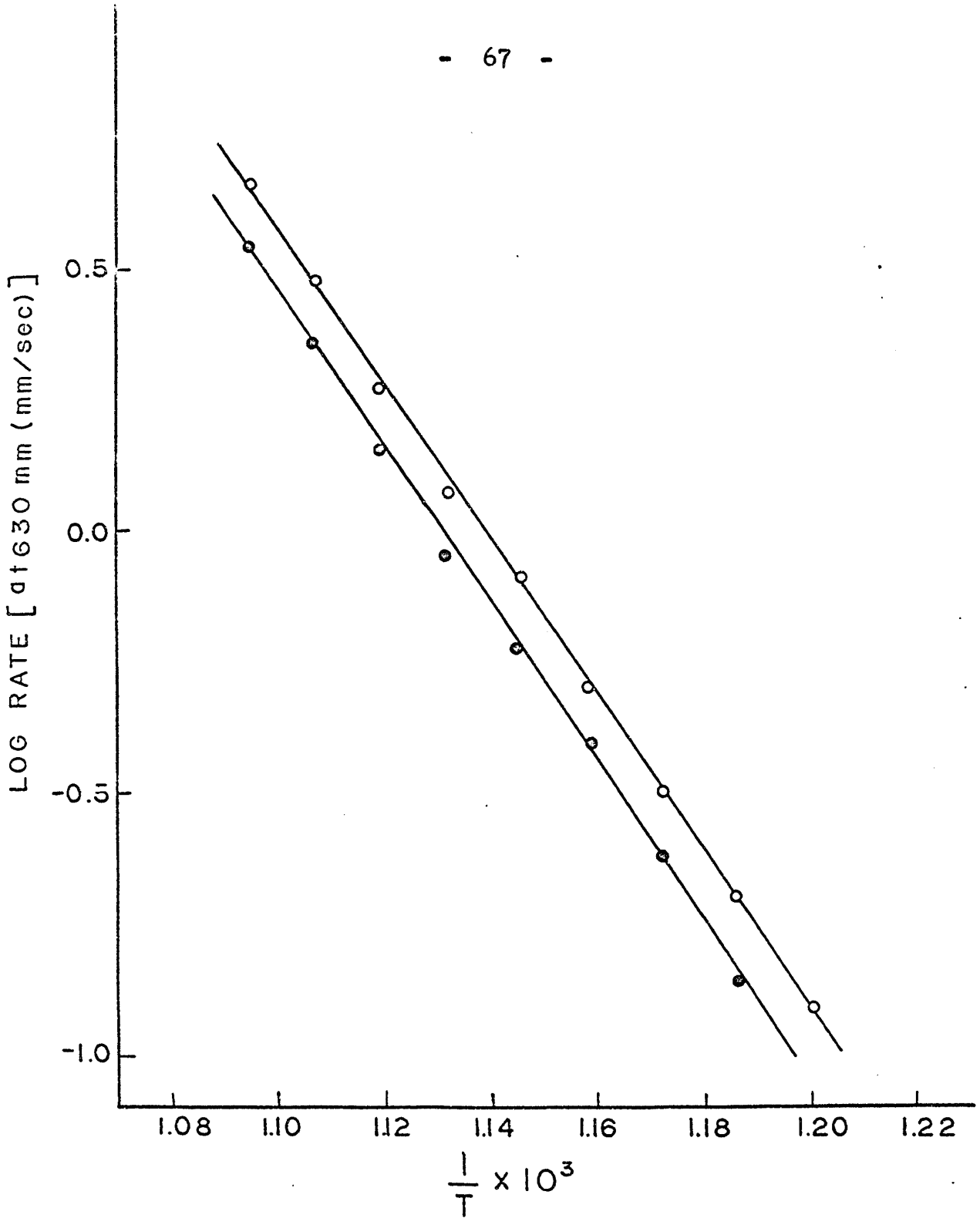

Figure 19 Comparison of rates of the inhibited pyrolysis of propane at high pressure measured in the unpacked (O) and packed (●) vessels.

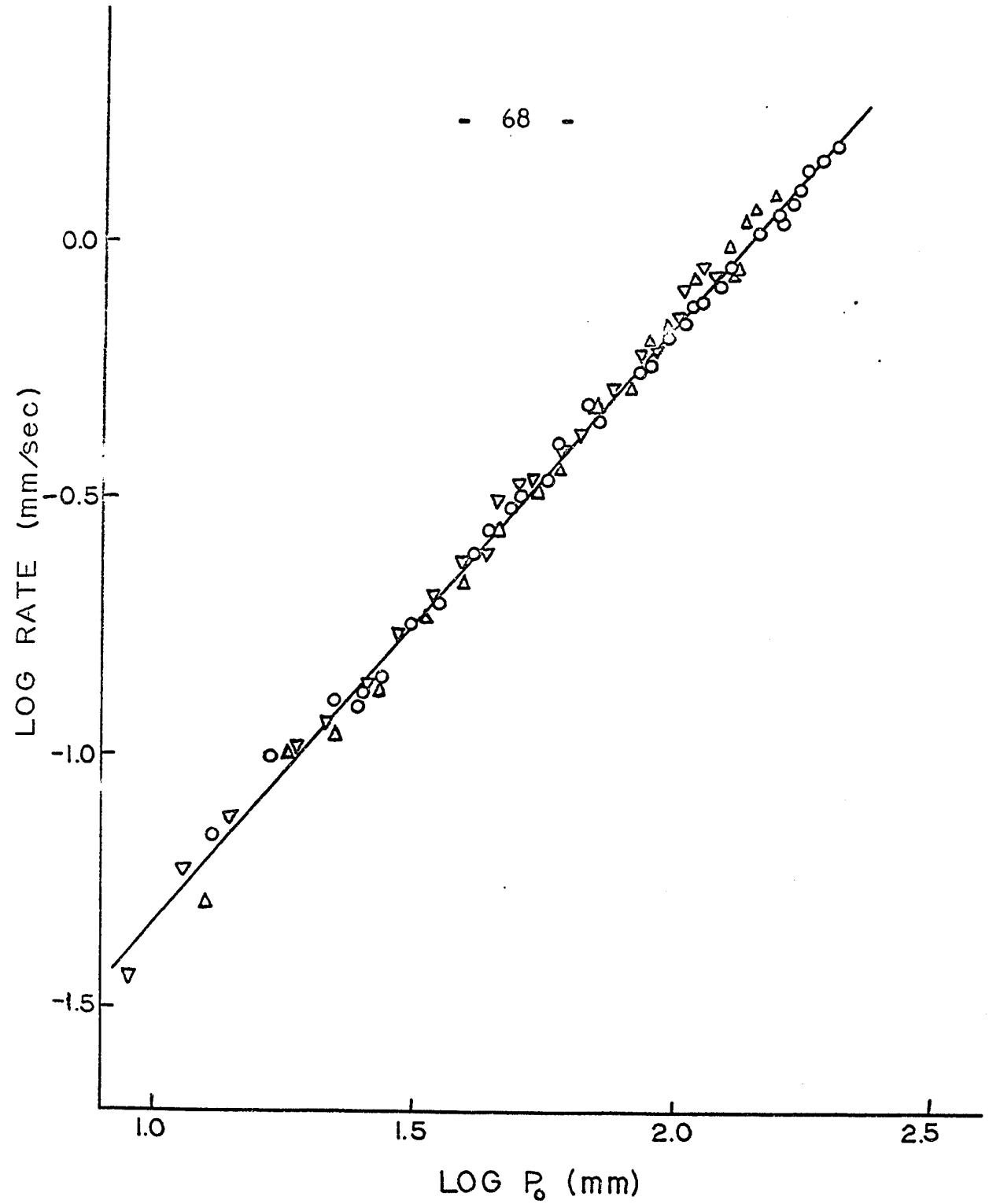

Figure 20 The effect of carbon dioxide on the inhibited pyrolysis of propane at 650°C. Rates measured with no added CO_2 are shown as O, with CO_2/C_3H_8 = 2.0 as Δ and with CO_2/C_3H_8 = 4.4 as ∇ .

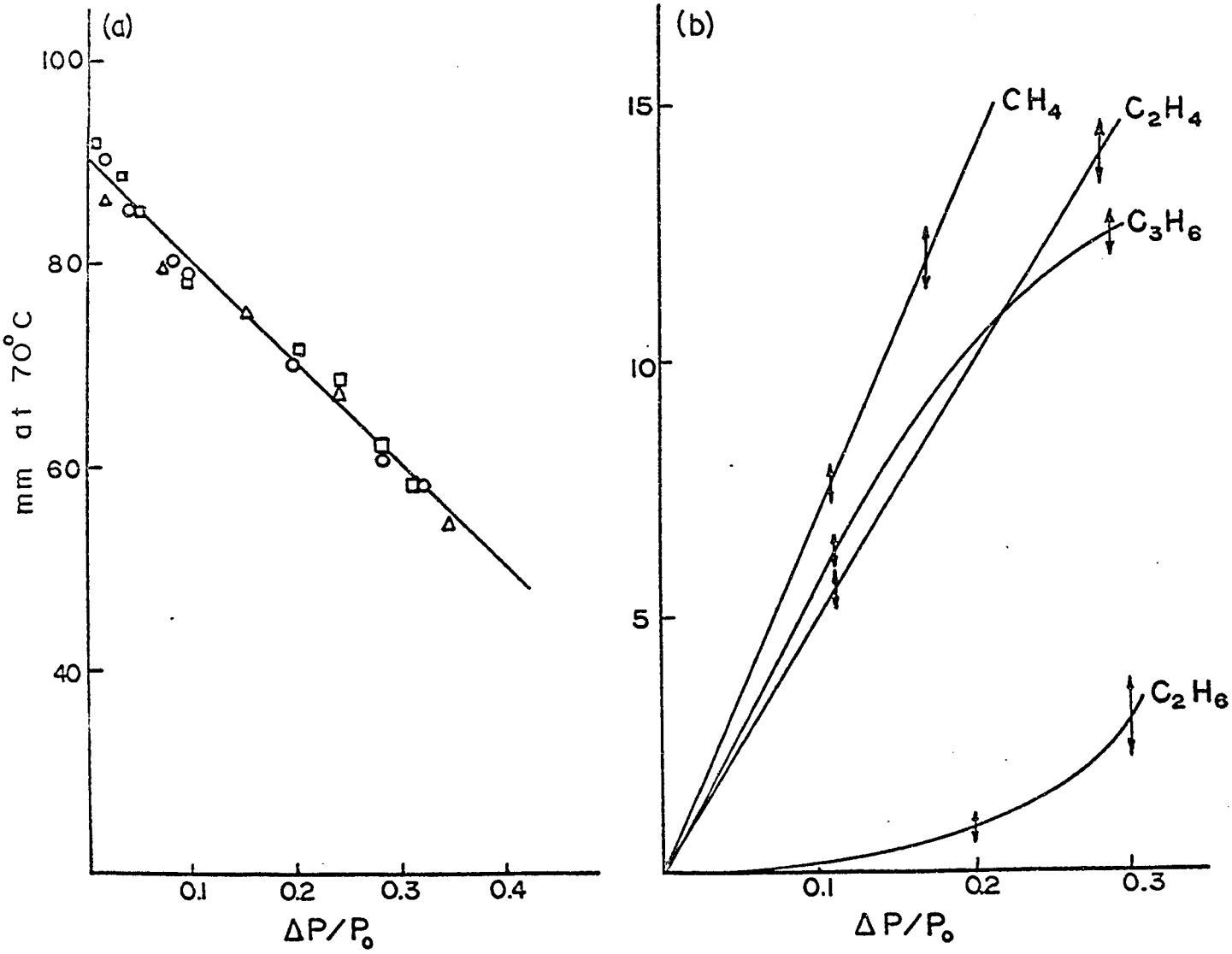

Figure 21 Analytical results for the inhibited pyrolysis of propane. The left hand plot (21a) shows the correlation between the pressure increase and amount of propane consumed at 570°C (□), at 600°C (Δ) and at 630°C (0). The right hand plot (21b) shows the relative rate of formation of several products.

the products are much the same as those of the uninhibited reaction and unit increase in total pressure is seen to correspond to unit decrease in the partial pressure of propene.

The increasing order of the inflexion rates on lowering the temperature may be ascribed to the lengthening of the induction periods as the pressures are lowered, thus removing the inflexion points further and further from initial conditions. Since it is assumed that once the reaction has passed the inflexion point the steady-state has been achieved, attempts were made to extrapolate the ΔP-time curves back to an 'initial' condition. Figure 22 shows a number of these initial rates compared with the measured inflexion-point rates. It is seen that the magnitude of the corrections is such as to bring the order close to unity.

DISCUSSION

Mechanism of the Fully Inhibited Reaction

It has been suggested by Rice and Polly (59) and by Laidler and Wojciechowski (56) (57) that NO reacts with a paraffin to produce HNO and a radical. Following this suggestion, it is postulated that initiation occurs by

$$(12) \qquad C_3H_8 + NO \longrightarrow C_3H_7 + HNO$$

The chain propagating steps are then the same as postulated

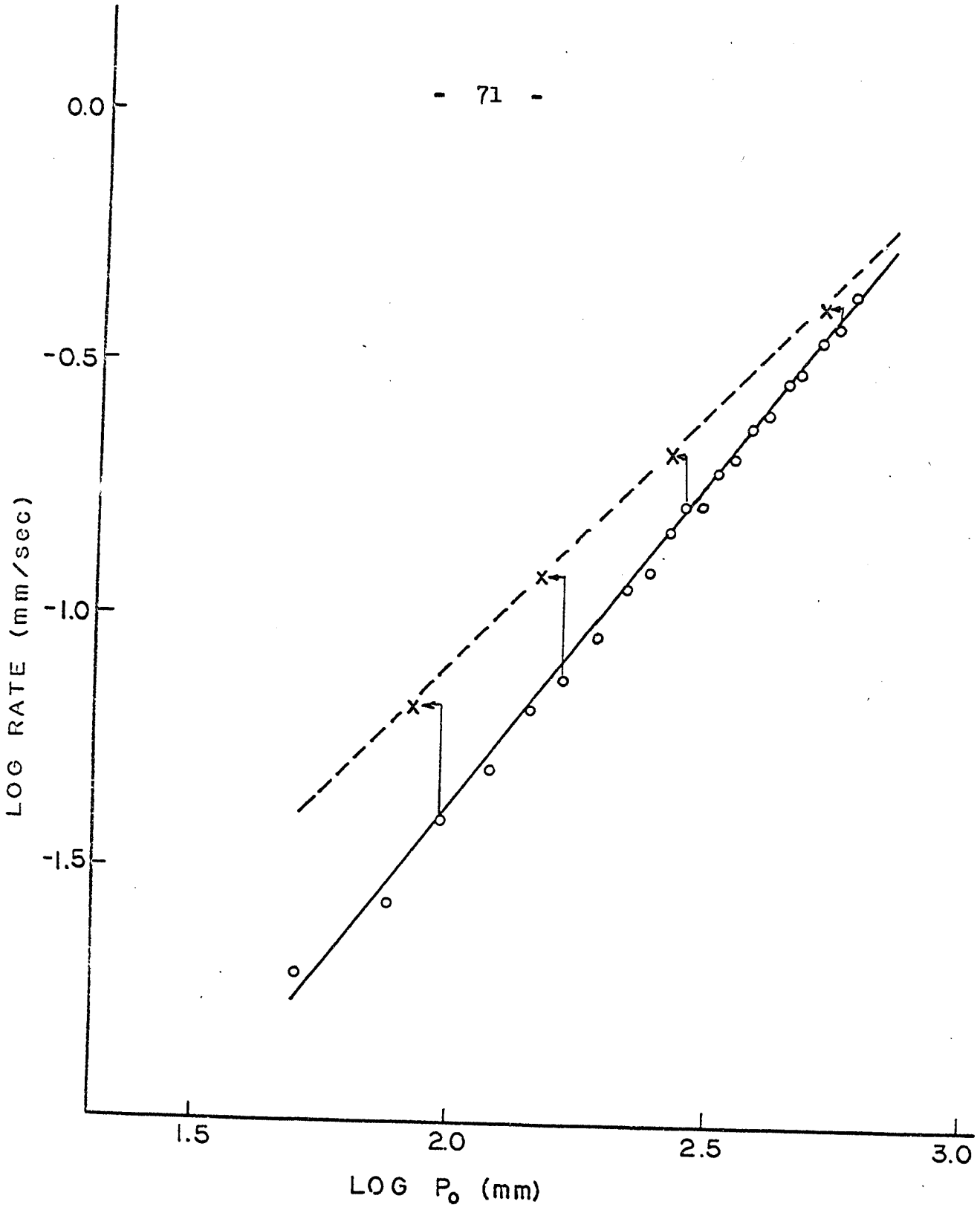

Figure 22 Inflexion point rates at 590°C (O) for the inhibited pyrolysis of propane extrapolated to initial time (X).

for the uninhibited reactions i.e. reactions 3 through 6. HNO is capable of dissociating into H + NO, and H unites with NO to form HNO. It has been shown by Clyne and Thrush (67) that both the forward and backward reactions require a third body. Initially this will be C_3H_8. In order for the over-all reaction order to be unity, termination must occur by the reaction of HNO with C_3H_7. Other equilibria such as

$$CH_3 + NO \rightleftharpoons CH_3NO$$

$$C_3H_7 + HNO \rightleftharpoons C_3H_7NO$$

undoubtedly occur, but these will not effect the kinetics of the reaction. The reaction mechanism thus becomes:

(12) $C_3H_8 + NO \longrightarrow C_3H_7 + HNO$

(5) $C_3H_7 \longrightarrow CH_3 + C_2H_4$

(6) $C_3H_7 \longrightarrow H + C_3H_6$

(3) $H + C_3H_8 \longrightarrow H_2 + C_3H_7$

(4) $CH_3 + C_3H_8 \longrightarrow CH_4 + C_3H_7$

(13) $X + H + NO \longrightarrow HNO + X$

(14) $X + HNO \longrightarrow H + NO + X$

(15) $C_3H_7 + HNO \longrightarrow C_3H_8 + NO$

When the steady-state treatment is applied to this scheme, the following concentrations of radicals are obtained:

$$[H] = \left(\frac{k_6 k_{12} k_{14}}{k_3 k_{13} k_{15}}\right)^{1/2} \qquad [23]$$

$$[CH_3] = \frac{k_5}{k_4}\left(\frac{k_3 k_{12} k_{14}}{k_6 k_{13} k_{15}}\right)^{1/2} \qquad [24]$$

$$[C_3H_7] = \left(\frac{k_3 k_{12} k_{14}}{k_6 k_{13} k_{15}}\right)^{1/2} [C_3H_8] \qquad [25]$$

The HNO concentration is

$$[HNO] = \left(\frac{k_6 k_{12} k_{13}}{k_3 k_{14} k_{15}}\right)^{1/2} [NO] \qquad [26]$$

The rate of reaction is given by

$$V_1 = (k_5 + k_6)\,[C_3H_7] \qquad [27]$$

Therefore

$$V_1 = (k_6 + k_6)\left(\frac{k_3 k_{12} k_{14}}{k_6 k_{13} k_{15}}\right)^{1/2} [C_3H_8] \qquad [28]$$

This mechanism gives first-order kinetics over all agreeing with the experimental behavior at high temperatures.

The initial rates are 3/2-order at most of the lower temperatures. This is attributed to the fact that the steady state has not yet been attained, that the concen-

tration of C_3H_7 has not reached its equilibrium level, and that termination is largely the result of of a combination of HNO with β radicals. If reaction 15 is removed from the mechanism and the following terminations substituted

(16) $H + HNO \longrightarrow H_2 + NO$

(17) $CH_3 + HNO \longrightarrow CH_4 + NO$

the initial rate becomes

$$V_{3/2} = (k_5+k_6)\left(\frac{k_4}{k_5}\right)\left(\frac{k_{12}k_{14}}{2k_{13}k_{16}}\right)^{1/2}[C_3H_8]^{3/2} \qquad [29]$$

The Initiating Step

Clement and Ramsay (68) have shown that the upper limit for the dissociation energy of HNO is 48.6 kcal. per mole, and Clyne and Thrush (67) have shown that reaction 13,

(13) $X + H + NO \longrightarrow HNO + X$

has a negative activation energy of 0.7 ± 0.3 kcal. per mole at 600°K. Thus 48.0 is a good value for the dissociation energy of HNO. If the bond strength of C_3H_7-H is taken as 97 kcal. per mole (38), then 51 kcal. per mole would be a good estimate for the activation energy of reaction 12. The frequency factor is taken as 10^{14}.

If the rate of initiation for the mechanism proposed

here is compared with that for the uninhibited reaction (V_{1a}), the ratio of rates becomes

$$\frac{V_{1a}}{V_{12}} = \frac{k_{1a}}{k_{12}} \frac{[C_3H_8]}{[NO]} \qquad [30]$$

If $[C_3H_8] = 8\,[NO]$, this ratio is close to unity at 600°C, showing that initiation of chains by this means is quite plausible.

Chain Propagating Steps

As shown in figure 21, the products of the inhibited reaction are virtually idential with those of the uninhibited reaction. Thus the same considerations apply here as applied for the uninhibited reaction.

Clyne and Thrush (67) found that the rate constant for reaction 13 was 4.8×10^{15} ml^2 mole^{-2} sec^{-1} at 21°C when the third body was hydrogen. The rate constant listed in table 8 for a temperature of 600°C was calculated using the Hinshelwood-Kassel-Rice-Ramsperger theory, as described in part I, using $s = 3$. The collision number, Z, was also calculated, and was used to estimate the frequency factor of reaction 14 at 600°C, using the same theory.

Chain Terminating Steps

It has been noted that in fully inhibited hydro-

Table 8

Kinetic Parameters for Reactions of Inhibited Propane Pyrolysis

Reaction	A*	E(kcal/mole)	k_{600}*	Reference
3	1.0×10^{12}	8.2	8.85×10^{9}	calc. from (48)
4	1.0×10^{13}	8.5	7.45×10^{10}	calc. from (49)
5	8.0×10^{13}	31	1.39×10^{6}	(38)
6	1.3×10^{14}	37	7.12×10^{4}	(38)
7(a)		[-16.5]	1.3×10^{19}	calculated
12	1.0×10^{14}	49	54.3	estimated
13	3.16×10^{14}	0	3.16×10^{14}	calc. from (67)
14	2.1×10^{16}	48.0	2.17×10^{4}	calc. from (67)
15	1.0×10^{12}	0	1.00×10^{12}	estimated
16	5.0×10^{12}	0	5.00×10^{12}	estimated from (67)
17	2.0×10^{12}	0	2.00×10^{12}	estimated

* Frequency factors and rates are in sec^{-1}, ml. $mole^{-1}$ sec^{-1} or ml^{2} $mole^{-2}$ sec^{-1}.

carbon pyrolyses, nitric oxide is not used up quickly and must therefore be regenerated in the over-all mechanism. Two likely processes for this are reactions 15 and 16.

$$(15) \qquad C_3H_7 + HNO \longrightarrow C_3H_8 + NO$$

$$(16) \qquad H + HNO \longrightarrow H_2 + NO$$

Comparing the rates of these two reactions

$$\frac{V_{15}}{V_{16}} = \frac{k_{15}}{k_{16}} \frac{[C_3H_7]}{[H]} = \frac{k_3}{k_6} \frac{k_{15}}{k_{16}} [C_3H_8] \qquad [31]$$

These two rate are equal when

$$[C_3H_8] = \frac{k_6}{k_3} \frac{k_{16}}{k_{15}} \qquad [32]$$

which, at 600°C, is at a pressure of the order of the experimental range. In view of the assumptions inherent in estimating the individual rate constants, this is considered satisfactory.

The ratio of the rates of termination by reaction (15) in the fully inhibited reaction and by reaction (7a) in the uninhibited reaction is

$$\frac{V_{15}}{V_{7a}} = \frac{k_{15}}{k_{7a}} \frac{[HNO][C_3H_7]}{[CH_3][C_3H_7][C_3H_8]} = \frac{k_4k_6k_{13}k_{15}}{k_3k_5k_{7a}k_{14}} \frac{[NO]}{[C_3H_8]} \qquad [33]$$

With 12.5% NO at 600°C this gives rise to the ratio 155.

Termination by this scheme is therefore quite fast compared with that proposed for the uninhibited reaction. It can be seen from this that, although initiation will occur in the inhibited reaction by the same mechanism as in the uninhibited, i.e. by reaction 1a as well as reaction 12, termination is almost all by reaction 15, and it is largely by a change in the termination step that the inhibited mechanism takes over from the uninhibited mechanism as more and more NO is added.

The Induction Period

It is seen in figure 13 that the ΔP-time curve is sigmoidal in shape, implying the existence of an induction period. The initial rate, corresponding to pre-steady-state conditions is of the 3/2 order in that part of the temperature range where a rather well-defined induction period exists. It was suggested above that the concentration of C_3H_7 had not reached its equilibrium value, and that termination was by the recombination of HNO and a β radical; this termination leads to 3/2-order kinetics.

It is also to be noted that the rates at the inflexion point are proportional to the pressure at the highest temperatures, but that the order increases as the temperature is lowered. This may be explained by noting that, at lower temperatures, the induction periods become longer and the inflexion points move further from the initial

conditions. In order to test this hypothesis, an empirical expression was fitted to the ΔP-time curve covering a region well beyond the inflexion point. This expression was used to extrapolate back to initial time, and an 'initial' rate was calculated. The results of these extrapolations are shown in figure 22, and it may be seen that the magnitude of the corrections is sufficient to bring the order back almost to unity.

Mechanism in the Presence of Other Inhibitors

It was shown by Laidler and Wojciechowski (57) that an inhibited mechanism of the type proposed for ethane will give the same limiting rate for any inhibitor that is capable of undergoing the same type of free-radical mechanism. This is also true for the propane decomposition. In the rate equation, the expression $k_{12}k_{14}/k_{13}k_{15}$ corresponds to the equilibrium constant K for the reaction

$$C_3H_8 \rightleftharpoons C_3H_7 + H$$

The rate expression then reduces to

$$v_1 = (k_5 + k_6)\left(K\frac{k_3}{k_6}\right)^{1/2}[C_3H_8] \qquad [34]$$

and contains only constants that do not depend in any way on the nature of the inhibitor.

Activation Energy and Rate Constant

Using the same method employed in part I to estimate an activation energy for (k_5+k_6), the activation energy corresponding to the proposed mechanism is

$$E = \tfrac{1}{2}(E_5 + E_6) + \tfrac{1}{2}(E_K + E_3 - E_6) \qquad [35]$$

where E_K is the energy change for the equilibrium

$$C_3H_8 \rightleftharpoons C_3H_7 + H,$$

and is equal to $E_{12} + E_{14} - E_{13} - E_{15}$. Using the values of the activation energies listed in table 8, the value of E is found to be 68.1 kcal. per mole. This is in excellent agreement with the experimental value of 69.4 kcal. per mole, especially when the uncertainties in the value of E_5 are taken into account.

In the same way the frequency factor is calculated to be

$$A = \left(\frac{A_3A_5A_{12}A_{14}}{A_{13}A_{15}}\right)^{1/2} = 4.6 \times 10^{14} \text{ sec}^{-1} \qquad [36]$$

The experimental value is 2.99×10^{14} sec^{-1}. Absolute rate constants are also in good agreement; at 600°C the experimental value is 1.35×10^{-3} sec^{-1}, the calculated 7.26×10^{-3} sec^{-1}.

Effect of Surface

The effect of increasing the surface to volume ratio is to lower the rate of reaction somewhat, although the order and activation energy remain approximately the same. The effect of packing was less marked than with the uninhibited reaction. In order to explain the results it is suggested that surface sites act very much like nitric oxide molecules and abstract hydrogen atoms from the substrate, as mentioned in part I. It is therefore easy to see why the effect of packing the vessel is less marked in the inhibited reaction, since adding surface to the uninhibited reaction is equivalent to adding a small amount of inhibitor. If a reaction is already proceeding by an inhibited mechanism, the effect of providing more surface should be relatively smaller.

Effect of Inert Gas

Carbon dioxide, which does not enter chemically into the reaction, has no effect on the rate of the inhibited reaction. This behavior is consistent with the mechanism proposed. Inert gases are involved in establishing the equilibrium

$$X + H + NO \rightleftharpoons HNO + X$$

but act in the same way on the reaction in both directions and have no resultant effect. Reactions 5 and 6 are presumed to be in the high-pressure first-order regions, so that no inert gas effect is observed in either the inhibited or uninhibited reactions. The apparent effect of sulphur hexafluoride on the kinetics of the reaction, observed by Jach and Hinshelwood (64), was seen above not to be a true inert gas effect, since this substance undergoes chemical reaction.

CONCLUSIONS

It has been shown that free radicals are involved in the nitric oxide inhibited decomposition of propane. A mechanism has been postulated to account for the experimental variation of the rate with pressure and temperature and, although certain details may not be quite correct, it is felt that the overall principles of abstraction of H atoms by NO and termination involving HNO are sound. An attempt has also been made to explain the induction periods and the effect of other inhibitors and surface. The rate constants for the inflexion rates at high pressure are given by

$$k_1 = 2.99 \times 10^{14} e^{-69,400/RT} \text{ sec}^{-1}.$$

Part III

THE UNINHIBITED PYROLYSIS OF n-BUTANE

INTRODUCTION

After the pyrolysis of propane had been studied it seemed natural that the pyrolysis of n-butane should be the next subject for investigation. There are, however, a number of other reasons for studying the pyrolysis of this hydrocarbon. Earlier work, reviewed in the following section, had shown that hydrogen atoms were not important chain carriers in this system, and so a different type of mechanism was necessary. Also, n-butane has been the chief hydrocarbon used in studies of hydrocarbon pyrolyses done after 1958 when renewed interest developed in this subject. It therefore seemed wise at this time to study the over-all kinetics of the reaction and to try to present a mechanism explaining these new results. Finally, as with propane, n-butane is an industrially important gas, and a detailed knowledge of its behavior on pyrolysis is definitely of economic value.

Review of Earlier Work

The first data on the thermal decomposition of n-butane were obtained by Pease (1) and Pease and Durgan (3). They established that the reaction was largely homogeneous

and approximately first-order although the first-order rate constants decreased as the pressure was lowered. The activation energy was around 65 kcal. per mole and the reaction could be represented by

$$C_4H_{10} \rightarrow C_4H_8 + H_2$$

$$C_4H_{10} \rightarrow C_3H_6 + CH_4$$

$$C_4H_{10} \rightarrow C_2H_4 + C_2H_6$$

Further work by Hurd and Spence (69) showed that only the last two reactions were important in the pyrolysis of n-butane, and Cambron (70) postulated that the reaction

$$C_4H_{10} \rightarrow 2C_2H_4 + H_2$$

also occurs.

Other early work included that of Frey and Hepp (8) who investigated the reaction at 575°C and made analyses by low-temperature distillation. Two additional runs done at 425°C gave a first-order rate constant

$$k = 3.4 \times 10^{13} \; e^{-61,400/RT} \; sec^{-1}$$

Analytical work was also done by Marek and Neuhaus (71) (72). Their results were in excellent agreement with the predictions of the Rice theory, which is discussed below.

Paul and Marek (7) were among the first to obtain

data on the temperature dependence of the reaction, and in the range 550 to 610°C found the first-order rate constants to be given by

$$k = 1.12 \times 10^{17} \; e^{-73,900/RT} \; sec^{-1}$$

The extremely large pre-exponential factor throws considerable doubt on their value for the activation energy. One source of error in their work was the use of a pre-heater held at so high a temperature that almost 20% of the reaction occurred there.

All the above-mentioned work was done in flow systems. A thorough investigation of the kinetics of the reaction, using a static system, was made by Steacie and Puddington (73). They worked at temperatures from 513 to 572°C and pressures of 50 to 600 mm., and obtained first-order rate constants, extrapolated to infinite pressure, of

$$k = 5.13 \times 10^{12} \; e^{-58,700/RT}$$

Since the reaction is now believed to be free-radical in nature, rather than molecular, the extrapolation to infinite pressure is probably meaningless. Analytical results showed that the reaction products were, initially, about 1/3 CH_4, 1/3 C_3H_6, 1/6 C_2H_4 and 1/6 C_2H_6, with slightly more C_2H_4 being produced than C_2H_6. Hydrogen was found to be less than 1% of the products and butenes were not detected.

Echols and Pease (74), also working with a static

system, found the reaction to be complicated and to have an over-all order of about 1.3, with an activation energy of about 58 kcal. per mole. They postulated a mechanism involving termination by the recombination of ethyl radicals, leading to 3/2-order kinetics. Analytical results showed that pressure increase was a satisfactory measure of the extent of reaction.

The history of the development of free-radical mechanisms parallels that of propane. While the above mentioned work was in progress on the over-all kinetics of the reaction, other people were developing free-radical mechanisms for the pyrolysis of n-butane.

It was shown by Rice, Johnston and Evering (13) that free radicals could be detected in the high-temperature decomposition of n-butane and Rice and Johnston (14) later showed that the activation energy for the split into free radicals was 65.4 kcal. per mole. Rice and Rice (75) proposed the following partial free-radical mechanism:

$$C_4H_{10} \longrightarrow CH_3 + n\text{-}C_3H_7$$

$$C_4H_{10} \longrightarrow 2C_2H_5$$

$$n\text{-}C_3H_7 \longrightarrow C_2H_4 + CH_3$$

$$C_4H_{10} + R \longrightarrow RH + n\text{-}C_4H_9$$

$$\longrightarrow RH + C_2H_4 + C_2H_5$$

$$C_4H_{10} + R \longrightarrow RH + S\text{-}C_4H_9$$

$$\rightarrow \quad RH + C_3H_6 + CH_3$$

where R is CH_3 or C_2H_5.

This partial mechanism leads to the equation

$$3\ C_4H_{10} \quad \rightarrow \quad 3\ C_2H_4 + 3\ C_2H_6$$

$$4\ C_4H_{10} \quad \rightarrow \quad 4\ C_3H_6 + 4\ CH_4$$

in reasonable agreement with experiment. The scheme ignores the small amount of hydrogen produced, and since no termination steps are proposed, no conclusions are reached about the overall order of the reaction. This original mechanism has been somewhat altered by other authors such as Steacie (48), Semenov (54) and Benson (76). Various terminating steps (76) of the type

$$C_2H_5 + C_2H_5 \quad \rightarrow \quad \text{products}$$

or

$$CH_3 + CH_3 \quad \rightarrow \quad C_2H_6$$

are often used and since both ethyl and methyl radicals are β (in the terminology of Goldfinger, Letort and Niclause (39)) these terminating reactions lead to 3/2-order kinetics over all.

Belchetz and Rideal (18), investigating the decomposition of butane at low pressures on a carbon filament found a much higher activation energy (93.2 kcal. per mole)

for the primary split than did Rice and co-workers (13). However, as in the propane case, it is likely that the presence of the carbon filament made comparison of their results with those of other workers impossible. Robertson (77) detected only ethyl radicals in the decomposition of butane near a platinum filament at 1050°C. His results are also likely complicated by heterogeneous processes. The presence of radicals in the ordinary decomposition of n-butane has been confirmed by Hurd and Azorlosa (78) who found that after pyrolyzing $CH_3CH_2CH_2CH_2D$, the butane remaining contained less deuterium than the original starting material.

It has been well established that the decomposition of n-butane can be sensitized by certain substances at a temperature below that normally necessary for appreciable reaction. Heckert and Mack (79) found that n-butane was 'cracked' by decomposing ethylene oxide. Frey (80) found that as little as 1% dimethyl mercury at 525°C could set up chains twenty molecules long. Echols and Pease (21) later repeated the work on the sensitizing action of ethylene oxide on n-butane. They found that the chain length was appreciable (i.e. Δ 10) only when the pressure of hydrocarbon was at least eight times that of ethylene oxide. Sickman and Rice (22) also found that n-butane was decomposed by radicals formed from decomposing azomethane. More recently Marzius, Markovich and Neiman (81) decomposed diethyl peroxide in the

presence of n-butane at temperatures up to 529°C. They did not detect any sensitizing effect which as Steacie (48) says "seems rather surprising". Bryce and Ruzicka (82), working at 506°C, found that allyl radicals formed from decomposing diallyl were also capable of sensitizing the pyrolysis of n-butane.

The effect of other additives was studied by Stepukhovich and his co-workers (24) (25) (26). They investigated the effects of added acetylene, allene and bivinyl on the reaction and found that its rate was unaffected by all three. This was taken as evidence that hydrogen atoms are not important chain carriers in the case of n-butane. However, in view of the new theory of inhibition proposed by Wojciechowski and Laidler (56), his reasons for reaching this conclusion are, perhaps, unsound.

Crawford and Steacie (83), working at one temperature (442°C), did an analytical study of the products of the reaction at pressures from 40 to 130 mm. Only H_2, CH_4, C_2H_4 and C_2H_6 were analyzed for quantitatively, and no significant variation of products was noted over the pressure range. At these lower pressures, they found that the amount of ethane, relative to ethylene, was decreased considerably, and that the orders for the rate of formation of all products were above unity.

A few experiments on the pyrolysis of n-butane alone

were done by Engle, Compt, Letort and Niclause (84). They found that the over-all order at moderate pressures was about 1.4. Much of the work of this group has been concerned with the pyrolysis of hydrocarbons to which small amounts of oxygen have been added (85), greatly accelerating the reaction.

A number of important papers on the thermal decomposition of n-butane have appeared recently. The effect of various surfaces was studied in some detail by Purnell and Quinn (86). They followed the rate by analysing the reaction mixture after one minute residence time, using a gas chromatographic technique. They concluded that any 'conditioning' which deposited a carbon layer on a reaction vessel increases the rate of the heterogeneous mode of termination of the free radical chains, and thus recommended that pyrolyses are best carried out at low conversions in clean reaction vessels.

An analytical study of the products of the reaction was recently carried out by Stepukhovich, Kosyreva and Petrosyan (87), who obtained extremely reproducible, consistent results. They confirmed the results of earlier workers that the products were about 30% of both CH_4 and C_3H_6, about 14% C_2H_4, 12% C_2H_6 and about 6% of both hydrogen and butenes. It should be noted that their yields for hydrogen and butenes are somewhat higher than those of other workers, and that their ratio of C_2H_6/C_2H_4 is closer to that of Steacie and Puddington (73) than to that of Crawford and Steacie (83). They also

detected about 4% of propane, which they ascribe to the chain termination being

$$CH_3 + C_2H_5 \longrightarrow C_3H_8.$$

Kuppermann and Larson (88) have recently presented data on the thermal decomposition of n-butane. Although their work is concerned mainly with the mechanism of the nitric oxide inhibited decomposition, and thus will be discussed in part IV of this thesis, nevertheless some work was done on n-butane alone. Extensive analytical work was carried out; their results agreed largely with those of Crawford and Steacie (83), the ratio of C_2H_6/C_2H_4 being between 0.7 and 0.5. They expressed the first-order rate constants as

$$k = 1.74 \times 10^{10} \; e^{-52,500/RT}$$

Thus their A and E are both significantly lower than those of other workers. Packing the vessel and adding carbon dioxide had little effect on this reaction rate. Their work also leads to a ratio of rate constants for the abstraction of a primary hydrogen atom from butane compared to that of a secondary one, by the same radical, as

$$\frac{k_p}{k_s} = 2.43 \; e^{-2,640/RT}$$

In numerous studies, such as those of Steacie and

Folkins (89), or Stubbs and Hinshelwood (61), a few runs have been done with n-butane alone while investigating the thermal decomposition of n-butane inhibited with nitric oxide. These results will be considered in part IV.

EXPERIMENTAL

Apparatus and Method

The apparatus was described in part I, and it was used in exactly the same way. Except for runs done to look for special surface effects, all data were obtained from vessels cleaned by three washings with concentrated nitric acid at 60°C, followed by rinsing with distilled water (86). Following such treatment runs were made only to very low conversion so that the surface remained clean.

The n-butane used was obtained from the Phillips Petroleum Company (Research Grade) and was stated to be 99.90% pure. Accordingly, it was used without further purification except for one bulb-to-bulb distillation and rigorous degassing.

The Perkin-Elmer Vapor Fractometer was again used for analyses. For analyses of C_1 to C_3 hydrocarbons and n-butane a two-meter silica gel column at 60°C was used. Butenes were analyzed using a three-meter column consisting of 30% (w/w) 2,5-hexanedione on firebrick (30-60 mesh).

Results

The pyrolysis of n-butane was studied in the temperature range 520 to 590°C and at pressures of 30 to 600 mm. The pressure change was followed automatically with time by the photo-pen recorder as described in part I, and a typical result is shown in figure 23. It may be seen that there is an extremely short induction period, but that it is too short to allow the measurement of initial rates. The rates of reaction were calculated from slopes drawn manually at the inflexion point, such a slope being the highest that could be drawn to a given curve.

Figure 24 shows the results of a number of runs in both packed and unpacked vessels. The rates are plotted logarithmically against the logarithm of the initial pressure, so that the over-all order of the reaction can be obtained. In the unpacked vessel this order is close to 3/2, but in the packed vessel is slightly lower. Table 9 lists the 3/2-order rate constants obtained in the unpacked vessel and table 10 lists the rates at 200 mm. in the packed vessel.

A comparison of rates in the packed and unpacked vessels at 550°C is shown in figure 25. It is immediately apparent that the order in the packed vessel is less than 3/2, and that the rate is somewhat lower, even at the lowest pressures used.

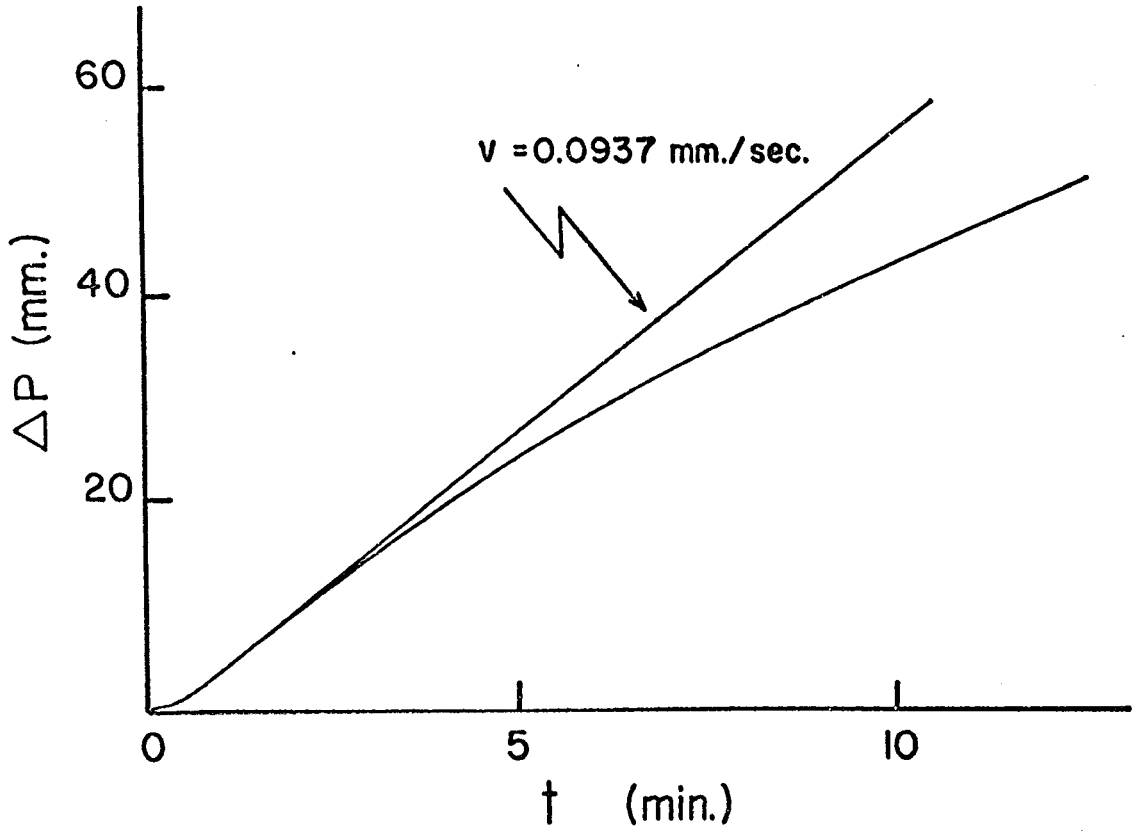

Figure 23 A typical pressure-time curve. Temperature = 530°C, initial butane pressure = 386 mm., unpacked vessel.

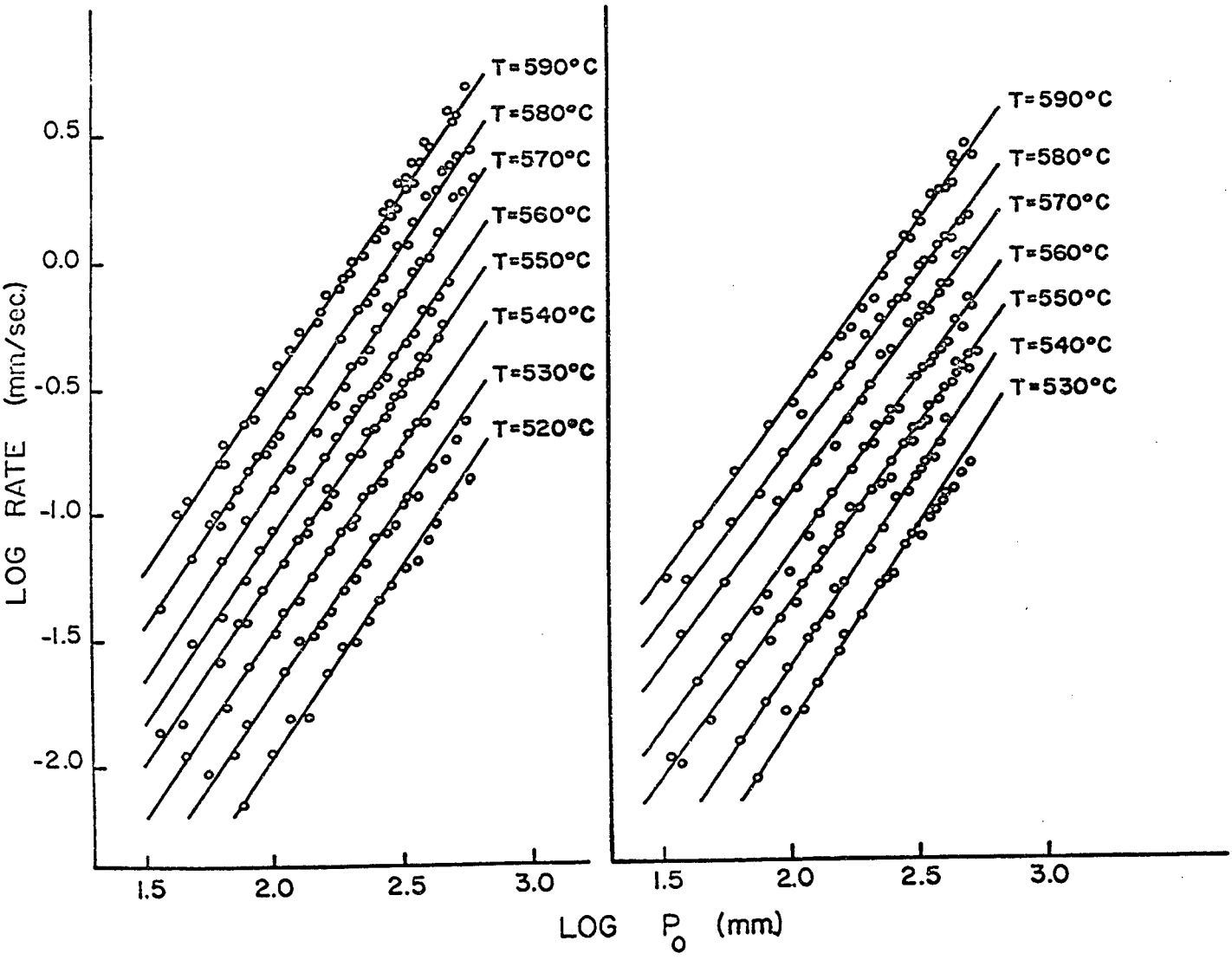

Figure 24 Logarithmic plots of rate against pressure. The left-hand plots are for the unpacked vessel, the right-hand ones for the packed vessel.

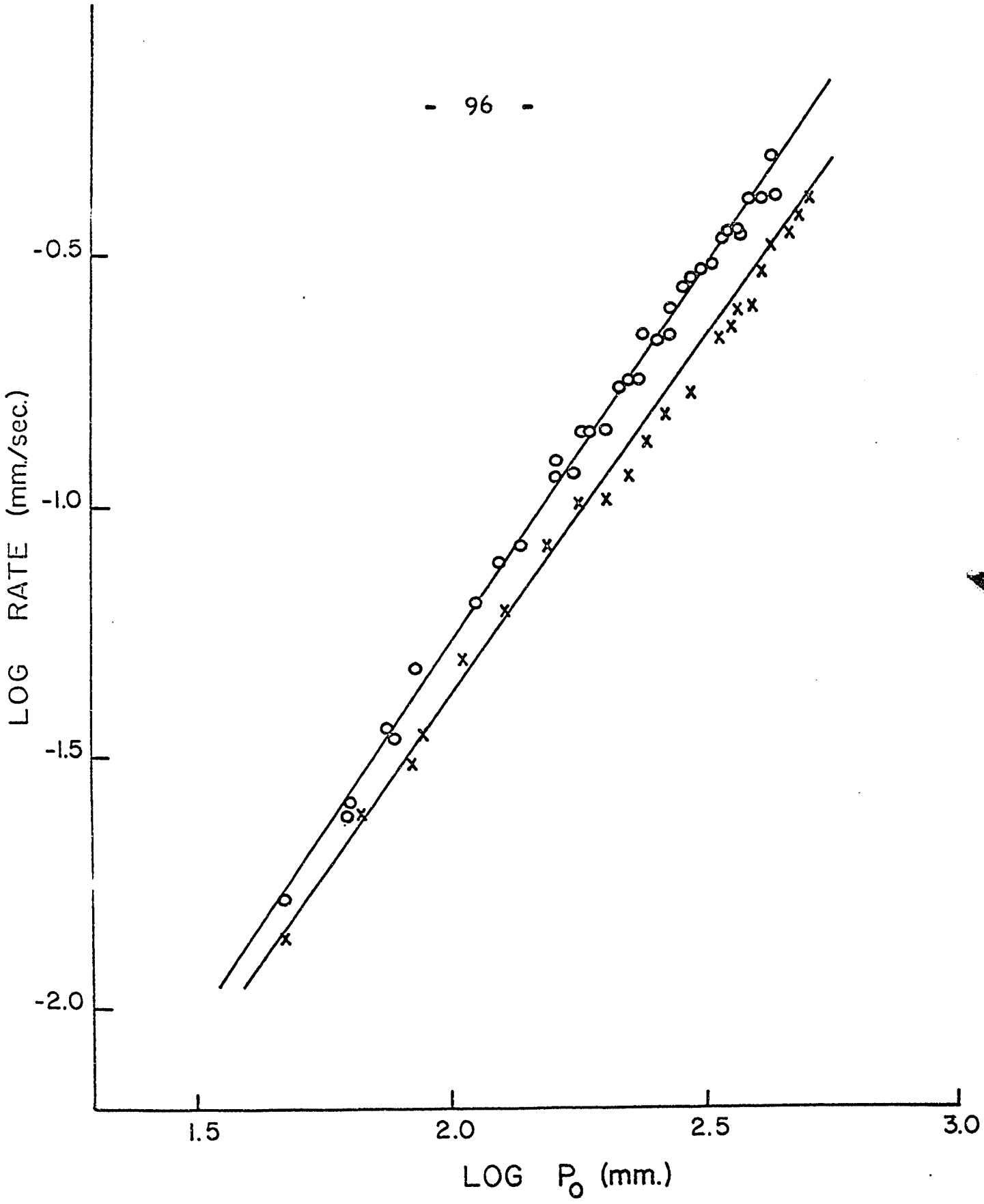

Figure 25 Rates in the packed (X) and unpacked (O) vessel at 550°C., plotted logarithmically against the initial pressure of butane.

Table 9

3/2-Order Rate Constants in the Unpacked Vessel

T°C	$10^5 k$ ($mm^{-1/2} sec^{-1}$)
520	1.093
530	1.94
540	3.29
550	5.50
560	7.92
570	13.02
580	20.4
590	32.5

Table 10

Rates at 200 mm. Initial Pressure in the Packed Vessel

T°C	10^2 rate (mm/sec)
530	4.32
540	7.24
550	10.97
560	16.80
570	28.05
580	43.7
590	70.5

In figure 26, the logarithms of the 3/2-order rate constants are plotted against the reciprocals of the absolute temperatures. This gives an activation energy of 59.9 kcal. per mole. The results of other workers such as Steacie and Puddington (73), Echols and Pease (74) and Frey and Hepp (8) are included for comparison. Since these authors occasionally expressed their rates as first-order high-pressure rate constants, rates have been calculated at 760 mm. ($\log P \approx 2.88$) and the appropriate 3/2-order rate constants then deduced.

Figure 27 shows the effect of adding carbon dioxide to the reaction at 580°C. Within the experimental error, it may be seen that a $2\frac{1}{2}$ fold excess of this gas caused no increase in the rate of reaction.

Figure 28 shows the effect of packing the reaction vessel, and of conditioning it by pyrolyzing 300 mm. of n-butane for 48 hours. It is seen that the reaction is quite sensitive to the state of the surface, and it is noted that almost any change from a clean unpacked vessel tends to raise the activation energy.

Finally, figure 29 gives some of the analytical results. Figure 29(a) shows that unit decrease in butane pressure corresponds closely to unit increase of total pressure, while 29(b) gives graphically the production of two important saturates, CH_4 and C_2H_6. Table 11 shows more of the analytical

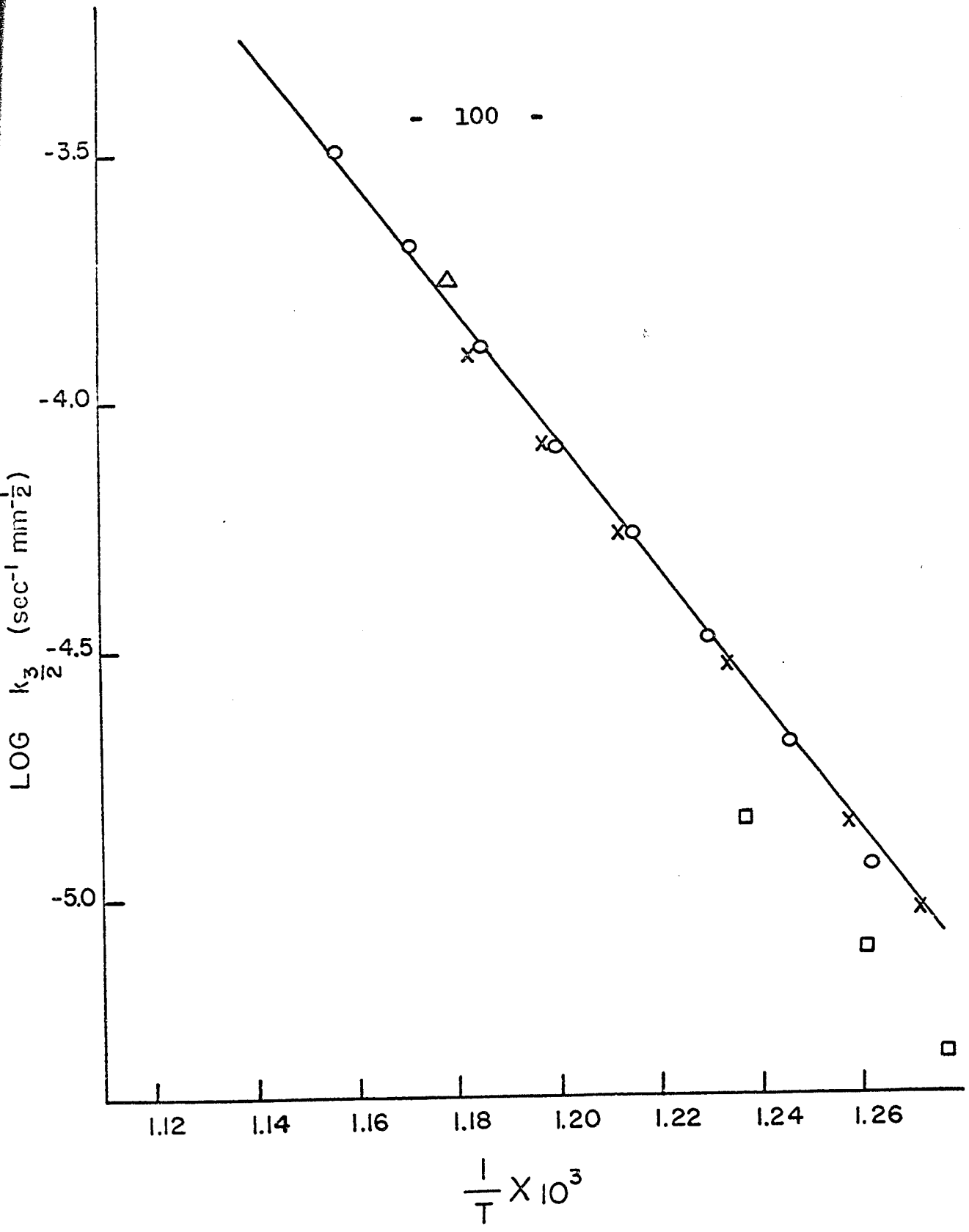

Figure 26 Arrhenius plot of the 3/2-order rate constants for the uninhibited pyrolysis of n-butane. The results of this investigation are shown as O, those of Steacie and Puddington (73) as X, those of Echols and Pease (74) as □ and that of Frey and Hepp (8) as Δ.

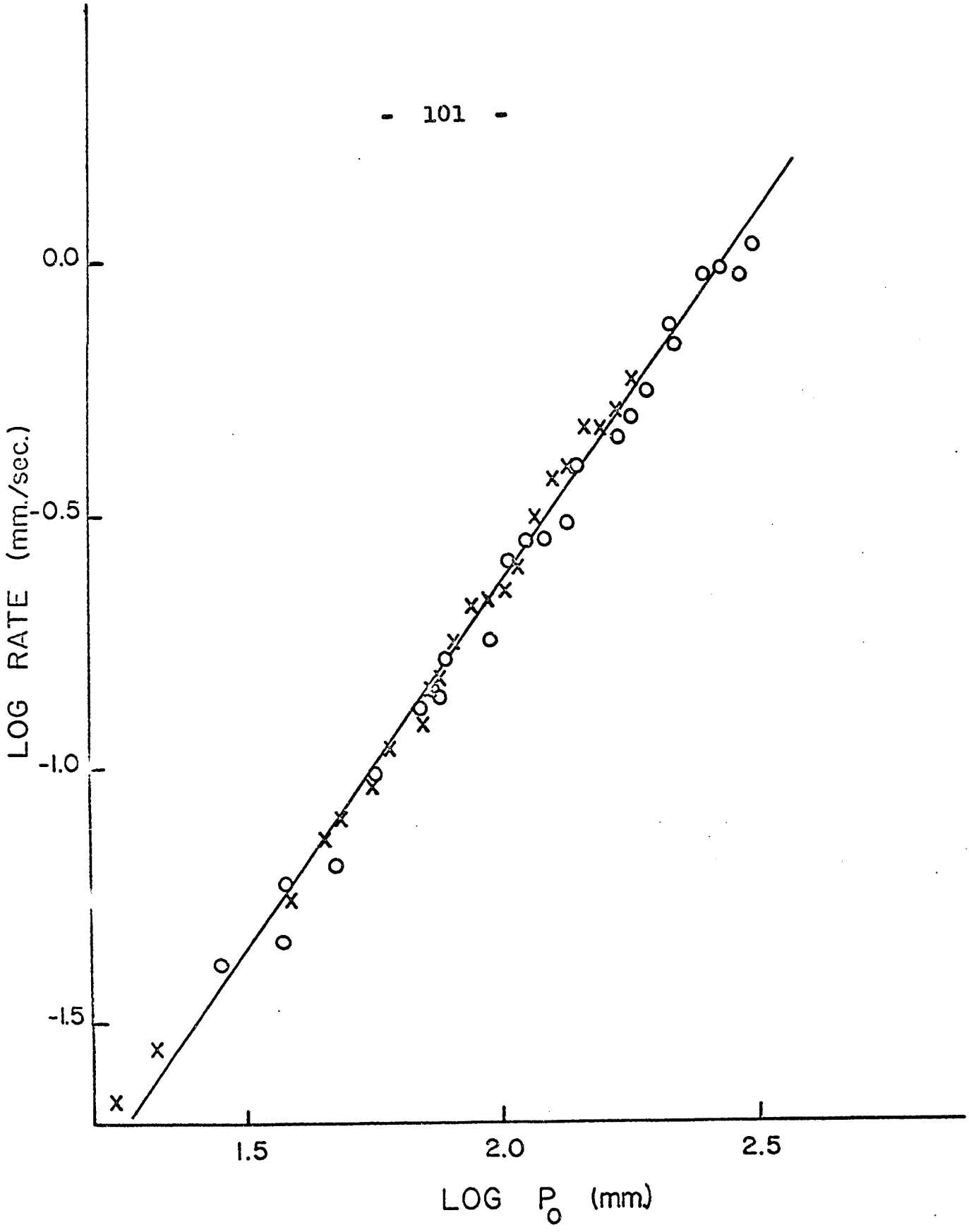

Figure 27 Plot of the logarithm of the rate against the logarithm of the pressure at 580°C, showing the effect of added CO_2. The circles denote no added CO_2, the crosses denote rate measured with $CO_2/C_4H_{10} \approx 2.5$.

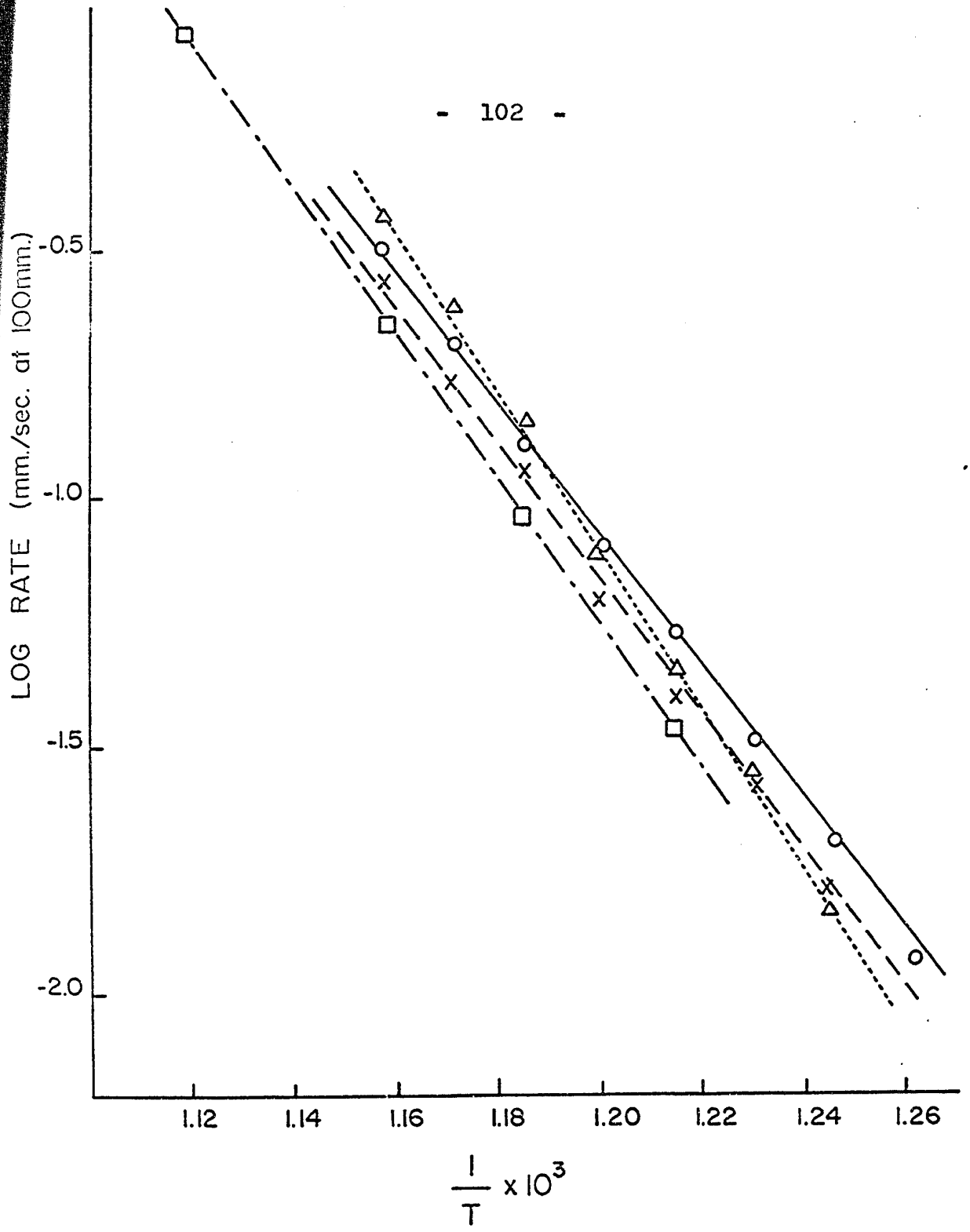

Figure 28 Arrhenius plot showing the effect of surface. Rates measured in the clean, unpacked vessel are given by O, in a clean packed vessel by X, in a conditioned unpacked vessel by Δ and in a conditioned packed vessel by □.

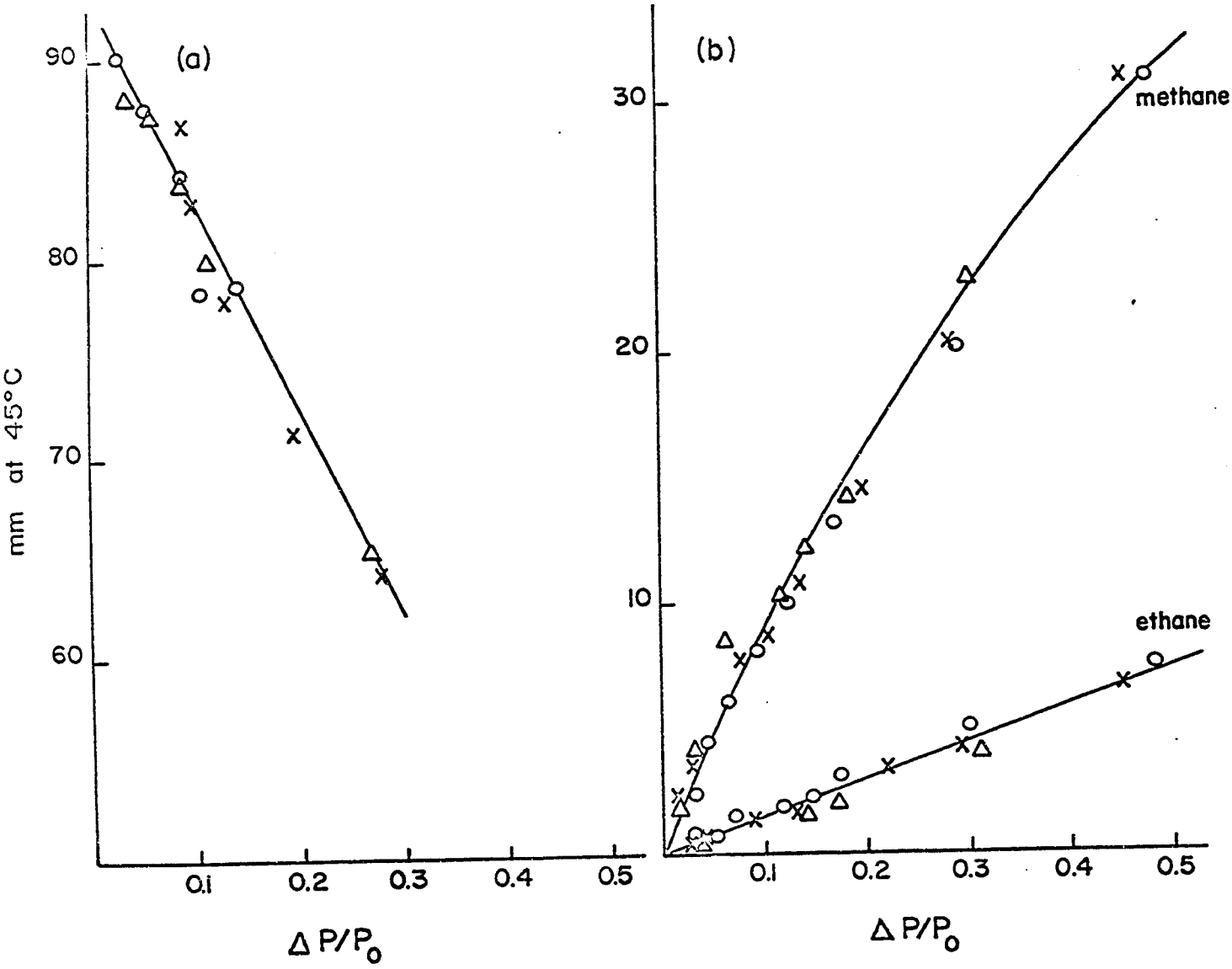

Figure 29 Analytical results. The left-hand plot shows the correlation between the increase in total pressure and decrease in partial pressure of butane, the right-hand gives that between the increase in total pressure, and appearance of methane and ethane, at 550°C (O), 570°C (X) and 590°C (Δ).

Table 11

Ratios of Decomposition Products

Initial Pressure 202 mm.

T°C	$\frac{C_2H_6}{C_2H_4}$	$\frac{\text{Alkanes}}{\text{Alkenes}}$	$\frac{CH_4 + C_3H_6}{C_2H_4 + C_2H_6}$	$\frac{C_4 \text{ products}}{C_1 \text{ to } C_3 \text{ products}}$
550	.616	1.08	1.92	0.012
570	.523	1.03	1.81	0.014
590	.467	1.02	1.80	0.021

data, giving the C_2H_6/C_2H_4, alkanes/alkenes, $(CH_4 + C_3H_6)/(C_2H_4 + C_2H_6)$ and (C_4 products)/(C_1 to C_3 products) ratios, all at about 200 mm. initial pressure, and at three different temperatures.

If unit increase in pressure corresponds to unit decrease in n-butane partial pressure, the rate constants may be given by

$$k_{3/2} = 3.24 \times 10^{15} \; e^{59,900/RT} \; ml^{1/2} \; mole^{-1/2} \; sec^{-1}$$

DISCUSSION

Mechanism and Over-All Order of the Reaction

Many earlier mechanisms were written on the assumption that the experimental order of the reaction was first. However the results quoted above show that it is best described as only a little less than 3/2. This fact was probably first realised by Echols and Pease (74). The proposed mechanism, following that outlined by Echols and Pease (74) is:

(18) $\quad C_4H_{10} \longrightarrow 2\,C_2H_5$

(19) $\quad C_2H_5 + C_4H_{10} \longrightarrow C_2H_6 + C_4H_9$

(20) $\quad C_4H_9 \longrightarrow CH_3 + C_3H_6$

(21) $C_4H_9 \rightarrow C_2H_5 + C_2H_4$

(22) $CH_3 + C_4H_{10} \rightarrow CH_4 + C_4H_9$

(2) $C_2H_5 \rightarrow C_2H_4 + H$

(23) $H + C_4H_{10} \rightarrow H_2 + C_4H_9$

(24) $C_2H_5 + C_2H_5 \rightarrow C_4H_{10}$ or $C_2H_6 + C_2H_4$

Table 12 lists the known and estimated rate constants, activation energies and frequency factors.

The proposed scheme gives the following steady-state concentrations of radicals:

$$[H] = \frac{k_2}{k_{23}} \left(\frac{2\,k_{18}}{k_{24}}\right)^{1/2} [C_4H_{10}]^{-1/2} \qquad [37]$$

$$[C_2H_5] = \left(\frac{2\,k_{18}}{k_{24}}\right)^{1/2} [C_4H_{10}]^{1/2} \qquad [38]$$

$$[CH_3] = \frac{k_{19}k_{20}}{k_{21}k_{22}} \left(\frac{2\,k_{18}}{k_{24}}\right)^{1/2} [C_4H_{10}]^{1/2} + \frac{k_6k_{20}}{k_{21}k_{22}} \left(\frac{2\,k_{18}}{k_{24}}\right)^{1/2} [C_4H_{10}]^{-1/2} \qquad [39]$$

$$[C_4H_9] = \frac{k_{19}}{k_{21}} \left(\frac{2\,k_{18}}{k_{24}}\right)^{1/2} [C_4H_{10}]^{3/2} + \frac{k_2}{k_{21}} \left(\frac{2\,k_{18}}{k_{24}}\right)^{1/2} [C_4H_{10}]^{1/2} \qquad [40]$$

Table 12

Kinetic Parameters for Reactions of Part III

Reaction	A*	E(kcal/mole)	k_{570}*	Reference
2	3.0×10^{14}	39.5	1.74×10^{4}	(47)
10		[-14.8]	1.0×10^{18}	calc. from (42)
18	1.0×10^{17}	80.0	1.85×10^{-4}	(46)
19	7.7×10^{11}	10.4	1.55×10^{9}	estimated from (90)
20	6.5×10^{11}	24.0	3.92×10^{5}	(91)≠
21	1.6×10^{11}	22.0	3.18×10^{5}	(92)
22	2.7×10^{11}	9.0	1.26×10^{9}	(93)
23	1.0×10^{14}	7.9	8.97×10^{11}	(94)
24	2.2×10^{13}	0.0	2.20×10^{13}	(95)
25	1.0×10^{13}	0.0	1.00×10^{13}	assumed

* rates and frequency factors in sec^{-1} or $ml^{1/2}$ $moles^{-1/2}$ sec^{-1}.

≠ The data of Gruver and Calvert (91) has since been re-calculated by Calvert (96). However, the original values are used here since they are considered by Metcalfe and Trotman-Dickenson (97) to form a consistent set with those for reaction 21, and in all cases the important figures are k_{20}/k_{21} and $E_{20}-E_{21}$.

Assuming very long chains, the over-all rate is given by

$$V = (k_{20} + k_{21}) [C_4H_9] \qquad [41]$$

and the rate becomes

$$V = (1 + \frac{k_{20}}{k_{21}}) \left\{ k_{19} (\frac{2 k_{18}}{k_{24}})^{1/2} [C_4H_{10}]^{3/2} + k_2 (\frac{2 k_{18}}{k_{24}})^{1/2} [C_4H_{10}]^{1/2} \right\} \qquad [42]$$

The data from table 12 indicate that k_{20} and k_{21} are very close to each other, although k_{20} is, perhaps, higher.

The experimental evidence indicates that at all temperatures the first term of the rate expression predominates above 100 mm., since the order is definitely 3/2 at the higher pressures. Furthermore ethane is produced at a rate comparable with that for the production of ethylene, showing that the first term is at least of the same order of magnitude as the second. The values of the rate constants in table 12 predict that, at 570°C and 500 mm.

$$\frac{\text{term 1}}{\text{term 2}} = \frac{k_{19}}{k_2} [C_4H_{10}] = 0.85 \qquad [43]$$

The source of the small discrepancy may lie in the fact that

the ethyl radicals produced by the decomposition of butyl radicals may be colder than those produced by photochemical means. An ethyl radical needs 39.5 kcal. in order to decompose but only 10.4 in order to abstract a hydrogen atom from n-butane, and there is good evidence that only a few kilocalories are transferred in any one collision. It may easily be seen that any radical, having acquired 10.4 kcal., is quite likely to abstract in a subsequent collision, and may never survive long enough to be energised, by collisions, up to the 39.5 kcal. necessary for decomposition.

For convenience, all butyl radicals are treated as the same. In actual practice, s-butyl radicals are formed slightly more easily, as shown by Kuppermann and Larson (88) and McNesby (98), the difference in activation energies being about $2\frac{1}{2}$ kcal. per mole. Thus the chain involving secondary butyl radicals and giving ($CH_4 + C_3H_6$) is about twice as fast as that giving ($C_2H_4 + C_2H_6$). Kuppermann and Larson (88) showed that for abstraction reactions such as 19 and 22, the ratio of primary to secondary hydrogen atoms abstracted is:

$$\frac{k_p}{k_s} = 2.43\, e^{-2,640/RT}$$

At 570°C, therefore, $k_p/k_s = 0.503 \approx 1/2$. Thus the C_4H_9 is about 1/3 primary and 2/3 secondary, and the ratio

$(CH_4 + C_3H_6)/(C_2H_6 + C_2H_4)$ should equal 2, in reasonable agreement with experiment (table 11). Of course some isomerization of butyl radicals is possible, but at only slightly lower temperatures (up to 450°C) Gordon and McNesby (99) were unable to find any evidence of this.

The mechanism presented here does not explain the small quantities of butenes formed. The kinetic parameters for the reaction

$$C_4H_9 \longrightarrow C_4H_8 + H$$

have never been estimated when the C_4H_9 radicals are primary or secondary. It seems likely, however, from the data on the decomposition of iso-butyl radicals obtained by Bywater and Steacie (47) that the activation energy is above 40 kcal. per mole. Thus, if the frequency factors are comparable, the amount of butenes should be less than 0.1% of the total products. Actually they total about 1 to 2% of the products (table 11) and probably come from surface dehydrogenation, or a small molecular component of the reaction. It may be noted here that butadiene is produced at a rate almost one-third that for the production of butenes, and butadiene is certainly not a primary product of the chain reactions.

From table 4, it may be seen that to obtain 3/2-order kinetics one may use the reaction scheme ${}^{1}\beta\beta_{3/2}$ as postulated here or, alternatively, ${}^{2}\mu\beta_{3/2}$ or ${}^{2}\beta\beta M/_{3/2}$. The

scheme $^{2}\mu\beta_{3/2}$ would give a positive inert gas effect which was not observed and, in any case, can be shown to be unimportant at pressures above 40 mm. The reaction scheme $^{2}\beta\beta M_{3/2}$ is a possibility, but kinetically it gives the same results as the scheme selected, so that it is impossible to distinguish between them from the kinetics alone. The reasons for choosing $'\beta\beta_{3/2}$ are discussed below.

Effect of Inert Gas

It has been shown experimentally (figure 27) that, at partial pressures up to $2\frac{1}{2}$ times those of n-butane, carbon dioxide has little effect on the rate of reaction. This means that the molecularity of the initiating step is the same as that of the terminating step, assuming that none of the chain propagating steps is pressure dependent. Small inert gas effects have been noted in this system by Jach and Hinshelwood (64) (100). However their results are suspect, since most of the work was done using SF_6 as an 'inert gas'.

The Initiating Reaction

The initiating reaction has been postulated to be the first-order breakdown of n-butane to two ethyl radicals. Brinton and Steacie (101) have shown that the recombination of ethyl radicals is certainly first-order at pressures of 0.5 mm. and higher at 250°C. The Rice-Ramsperger-Kassel

theory predicts that the transition should vary as the $(s-\frac{1}{2})$th power of the temperature. Thus the breakdown of butane into ethyl radicals should be first-order above 200 mm., taking s as 12. However, the results of Brinton and Steacie (101) show that large excesses of perfluorodimethylcyclohexane added to their system in its third-body dependent region did not substantially increase the rate of reaction as it had for the case of the recombination of methyl radicals studied by Dodd and Steacie (55). Thus they concluded that the recombination of ethyl radicals may be independent of pressure down to 0.02 mm. total pressure at 250°C. Thus s could be as large as 19, and the split into ethyl radicals would remain first-order down to 100 mm. at 570°. Further support for this view is provided by the fact that for the ethane decomposition the evidence strongly supports the conclusion that the ethyl radical recombination is in its second-order region (40) (41).

The other possible initiation reaction is the splitting of a methyl radical from a butane molecule, probably in its second-order region. However Trotman-Dickenson (46) has estimated that the dissociation energy for this process is some 4 kcal. higher than that for reaction 18. On the other hand the frequency factor may be higher by a small amount. However it is unlikely that this factor will be as

high as the 10 necessary to offset the difference in activation energy, so that reaction 18 should predominate.

Chain Terminating Reactions

Assuming first-order initiation, the only possible chain terminating step is the recombination of β radicals. Since it has been shown (41) that the recombination of methyl radicals requires a third body, the termination must be reaction 24

$$(24) \qquad C_2H_5 + C_2H_5 \longrightarrow C_4H_{10}$$

$$\text{or } C_2H_6 + C_2H_4$$

A comparison of the rate of this reaction with that for the recombination of methyl radicals gives

$$\frac{V_{24}}{V_{10}} = \frac{k_{24}}{k_{10}} \frac{[C_2H_5]^2}{[CH_3]^2[C_4H_{10}]} = \frac{k_{24}}{k_{10}} \left(\frac{k_{21}k_{22}}{k_{20}k_{19}}\right)^{1/2} \frac{1}{[C_4H_{10}]} \qquad [44]$$

which, at 570°C and 500 mm., yields

$$\frac{V_{24}}{V_{10}} = 1.01$$

Thus there is no difficulty in accepting the evidence of the inert gas experiments and assuming reaction 24 to be slightly predominant.

Another possible termination reaction is

(25) $C_2H_5 + C_4H_9 \longrightarrow C_6H_{14}$

or $C_2H_6 + C_4H_8$

At 570°C and 500 mm.

$$\frac{V_{24}}{V_{25}} = \frac{k_{24}}{k_{25}} \frac{k_{21}}{k_{19}} \frac{1}{[C_4H_{10}]} = 47 \qquad [45]$$

and so reaction 24 is considerably faster.

The Induction Period

A very small induction period was noticed which became longer at lower pressures, and slightly shorter at higher temperatures. In an effort to see if the experimentally high activation energy could be a result of the variation of this induction period, an attempt was made to extrapolate that part of the pressure-time curve beyond the inflexion point back to zero time by using an appropriate power series, and to then calculate the 'initial' rate. The results of this procedure are shown in figure 30 in the form of an Arrhenius plot. The activation energy is 59.0 kcal. per mole, slightly lower than that obtained at the inflexion point, but still not close to the predicted value of 52.4 kcal. per mole.

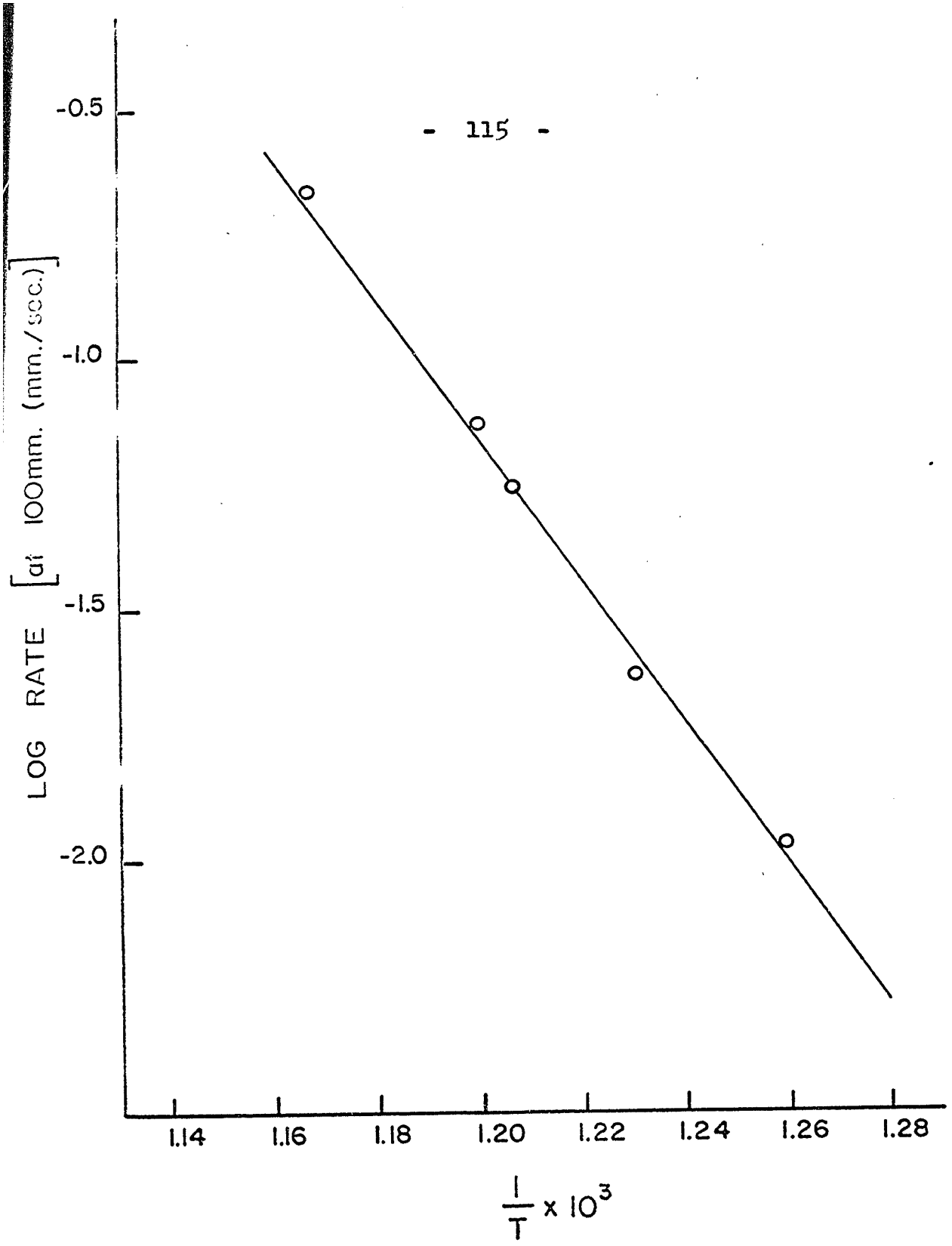

Figure 30 Rates of the uninhibited pyrolysis of n-butane obtained by extrapolation of that part of the ΔP-time curve beyond the inflexion point to zero time.

The Effect of Surface

In an effort to determine the effect of surface on the reaction, runs were carried out in a vessel whose surface to volume ratio had been increased by a factor of 11.6. Also, runs were done in both the packed and unpacked vessels after a thin layer of carbon was deposited on the interior surfaces of the reaction vessel, as previously described. The results of this work are shown in figure 28, plotted in the form of the logarithm of the rate at 100 mm. against the reciprocal of the absolute temperature.

The rates in the packed, clean vessel are seen to be lower than those in the unpacked clean vessel at all temperatures. They are most depressed at lower temperatures and so the activation energy in the packed vessel is slightly higher, being 62.3 kcal. per mole. It is suggested that the free valencies in the surface layer of the quartz (S) can abstract hydrogen from the butane molecule, forming an S-H bond, in a manner analogous to NO (part IV). Thus a small portion of the reaction may be following a mechanism such as

(26s) $C_4H_{10} + S \rightarrow SH + C_4H_9$

(20) $C_4H_9 \rightarrow C_3H_6 + CH_3$

(21) $C_4H_9 \rightarrow C_2H_4 + C_2H_5$

(19) $C_2H_5 + C_4H_{10} \rightarrow C_2H_6 + C_4H_9$

(22) $CH_3 + C_4H_{10} \longrightarrow CH_4 + C_4H_9$

(14s) $SH \longrightarrow S + H$

(27s) $S + C_2H_5 \longrightarrow C_2H_5S$

(28s) $C_2H_5S \longrightarrow C_2H_5 + S$

(29s) $C_2H_5S + C_2H_5 \longrightarrow C_4H_{10} + S$

or $C_2H_6 + C_2H_4 + S$

The over-all rate is then given by

$$v \approx k_{19} \left(\frac{k_{20}}{k_{22}}\right) \left(\frac{k_{26s}k_{28s}}{k_{27s}k_{29s}}\right)^{1/2} [C_4H_{10}]^{3/2}$$

$$+ 2\left(\frac{k_{20}}{k_{21}}\right) k_{26s} [C_4H_{10}] [S] \qquad [46]$$

No reliable estimates of rate constants for the reactions subscripted by 's' are available, although an estimate for the activation energy of breaking the C-Si bond (78 kcal. per mole) is available from Cottrell (102). As with any surface reaction, a range of sites with varying heats of adsorption will be available, and furthermore these heats of adsorption will vary with coverage in some fashion, perhaps in a linear fashion as predicted by the well known Temkin (103) isotherm.

The results in the conditioned vessel are of some interest. The reaction in the unpacked vessel has an extremely

high activation energy and, at the highest temperatures, a rate higher than that in the clean vessel. The effect of packing is much more pronounced than in the clean vessel. These results suggest that at least some of the initiation and termination is taking place on the vessel walls. The larger effect of packing indicates that the carbon surface is a better initiator and terminator of chains than the clean silica. As graphite consists of a two-dimensional fused-ring system, it is not surprising that atoms and small free radicals can be adsorbed with only a small activation energy (104).

In any case, it is important to note that the reaction is extremely sensitive to the nature of the surface, rates varying almost by a factor of 2 at the lower temperatures. This will be contrasted later with the results for the reaction inhibited by NO.

Kinetic Parameters

The activation energy predicted using the values in table 12 is

$$E = E_{19} + E_{20} - E_{21} + \frac{1}{2}(E_{18} - E_{24}) \qquad [47]$$

$$= 52.4 \text{ kcal. per mole.}$$

This compares with the experimental value of 59.9 kcal. per

mole. The pre-exponential factor is

$$A = \frac{A_{19}A_{20}}{A_{21}} \left(\frac{A_{18}}{A_{24}}\right)^{1/2} = 2.1 \times 10^{14}\ ml^{1/2}\ mole^{-1/2}\ sec^{-1} \quad [48]$$

compared to the experimental value of 3.24×10^{15}. Absolute rate constants, are in somewhat better agreement, the calculated rate at 570°C being 5.5 $ml^{1/2}\ mole^{-1/2}\ sec^{-1}$, and the experimental value 0.97 $ml^{1/2}\ mole^{-1/2}\ sec^{-1}$.

As has been shown above, all surface treatments tend to raise the activation energy somewhat, so that even the activation energy obtained in the clean unpacked vessel is too high.

CONCLUSIONS

It is concluded that the thermal decomposition of n-butane is largely homogeneous and is described well by a 3/2-order rate law between 520 and 590°C. A free-radical reaction mechanism is postulated involving first-order initiation and termination by the second-order recombination of ethyl radicals; it is shown that the experimental facts are quite well fitted by this mechanism. The values of various rate constants, either quoted from the literature or, where necessary, assumed, are also shown to be consistent with this mechanism.

The experimental 3/2-order rate constants are given by

$$k = 3.24 \times 10^{15} e^{-59,900/RT} \text{ ml}^{1/2} \text{ mole}^{-1/2} \text{ sec}^{-1}$$

at an average temperature of 570°C.

Part IV

THE PYROLYSIS OF n-BUTANE INHIBITED BY NITRIC OXIDE

INTRODUCTION

As in the case of other hydrocarbons, the mechanism of the thermal decomposition of n-butane, in the presence of enough NO to reduce the rate of reaction to a minimum, has been greatly disputed. Much interest has redeveloped in this subject in recent years, and the pyrolysis of n-butane when fully inhibited has been the subject of several papers. None of these, however, has given a detailed mechanism of the reaction and none has presented the overall kinetics in detail. The purpose of this work was to see if the mechanisms proposed in this laboratory (56) for the lower alkanes could be applied to the inhibited decomposition of n-butane, and to propose a new one if necessary.

Review of Earlier Work

Following Staveley's (58) discovery that the thermal decomposition of some organic compounds could be inhibited with nitric oxide, Nichols and Pease (105) found that NO also inhibited the decomposition of n-butane. Rice and Polly (59) found that propylene greatly reduced the rate of decomposition of n-butane at 512°C, and proposed a free-radical mechanism to explain their results. This mechanism has been discussed

in part II, as have the modifications made to it by Goldansky (60).

Echols and Pease (105) (106) (107) (74) found that the inhibition brought about by nitric oxide was only transitory and that after 20% reaction the rate became normal again. They suggested that on equilibrium

$$R + NO \rightleftharpoons RNO$$

was set up and that radicals were then fed back into the system, R being largely methyl radicals. However, in the view of Goldansky (60) this would necessitate acceleration of the reaction at the later time. The rates measured by Echols and Pease also seem lower than those of other workers (e.g. (61)).

Goldfinger (108) suggested that the 3/2-order over all reaction could come from terminations of the sort:

$$R_1 + R_2 + NO \longrightarrow \text{products}$$

However postulating NO as a very efficient third body is equivalent to

$$R + NO \longrightarrow RNO$$

$$RNO \longrightarrow R + NO$$

$$R + RNO \longrightarrow \text{Products}$$

It is of interest that this sort of termination, together

with initiation of the type postulated by Laidler and Wojciechowski (57) for the inhibited pyrolysis of ethane, is essentially the mechanism proposed here.

Hobbs and Hinshelwood (35) had proposed earlier that the fully inhibited decomposition of any organic compound was the 'residual reaction' left after NO had suppressed all the chain reaction. However Steacie and Folkins (109) found that a small amount of ethylene oxide could sensitize the decomposition of n-butane, even when enough nitric oxide had been added to 'fully inhibit' the chain reaction and that, at 450°C, a chain length of four was obtained. They also found (89) that the products of the inhibited reaction were identical with those of uninhibited, and thus considered that both reactions were of a similar type, the inhibited reaction also consisting of chains, but of a shorter length.

Partington and Danby (110) obtained similar results on larger hydrocarbons, but Ingold, Stubbs and Hinshelwood (111) felt that the reactions involving a split of one radical into another radical and an olefin, and the split of a molecule into two products were similar enough that the activation energy differences, and ratios of frequency factors should be similar. For example

$$\text{I} \quad CH_3CH_2CH_2CH_2R \longrightarrow CH_4 + CH_2{=}CHCH_2R$$

and

II $CH_3CH_2CH_2CH_2R \longrightarrow C_2H_6 + CH_2{=}CHR$

compared with

III $CH_2CH_2CH_2CH_2R \longrightarrow CH_3 + CH_2{=}CHCH_2R$

and

IV $CH_2CH_2CH_2CH_2R \longrightarrow C_2H_5 + CH_2{=}CHR$

should give the result that:

$$E_{III} - E_{IV} = E_I - E_{II} \qquad [49]$$

and

$$\frac{A_{III}}{A_{IV}} = \frac{A_I}{A_{II}} \qquad [50]$$

However Steacie (48) pointed out that this simplified argument will be valid only if no secondary hydrogens are abstracted by radicals. Furthermore, later work by Crawford and Steacie (83) showed that the products of the inhibited reaction are actually somewhat deficient in ethane. This is to be expected from the mechanism proposed here.

Stubbs, Ingold and Hinshelwood (61) (62) (36) (63) obtained kinetic parameters for the maximally inhibited decomposition of n-butane. They considered the reaction to be approximately first-order from an examination of the pressure-rate relationship and found an activation energy of about 60 kcal. per mole at higher pressures and 79 at lower (10 mm.)

pressure.

The effect of added inert gas has been studied in some detail by Jach and Hinshelwood (64) (100). They found that an excess of added inert gas caused some increase in rate, and, moreover, found that the absolute increase in rate was the same whether the reaction was fully inhibited or uninhibited. This fact was taken to be a further proof for the molecular nature of the maximally inhibited reaction. Their results are somewhat suspect since SF_6 was the chief inert gas used and, as has been pointed out in part II, this compound may not be truly inert. Furthermore, later work using CO_2 as the inert gas (88) has not shown any increase in rate on adding an excess of this gas.

Interest in the nature of the fully inhibited thermal decomposition of paraffins and in particular of n-butane has revived in recent years. Purnell and Quinn (112), looking at the propylene inhibited decomposition of n-butane, found that the production of ethylene, relative to that of ethane, was increased as the pressure was lowered, and attributed this result to competition between decomposition of and abstraction by the ethyl radical,

$$(2) \qquad C_2H_5 \rightarrow C_2H_4 + H$$

$$(19) \qquad C_2H_5 + C_4H_{10} \rightarrow C_2H_6 + C_4H_9$$

decomposition being more important at lower pressures and

higher temperatures. Thus their work is evidence for a free-radical mechanism for the maximally inhibited reaction.

The non-molecular nature of the nitric oxide inhibited decomposition has been established by Kuppermann and Larson (113) using deuterium mixing techniques. They pyrolyzed an equimolar mixture of C_4D_{10} and C_4H_{10} and found that the methanes gave the same CD_3H/CD_4 ratio, whether uninhibited or maximally inhibited with up to 27.6% NO. Furthermore, they showed that secondary processes were of little importance since, on pyrolyzing a mixture of CD_4 and C_4H_{10}, no CD_3H was detected at all. These authors (88) later presented a fuller account of further analytical and kinetic work done on the $n\text{-}C_4H_{10}$, $n\text{-}C_4D_{10}$ system. They confirmed their earlier conclusion that the extent of mixing, as measured by the CD_3H/CD_4 and C_2H_5D/C_2D_6 ratios, was essentially independent of the amount of NO present. An interesting result was that, while methanes and ethanes were mixed, ethylenes and propylenes were essentially unmixed. This result is consistent with the accepted view that propylene and ethylene are formed from the unimolecular decomposition of larger radicals. Kuppermann and Larson (88) also found that the addition of NO increased the amount of ethylene relative to ethane. They interpreted this result as a disagreement with the mechanisms proposed by Laidler and Wojciechowski (57) for the thermal decomposition of ethane, feeling that chain termination by

$$C_2H_5 + HNO \longrightarrow C_2H_6 + NO$$

$$CH_3 + HNO \longrightarrow CH_4 + NO$$

should increase the amount of ethane produced. However it will be shown below that the above reactions are not, in fact, important chain terminating steps.

EXPERIMENTAL

Apparatus and Method

The apparatus was described in part I of this thesis. The n-butane was prepared as in part III, the nitric oxide as in part II, and analyses were performed as in part III.

Results

The inhibited pyrolysis of n-butane was studied at temperatures ranging from 540 to 610°C and at partial pressures of butane from 30 to 550 mm. The pressure change was followed automatically as previously described. The pressure-time curve is slightly sigmoidal as shown in figure 31, a typical run at 570°C and 225 mm. butane. The induction period was lengthened at lower pressures of butane, but did not seem to be much affected by changes in the partial pressure of nitric oxide.

A number of preliminary experiments showed that about 12% NO gave complete inhibition. Large amounts of NO

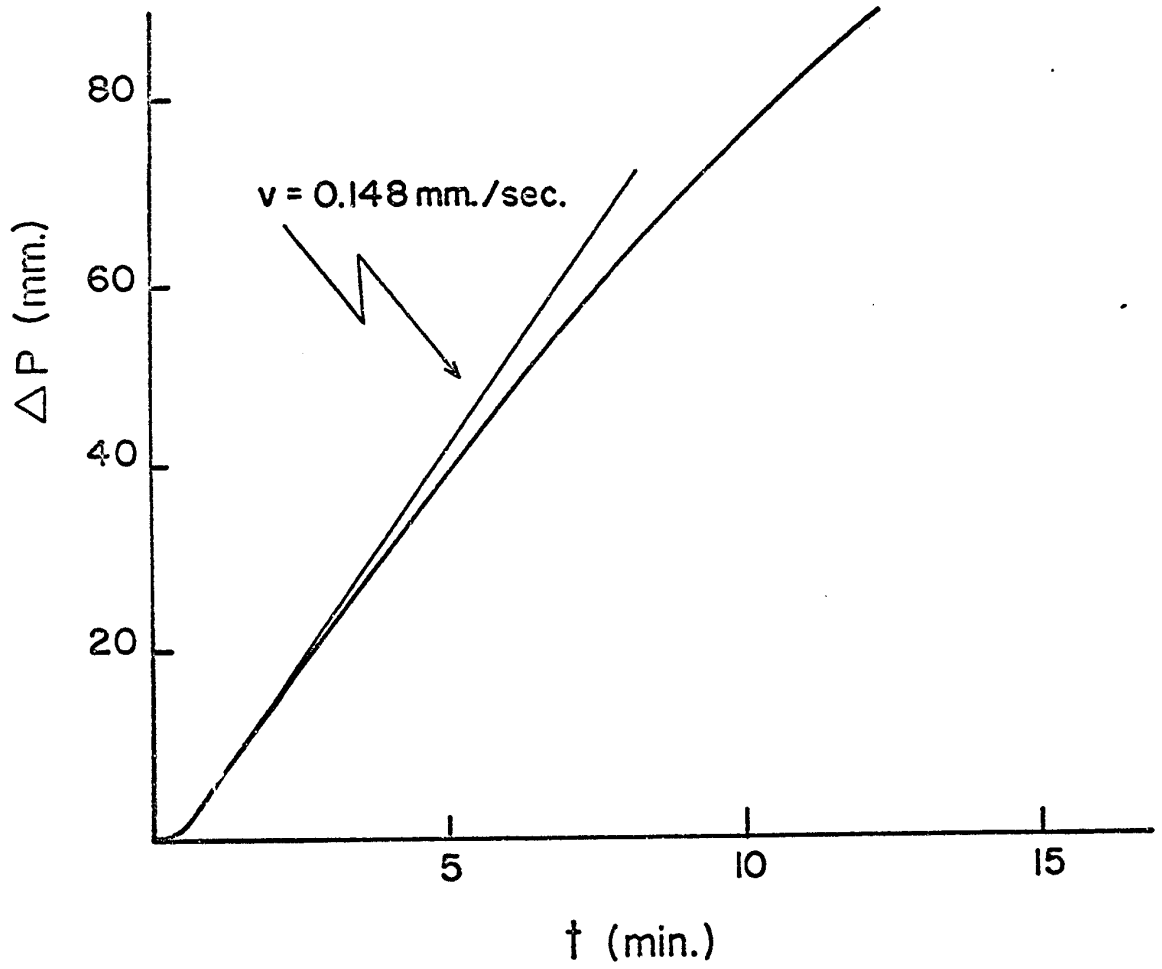

Figure 31 A typical pressure-time curve, obtained at 570°C, with an initial butane pressure of 225 mm. Hg, and a nitric oxide pressure of 32 mm. Hg, in an unpacked vessel.

(more than 40%) accelerated the inhibited reaction somewhat, so most of the experiments were done with about 15% NO.

Following the procedures normally used in this laboratory, the logarithms of the rates at the inflexion point are plotted against the logarithms of the partial pressures of butane in figure 32. It may be seen that the reaction is best described as being 3/2-order, and table 13 lists the 3/2-order rate constants obtained in the packed and unpacked reaction vessels.

Figure 33 shows a comparison of the maximally inhibited and uninhibited rates at 570°C. It is seen that both are close to 3/2-order and that the ratio of rates does not vary as much with pressure as has been reported by Stubbs and Hinshelwood (62), although they worked at 530°C so that a comparison is not strictly valid.

Figure 34 gives the logarithms of the 3/2-order rate constants plotted against the reciprocal of the absolute temperature. Rates obtained by other workers such as Steacie and Folkins (89) and Ingold, Stubbs and Hinshelwood (36) are also included. The 3/2-order rate constants may be given as

$$k = 4.55 \times 10^{12} e^{-65,100/RT} \text{ mm.}^{-1/2} \text{ sec}^{-1}$$

The effect of added carbon dioxide on the rate of reaction at 590°C is given in figure 35. The partial pressure

Table 13

Rate Constants for the Inhibited Decomposition of n-Butane

	Unpacked Vessel	Packed Vessel
$T^{\circ}C$	10^5 k($mm^{-1/2}sec^{-1}$)	10^5 k($mm^{-1/2}sec^{-1}$)
540	1.46	-
550	2.29	1.79
560	3.68	3.08
570	6.32	5.48
580	9.55	8.32
590	14.38	13.17
600	24.45	22.40
610	37.6	35.6

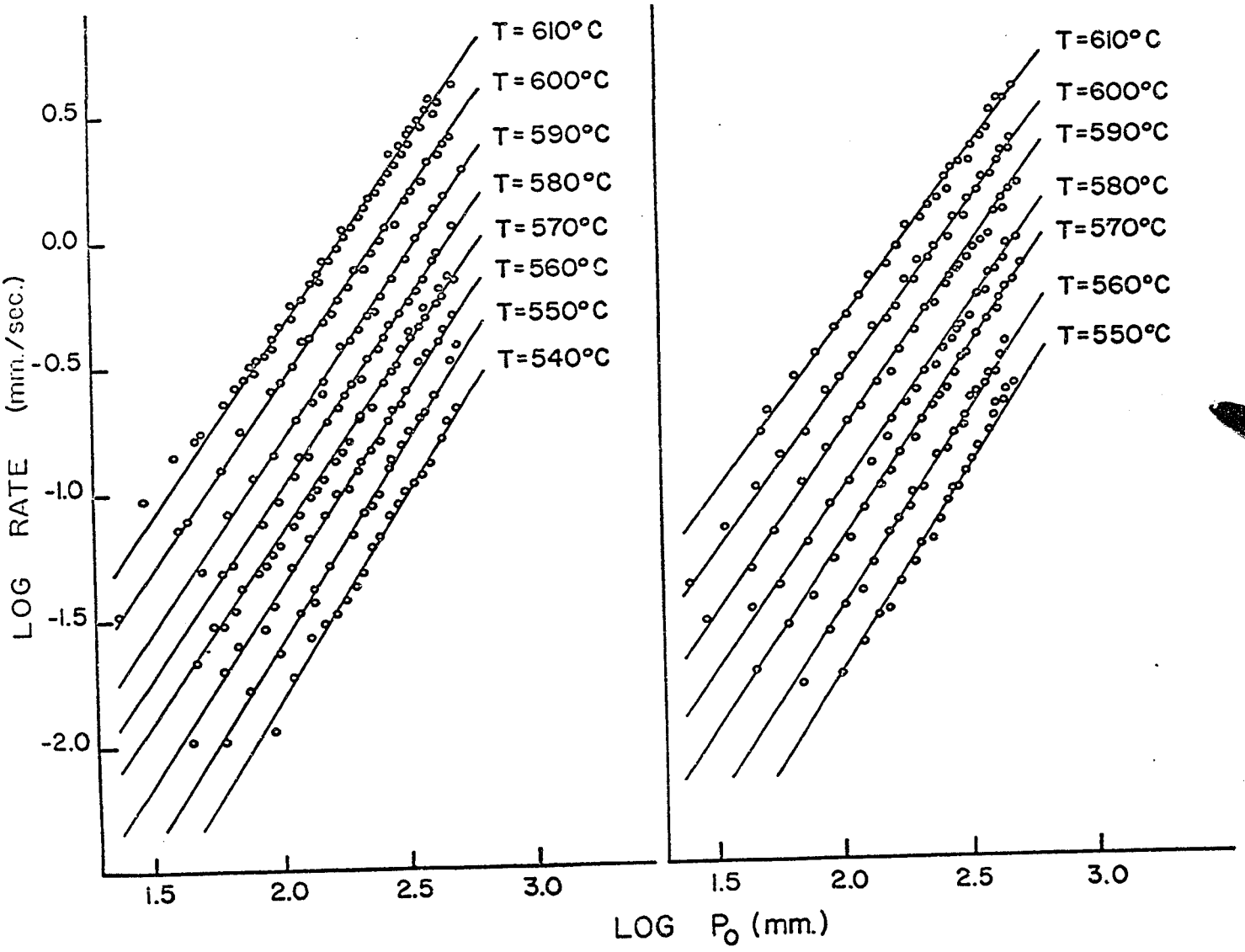

Figure 32 Logarithmic plots of rate against pressure. The plot on the left-hand side is for the unpacked vessel, that on the right-hand side for the packed vessel.

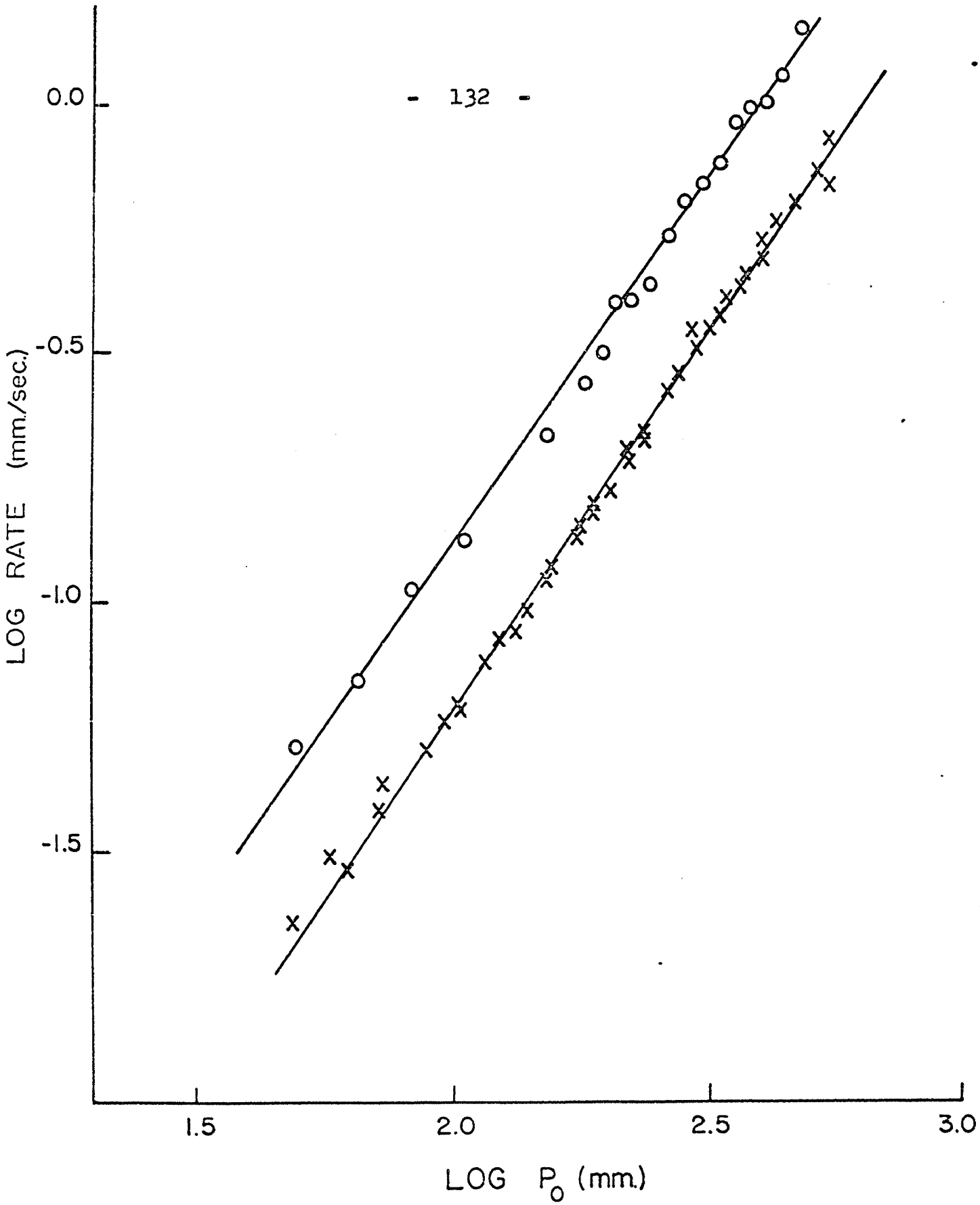

Figure 33 Plots of the logarithm of the rate against the logarithm of the pressure for the uninhibited (X) and inhibited (O) reaction at 570°C.

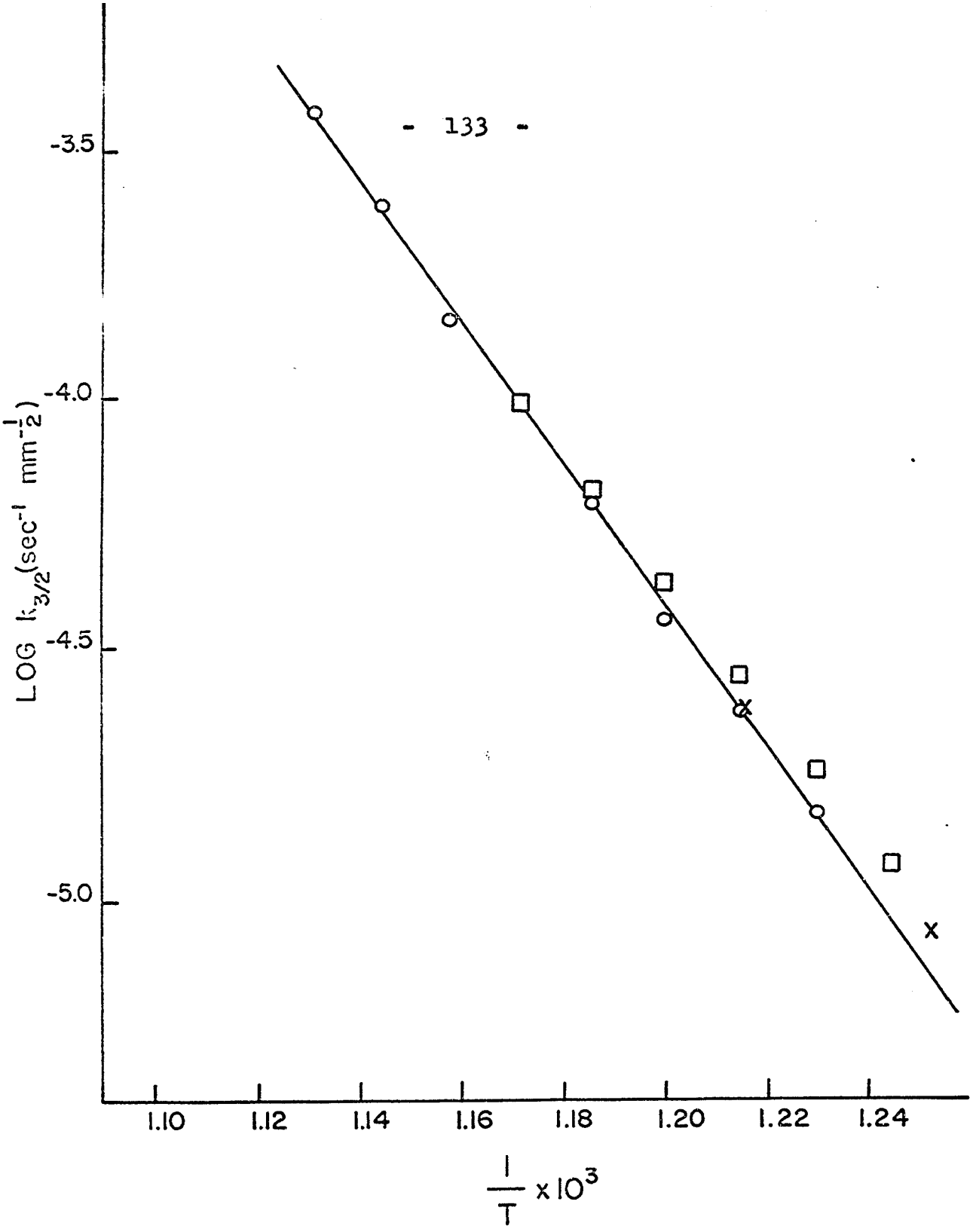

Figure 34 Arrhenius plot for the inhibited pyrolysis of n-butane. The results of this investigation are shown as O, those of Ingold, Stubbs and Hinshelwood (36) as □ and those of Steacie and Folkins (89) as X.

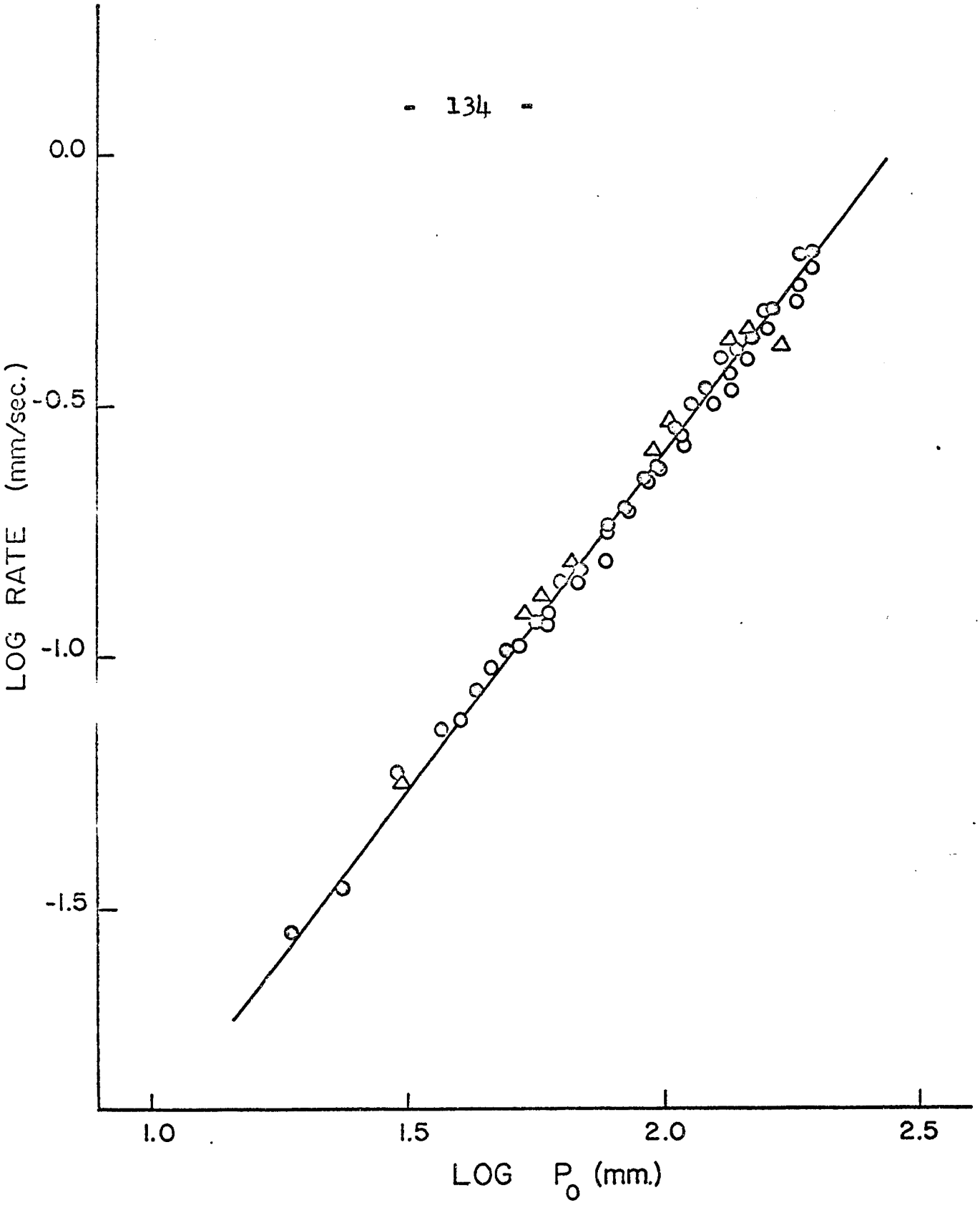

Figure 35 Plots of the logarithm of the rate against the logarithm of the pressure, showing the effect of added carbon dioxide. O denotes results with no added CO_2, Δ denote rates with $CO_2/C_4H_{10} \approx 3$, and ● denotes rates with $CO_2/C_4H_{10} \approx 2.1$.

of added CO_2 was 2.1 and 3.0 times that of the butane and it may be seen that, within the limits of experimental error, no effect of the added carbon dioxide on the rate was noticed.

Figure 36 shows the effect of various types of surfaces, the data being presented in Arrhenius form. Reactions done in a 'clean vessel' were performed in a vessel washed three times with warm concentrated nitric acid and rinsed with distilled water as described in part III, and as done by Purnell and Quinn (86). The 'conditioned vessel' was prepared by pyrolyzing 300 mm. of n-butane in a vessel for 48 hours before carrying out a set of reactions. The packed vessel had its surface to volume ratio increased by a factor of 11.6. These surface treatments gave rates close to those obtained in the clean unpacked vessel, although they were a little lower at the lowest temperatures, giving a slightly higher activation energy.

Figure 37 summarizes the analytical data. The left-hand drawing shows the correlation between the pressure increase and the amount of n-butane used up, and it may be seen that unit increase in total pressure corresponds closely to unit decrease in the partial pressure of n-butane. The right-hand drawing gives the production of methane and ethane, as well as indicating the equivalent data for the uninhibited case. It may be seen that methane is produced at about the same relative

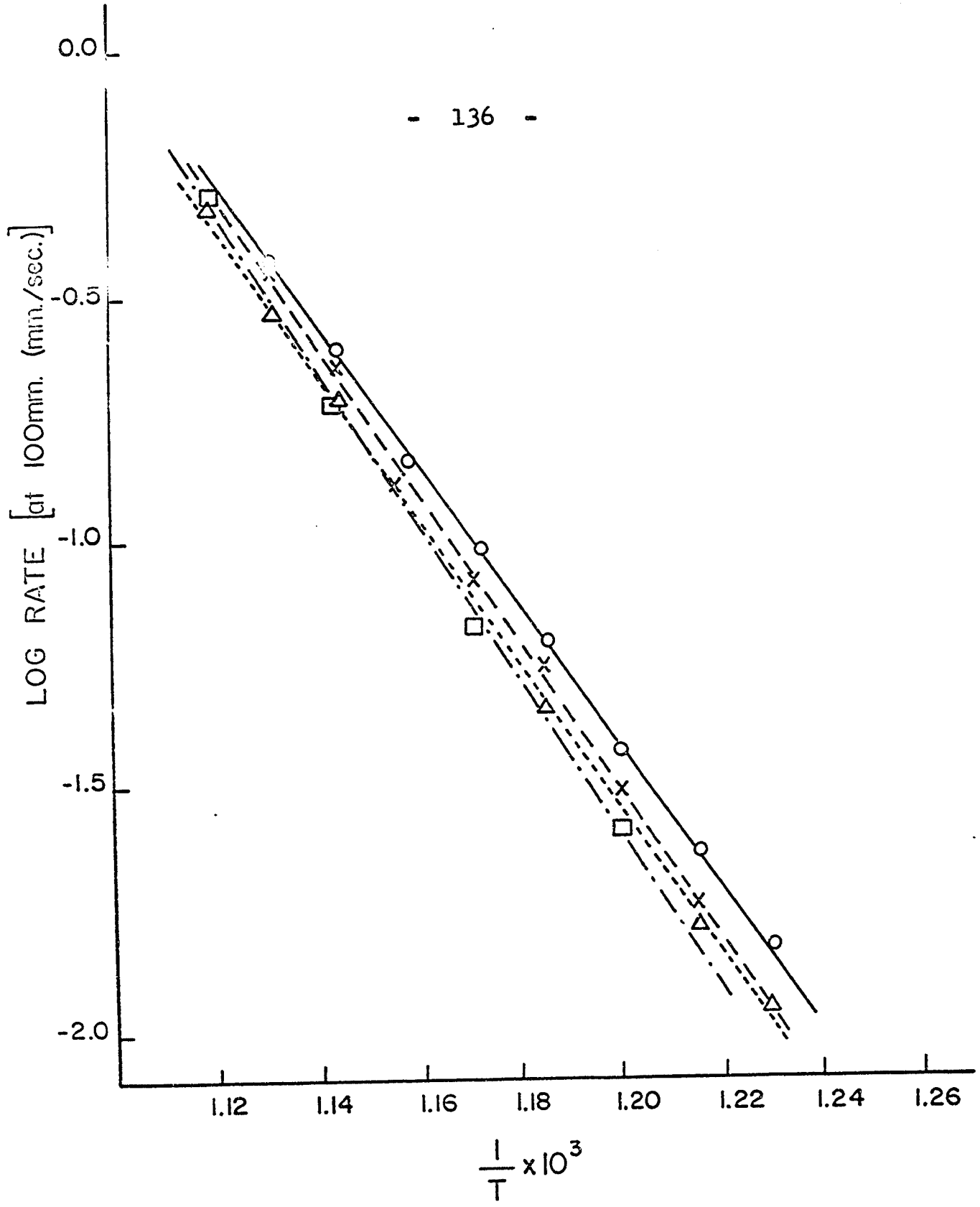

Figure 36 Arrhenius plots showing the effect of surface. Rates measured in a clean unpacked vessel are given as O, those in the clean packed vessel as X, those in the conditioned unpacked vessel as Δ, and those in the conditioned packed vessel as □ .

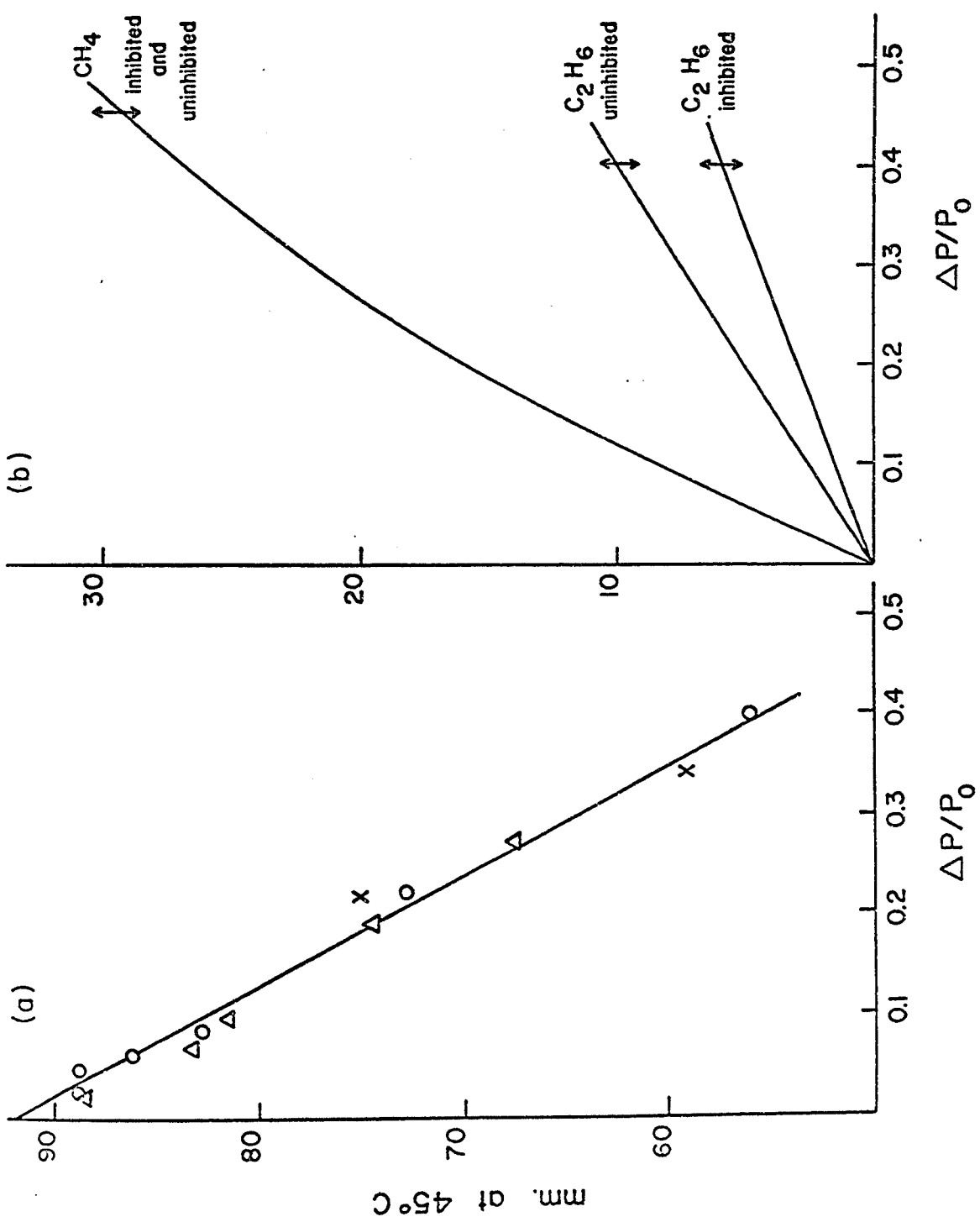

Figure 37 Analytical results showing the partial pressure of butane (left-hand side) and of methane and ethane (right-hand side) plotted against the extent of reaction for 570°C (O), 590°C (X) and 610°C (Δ).

rate whether NO is present or not, but that when NO is present, relatively less C_2H_6 is formed. Table 14 lists the C_2H_6/C_2H_4 ratios as well as other product ratios at three temperatures, all at about 200 mm. butane pressure.

Taking the result that unit increase in pressure corresponds to unit decrease in n-butane pressure, the rate constants are given as

$$k_{3/2} = 5.30 \times 10^{16} e^{-65,900/RT} \text{ ml}^{1/2} \text{ mole}^{-1/2} \text{ sec}^{-1}$$

DISCUSSION

Mechanism and Over-All Order of the Reaction

It is proposed, as suggested by Laidler and Wojciechowski (57), that initiation is the attack of NO on the n-butane

(26) $NO + C_4H_{10} \longrightarrow HNO + C_4H_9$

The usual chain propagating steps then follow. HNO will dissociate into H + NO, and other equilibria involving NO and various radicals will be set up, such as

(27) $C_2H_5 + NO \longrightarrow C_2H_5NO$

(28) $C_2H_5NO \longrightarrow C_2H_5 + NO$

To give 3/2-order over all kinetics, termination must by the

Table 14

Ratios of Decomposition Products

Initial pressure n-butene = 200 mm. 15% decomposition

Initial pressure nitric oxide = 29 mm.

T°C	$\frac{C_2H_6}{C_2H_4}$	$\frac{\text{Alkanes}}{\text{Alkenes}}$	$\frac{C_4 \text{ products}}{C_1C_2 \text{ and } C_3 \text{ products}}$	$\frac{CH_4 + C_3H_6}{C_2H_4 + C_2H_6}$
570	0.405	0.927	0.014	1.74
590	0.381	0.988	0.016	1.69
610	0.366	0.905	0.014	1.66

reaction between a β radical (H, CH_3 or C_2H_5) and a βNO molecule (HNO, CH_3NO or C_2H_5NO).

It is suggested that most of the known facts are explained by the following mechanism

(26)	$NO + C_4H_{10}$	→	$HNO + C_4H_9$
(20)	C_4H_9	→	$CH_3 + C_3H_6$
(21)	C_4H_9	→	$C_2H_4 + C_2H_5$
(19)	$C_2H_5 + C_4H_{10}$	→	$C_2H_6 + C_4H_9$
(22)	$CH_3 + C_4H_{10}$	→	$CH_4 + C_4H_9$
(2)	C_2H_5	→	$C_2H_4 + H$
(14)	$X + HNO$	→	$H + NO + X$
(23)	$H + C_4H_{10}$	→	$H_2 + C_4H_9$
(27)	$C_2H_5 + NO$	→	C_2H_5NO
(28)	C_2H_5NO	→	$C_2H_5 + NO$
(29)	$C_2H_5 + C_2H_5NO$	→	$C_4H_{10} + NO$ or $C_2H_4 + C_2H_6 + NO$
(30)	C_2H_5NO	→	$CH_3CH{=}NOH$ → Products

where X represents a third body.

The accepted values of rate constants, activation energies and frequency factors are listed in table 15.

This scheme gives the following steady-state concentration of radicals:

Table 15

Kinetic Parameters for Elementary Reactions

Reaction	A*	E(kcal/mole)	k_{570}*	Reference
2	3.0×10^{14}	39.5	1.74×10^{4}	(47)
14	1.92×10^{16}	48.0	6.90×10^{3}	calc. from (67) using S=3
19	7.7×10^{11}	10.4	1.55×10^{9}	estimated from (90)
20	6.5×10^{11}	24.0	3.92×10^{5}	(91)
21	1.6×10^{11}	22.0	3.18×10^{5}	(92)
22	2.7×10^{11}	9.0	1.26×10^{9}	(93)
23	1.0×10^{14}	7.9	8.97×10^{11}	(94)
26	1.0×10^{15}	48	13408	estimated
27	3.0×10^{11}	0	3.00×10^{11}	estimated
28	5.0×10^{14}	59	2.56×10^{-1}	estimated from (114), and (115)
29	7.0×10^{9}	0	7.00×10^{9}	estimated
31	2.8×10^{14}	0	2.80×10^{14}	calc. from (67) using S=3
32	1.0×10^{14}	42	1.3×10^{3}	estimated
33	1.0×10^{12}	0	1.00×10^{12}	(57)
34	1.0×10^{10}	0	1.00×10^{10}	estimated
35	1.3×10^{11}	0	1.30×10^{11}	(116)
36	1.0×10^{15}	62	8.55×10^{-2}	(114)

(Continued on next page)

Table 15 (Continued)

37	1.0×10^{10}	0	1.00×10^{10}	(114)

* frequency factors and rate constants in sec^{-1}, ml. $mole^{-1}$ sec^{-1} or ml^2 $mole^{-2}$ sec^{-1}.

$$[C_2H_5] = \frac{k_{26}[C_4H_{10}]}{2k_{27}} + \frac{\left\{k_{26}^2 k_{24}^2 [C_4H_{10}]^2 + 4k_{26}k_{27}k_{28}k_{29}[C_4H_{10}]\right\}^{1/2}}{2k_{27}k_{29}} \quad [51]$$

which, at the butane pressures used, 10^{-7} to 2×10^{-5} moles/ml., reduces to

$$[C_2H_5] = \left(\frac{k_{26}k_{28}}{k_{27}k_{29}}\right)^{1/2} [C_4H_{10}]^{1/2} \quad [52]$$

$$[H] = \frac{k_{26}}{k_{23}}[NO] + \frac{k_2}{k_{23}}\left(\frac{k_{26}k_{28}}{k_{27}k_{29}}\right)^{1/2} [C_4H_{10}]^{-1/2} \quad [53]$$

$$[CH_3] = \frac{2k_{20}k_{26}}{k_{21}k_{22}}[NO] + \frac{k_2k_{20}}{k_{21}k_{22}}\left(\frac{k_{26}k_{28}}{k_{27}k_{29}}\right)^{1/2} [C_4H_{10}]^{-1/2} + \frac{k_{19}k_{20}}{k_{21}k_{22}}\left(\frac{k_{26}k_{28}}{k_{27}k_{29}}\right)^{1/2} [C_4H_{10}]^{1/2} \quad [54]$$

$$[C_4H_9] = \frac{2k_{26}}{k_{21}}[C_4H_{10}][NO] + \frac{k_{19}}{k_{21}}\left(\frac{k_{26}k_{28}}{k_{27}k_{29}}\right)^{1/2} [C_4H_{10}]^{3/2} + \frac{k_2}{k_{21}}\left(\frac{k_{26}k_{28}}{k_{27}k_{29}}\right)^{1/2} [C_4H_{10}]^{1/2} \quad [55]$$

and the steady-state concentrations of short-lived molecules are

$$[HNO] = \frac{k_{26}}{k_{14}}[NO] \qquad [56]$$

$$[C_2H_5NO] = \left(\frac{k_{26}k_{27}}{k_{28}k_{29}}\right)^{1/2} [C_4H_{10}]^{1/2}[NO] \qquad [57]$$

If the over-all rate is given by

$$v = (k_{20} + k_{21})[C_4H_9] \qquad [58]$$

then:

$$v = 2k_{26}\left(1 + \frac{k_{20}}{k_{21}}\right)[C_4H_{10}][NO] + k_2\left(1 + \frac{k_{20}}{k_{21}}\right)\left(\frac{k_{26}k_{28}}{k_{27}k_{29}}\right)^{1/2}[C_4H_{10}]^{1/2}$$

$$+ k_{19}\left(1 + \frac{k_{20}}{k_{21}}\right)\left(\frac{k_{20}k_{28}}{k_{27}k_{29}}\right)^{1/2}[C_4H_{10}]^{3/2} \qquad [59]$$

If the chains are reasonably long, the first term of equation 59 will be small, and for reasons discussed in part III, the second term is considered smaller than the last term. Since k_{20} is slightly larger than k_{21},

$$v = \frac{k_{19}k_{20}}{k_{21}}\left(\frac{k_{26}k_{28}}{k_{27}k_{29}}\right)^{1/2}[C_4H_{10}]^{3/2} \qquad [60]$$

This expression gives rise to 3/2-order kinetics, as observed experimentally.

Rates of Production of Methane, Ethane and Ethylene

The over-all rate as given by equation [59] applies to the rate of disappearance of n-butane.

The rate of production of C_2H_4 is given by

$$v_{(C_2H_4)} = k_4[C_4H_9] + k_6[C_2H_5]$$

$$= 2k_{26}[C_4H_{10}][NO] + k_{19}\left(\frac{k_{26}k_{28}}{k_{27}k_{29}}\right)^{1/2}[C_4H_{10}]^{3/2}$$

$$+ 2k_2\left(\frac{k_{26}k_{28}}{k_{27}k_{29}}\right)^{1/2}[C_4H_{10}]^{1/2} \qquad [61]$$

whereas the rate of production of ethane is given by:

$$v_{(C_2H_6)} = k_{19}[C_2H_5][C_4H_{10}]$$

$$= k_{19}\left(\frac{k_{26}k_{28}}{k_{27}k_{29}}\right)^{1/2}[C_4H_{10}]^{3/2} \qquad [62]$$

Thus there will always be more ethylene than ethane produced,

largely as a result of reaction 2, but in addition, when enough NO is added so that reaction 26 becomes reasonably fast, extra ethylene will be produced at the rate of $2 k_{26} [C_4H_{10}][NO]$.

Therefore this mechanism predicts that as more and more nitric oxide is added, the rate of production of ethylene should increase relative to that of ethane, as found experimentally. At 570°C, with 500 mm. butane and 75 mm. NO, the ratio of terms of equation [61] becomes

$$\frac{\text{term } 1}{\text{term } 2} = \frac{2k_{26}[C_4H_{10}][NO]}{k_{19}\left(\frac{k_{26}k_{28}}{k_{27}k_{29}}\right)^{1/2}[C_4H_{10}]^{3/2}} = 0.311 \qquad [63]$$

Thus about 31% extra ethylene should be produced by adding the usual amount of NO. This agrees well with the experimental result that 20-25% extra ethylene is produced.

It is easily verified that a similar comparison of the rates of formation of methane and propylene shows that these two rates should be equally accelerated by large amounts of NO, as has been found experimentally.

The Initiating Reaction

The initiating reaction is that proposed by Wojciechowski and Laidler (56) for most NO inhibited reactions.

The H-NO dissociation energy has been estimated as 48.0 kcal. per mole (67) and if the C-H dissociation energy is taken as 96.0 kcal. per mole, a reasonable estimate for the activation energy of reaction 26 is 50 kcal. per mole. The frequency factor was taken to be that for the reaction between nitric oxide and ethane (57).

The ratio of rates of initiating steps in the uninhibited reaction (V_{18}) and the inhibited reaction (V_{26}) is given by

$$\frac{V_{18}}{V_{26}} = \frac{k_{18}[C_4H_{10}]}{k_{26}[NO][C_4H_{10}]} \qquad [64]$$

At 75 mm. partial pressure of NO, this is of the order of unity. Thus, to within the certainty with which various rate constants are known, reaction 26 is capable of initiating chains.

The Chain Terminating Reactions

With the initiating step used, in order to get 3/2-order kinetics over all, termination must be by some reaction such as

$$\beta NO + \beta \longrightarrow \text{Products}$$

where β represents any β radical, and in this case may be H, CH_3 or C_2H_5. If reactions 31 and 32

(31) $X + H + NO \longrightarrow HNO + X$

(32) $C_4H_9 \longrightarrow C_4H_8 + H$

are included in the mechanism, then the termination reaction reaction 33

(33) $C_2H_5 + HNO \longrightarrow C_2H_6 + NO$

is possible. If the steady-state expression for βNO concentrations are obtained, then

$$\frac{V_{29}}{V_{33}} = \frac{k_{29}}{k_{33}} \frac{[C_2H_5NO]}{[HNO]} = \frac{k_{14}k_{20}k_{23}k_{27}k_{29}}{k_{22}k_{26}k_{31}k_{32}k_{33}} = 1.4 \times 10^4 \quad [65]$$

Thus termination by reaction 29 is much faster than by the reaction used as a termination in the inhibited decomposition of ethane and propane.

It should, perhaps, be noted that a similar calculation comparing termination by

(34) $CH_3NO + C_3H_7 \longrightarrow C_4H_{10} + NO$

with

(15) $HNO + C_3H_7 \longrightarrow C_3H_8 + NO$

for the inhibited decomposition of propane shows reaction 15 to be favoured by a factor of 6. These calculations are intuitively understood if it is realized that in the decom-

(31) $X + H + NO \longrightarrow HNO + X$

(32) $C_4H_9 \longrightarrow C_4H_8 + H$

are included in the mechanism, then the termination reaction reaction 33

(33) $C_2H_5 + HNO \longrightarrow C_2H_6 + NO$

is possible. If the steady-state expression for βNO concentrations are obtained, then

$$\frac{V_{29}}{V_{33}} = \frac{k_{29}}{k_{33}} \frac{[C_2H_5NO]}{[HNO]} = \frac{k_{14}k_{20}k_{23}k_{27}k_{29}}{k_{22}k_{26}k_{31}k_{32}k_{33}} = 1.4 \times 10^4 \quad [65]$$

Thus termination by reaction 29 is much faster than by the reaction used as a termination in the inhibited decomposition of ethane and propane.

It should, perhaps, be noted that a similar calculation comparing termination by

(34) $CH_3NO + C_3H_7 \longrightarrow C_4H_{10} + NO$

with

(15) $HNO + C_3H_7 \longrightarrow C_3H_8 + NO$

for the inhibited decomposition of propane shows reaction 15 to be favoured by a factor of 6. These calculations are intuitively understood if it is realized that in the decom-

position of propane, H atoms are major chain carriers, while in the decomposition of n-butane they are not.

For completeness, the reactions

(35) $CH_3 + NO \longrightarrow CH_3NO$

(36) $CH_3NO \longrightarrow CH_3 + NO$

should be included in the reaction scheme. However with the termination step used, they cancel out of the steady-state solution to the rate equations.

It is possible that termination could be by

(37) $CH_3 + CH_3NO \longrightarrow C_2H_6 + NO$

Comparing the rate of reactions 29 and 37

$$\frac{V_{29}}{V_{37}} = \frac{V_{29}[C_2H_5][C_2H_5NO]}{k_{37}[CH_3][CH_3NO]} \qquad [66]$$

since

$$[CH_3NO] \approx \frac{k_{35}}{k_{36}}[CH_3][NO] \qquad [67]$$

$$\frac{V_{29}}{V_{37}} \approx \frac{k_{29}}{k_{37}}\left(\frac{k_{21}k_{22}}{k_{19}k_{20}}\right)^2 \frac{k_{27}k_{36}}{k_{28}k_{35}} \qquad [68]$$

At 570°C, this is of the order of unity. Thus according to the rate constants given in table 15 either reaction 29 or 37

could terminate the chains. Termination by reaction 37 would, however, mean that more propylene should be produced relative to methane when NO is added, while the ratio C_2H_6/C_2H_4 should remain constant. Since, in fact, the amount of C_2H_4 increases relative to C_2H_6, while the CH_4/C_3H_6 ratio remains constant on adding NO, termination by reaction 29 seems to be more important.

Finally, comparing the rate of termination of the inhibited reaction to that of the uninhibited,

$$\frac{V_{29}}{V_{24}} = \frac{k_{29}[C_2H_5][C_2H_5NO]}{k_{24}[C_2H_5]^2} = \frac{k_{29}k_{27}}{k_{24}k_{28}}[NO] \qquad [69]$$

which, at 75 mm. pressure of NO and 570°C is 53.1. Thus the termination by reaction 29 will be the dominant process at all pressures of NO used.

Effect of Inert Gas

Reactions 2, 14, 20, 21, 27 and 28 may involve third body effects. Of these, the rate constants for the first two do not appear in the important term of the rate expression (equations 59 and 60). Reactions 20 and 21 are probably first-order down to quite low pressures, and reactions 27 and 28 form a reversible equilibrium, so that adding a third body to both will have no effect on the over-all kinetics of the

reaction. Thus no significant increase in rate on adding an excess of inert gas would be expected, and none was found.

Kinetic Parameters

On the basis of equation 60, the proposed activation energy for the reaction is:

$$E = E_{19} + E_{20} - E_{21} + \frac{1}{2}(E_{26} + E_{28} - E_{27} - E_{29}) \qquad [70]$$

Using the values given in table 15, E becomes 65.9 kcal. per mole. This is in excellent agreement with the experimental value of 65.9 kcal. per mole.

The predicted frequency factor is

$$A = \frac{A_{19}A_{20}}{A_{20}} \left(\frac{A_{26}A_{28}}{A_{27}A_{29}}\right)^{1/2} = 1.5 \times 10^{16}\ ml^{1/2}\ mole^{-1/2} sec^{-1} \qquad [71]$$

as compared with the experimental value of 5.3×10^{16} $ml^{1/2}$ $mole^{-1/2}$ sec^{-1}.

The actual rates, calculated at 570°C, are in good agreement, the calculated being 2.2×10^{-1} $ml^{1/2}$ $mole^{-1/2}$ sec^{-1}, compared to the experimental value, 4.42×10^{-1} $ml^{1/2}$ $mole^{-1/2}$ sec^{-1}.

The Effect of Surface

It is apparent that the amount and nature of the exposed surface has much less effect on the fully inhibited

reaction than on the uninhibited. This is to be expected on the basis of the surface mechanism proposed in part III, since the effect of adding more surface is equivalent to adding more inhibitor of a slightly different nature. Some effect is noted, and this is always in the direction of lower rates. Thus surface termination is probably more efficient than surface initiation, as discussed in part III. Activation energies are slightly higher than in the clean unpacked vessel, being as high as 69.5 kcal. per mole in the packed, conditioned vessel.

The Induction Period

Figure 38 shows rates obtained by extrapolating the pressure time curves back to initial time, as described in part III. The activation energy so obtained is 66.9 kcal. per mole, suggesting that some of the discrepancy between the calculated and experimental reaction parameters may be the result of using inflexion rates as a measure of the rate of reaction.

CONCLUSIONS

The thermal decomposition of n-butane, fully inhibited by nitric oxide, has been shown to proceed by a free-radical mechanism. This mechanism has satisfactorily

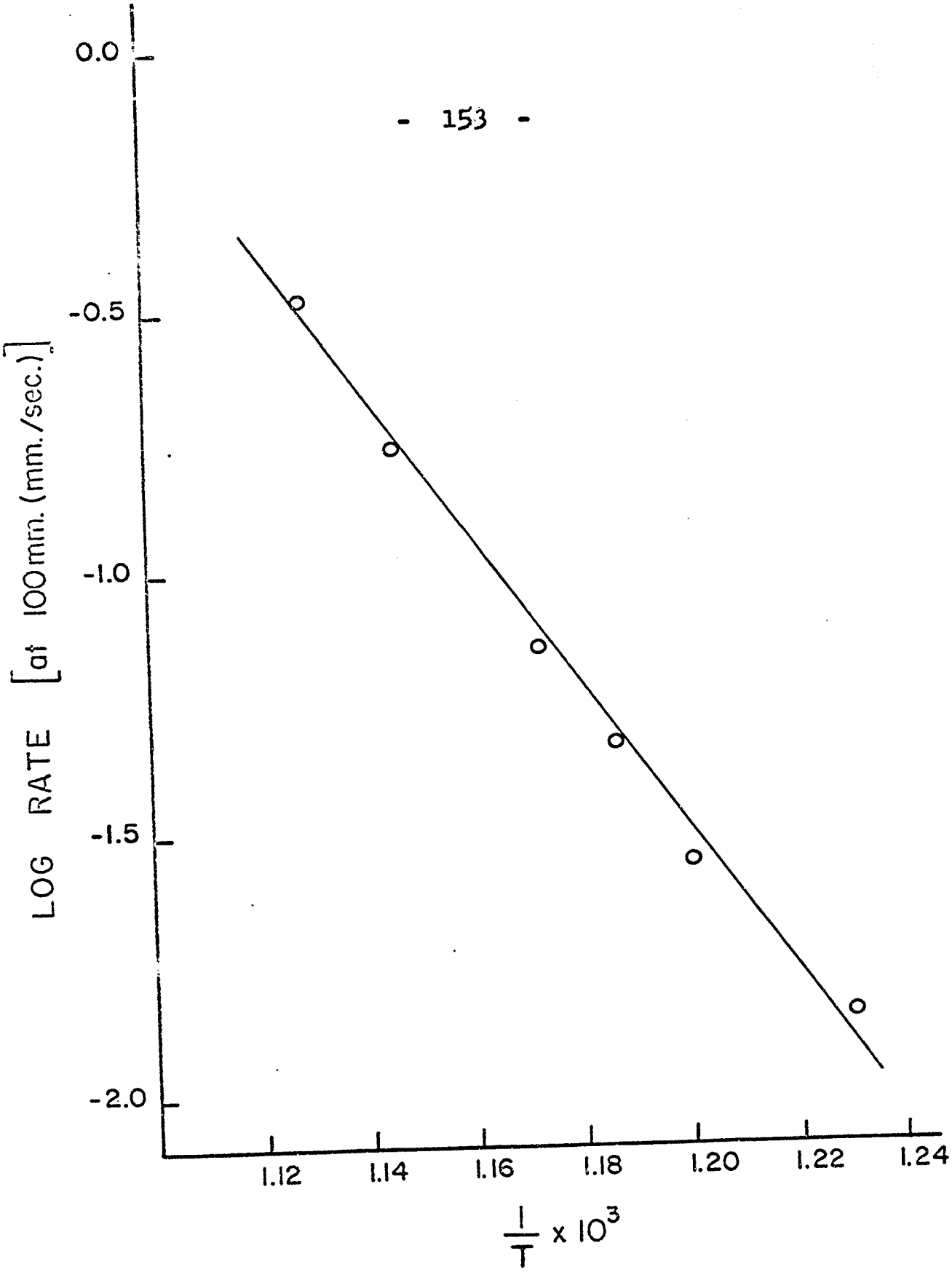

Figure 38 Rates of the inhibited pyrolysis of n-butane obtained by extrapolation of that part of the ΔP-time curve beyond the inflexion point to zero time.

predicted the kinetic parameters obtained, the effect of inert gas, the stoichiometry of the reaction and, to some extent, the effect of surface. The reaction shows 3/2-order over all kinetics in the temperature range from 540 to 610°C and at partial pressures of n-butane from 30 to 550 mm. The 3/2-order rate constants are well described by

$$k = 5.30 \times 10^{16} e^{-65,900/RT} \text{ ml}^{1/2} \text{ mole}^{-1/2} \text{ sec}^{-1}$$

CLAIMS TO ORIGINAL RESEARCH

1. The rate of pyrolysis of propane has been measured over a larger temperature range than heretofore, clearly showing for the first time the transition from first to 3/2-order kinetics.

2. A free-radical mechanism for the uninhibited pyrolysis of propane has been proposed, involving initiation by the second-order split of a propane molecule into a methyl and an ethyl radical. Termination in the first-order region is by the recombination of a methyl and a propyl radical, and in the 3/2-order region by the recombination of methyl radicals, both reactions being in their third-body dependent regions.

3. The pyrolysis of propane, maximally inhibited with nitric oxide, has been studied over a wide temperature range. The pressure-time curve was noted to have a marked induction period. The initial rates gave 3/2-order kinetics at most temperatures, while the inflexion point rates were close to unity at the higher temperatures.

4. A free-radical mechanism involving initiation by the abstraction of a hydrogen atom from propane by NO and termination by the reaction of a propyl radical with HNO was proposed. This mechanism is similar to that

proposed by Laidler and Wojciechowski (57) for the inhibited decomposition of ethane.

5. The kinetics of the uninhibited pyrolysis of n-butane have been re-investigated and found to be of the 3/2 order.

6. The mechanism proposed by Echols and Pease (74) for the thermal decomposition of n-butane has been verified.

7. The pyrolysis of n-butane, maximally inhibited with nitric oxide, has been studied over a wide range of temperature and pressure. The reaction was 3/2-order over the entire range.

8. A mechanism for the pyrolysis of n-butane, maximally inhibited with nitric oxide, has been proposed. The suggested initiation is the abstraction of a hydrogen atom from a butane molecule by NO, and the termination is the reaction between an ethyl radical and nitroso-ethane.

9. The effects of surface have been shown to be explicable on the assumption that reactive surface sites behave much like the nitric oxide molecule.

10. Sulfur hexafluoride has been shown to be not truly inert in pyrolytic reactions.

11. If a reaction shows two types of kinetics over a range of pressure and temperature, the relation between the 'break point activation energy' for the transition from one type of kinetics to another and the activation energies and orders of the two kinetic formulations has been pointed out for the first time.

REFERENCES

1. R.N. Pease, J. Am. Chem. Soc., 50, 1779 (1928).
2. F.E. Frey and D.F. Smith, Ind. Eng. Chem., 20, 948 (1928).
3. R.N. Pease and E.S. Durgan, J. Am. Chem. Soc., 52, 1262 (1930).
4. G.O. Ebrey and C.G. Engelder, Ind. Eng. Chem., 23, 1033 (1931).
5. V. Schneider and P.K. Frolick, Ind. Eng. Chem., 23, 1405 (1931).
6. L.F. Marek and W.B. McCluer, Ind. Eng. Chem., 25, 878 (1933).
7. R.E. Paul and L.F. Marek, Ind. Eng. Chem., 26, 454 (1934).
8. F.E. Frey and H.J. Hepp, Ind. Eng. Chem., 25, 441 (1933).
9. A.I. Dintses and A.V. Frost, J. Gen. Chem. U.S.S.R., 3, 747 (1933).
10. A.I. Dintses and A.V. Frost, Compt. Rend. Acad. Sci., U.R.S.S. 4, 153 (1933).
11. A.I. Dintses and A.V. Frost, Compt. Rend. Acad. Sci., U.R.S.S. 5, 513 (1934).
12. E.W.R. Steacie and I.F. Puddington, Can. J. Research, B16, 411 (1938).
13. F.O. Rice, W.R. Johnston and B.L. Evering, J. Am. Chem. Soc., 54, 3529 (1932).
14. F.O. Rice and W.R. Johnston, J. Am. Chem. Soc., 56, 214 (1934).

15. F.O. Rice, J. Am. Chem. Soc. 55, 3035 (1933).

16. F.O. Rice, Trans. Faraday Soc., 30, 152 (1934).

17. F.O. Rice and K.F. Herzfeld, J. Am. Chem. Soc., 56, 284 (1934).

18. L. Belchetz and E.K. Rideal, J. Am. Chem. Soc., 57, 2466 (1935).

19. F.P. Lossing, K.U. Ingold and I.H.S. Henderson in E.W.R. Steacie (48).

20. F. Patat, Z. physik. Chem., B32, 294 (1936).

21. L.S. Echols and R.N. Pease, J. Am. Chem. Soc., 58, 1317 (1936).

22. D.V. Sickman and O.K. Rice, J. Chem. Phys., 4, 608 (1936).

23. A.D. Stepukhovich and V.V. Tatarintsev, Doklady Akad. Nauk. S.S.S.R., 99, 1049 (1954).

24. A.D. Stepukhovich, L.S. Stal'makhova and V.V. Eremin, Zhur. Fiz. Khim., 28, 1878 (1954).

25. A.D. Stepukhovich and L.V. Derevenskikh, Zhur. Fiz. Khim., 28, 1720 (1954).

26. A.D. Stepukhovich and L.V. Derevenskikh, Zhur, Fiz. Khim., 29, 2129 (1955).

27. V.V. Voevodsky, Trans. Faraday Soc., 55, 65 (1959).

28. R. Martin, M. Niclause and M. Dzierzynski, Compt. rend., 254, 1786 (1962).

29. A.D. Stepukhovich, R.V. Kosyreva and V.I. Petrosyan, Rus. J. Phys. Chem., 35, 293 (1961).

30. M.B. Neiman, N.I. Medvedeva and E.S. Torsueva, Proc. Acad. Sci. U.S.S.R., Sect. Phys. Chem., 115, 477 (1957).

31. M.B. Neiman, Inter. J. Applied Radiation and Isotopes, 3, 20 (1958).

32. M.B. Neiman, N.I. Medvedeva and E.S. Torsueva, Zhur. Fiz. Khim., 36, 1016 (1962).

33. H.M. Frey, C.J. Danby and C.N. Hinshelwood, Proc. Roy. Soc. A234, 301 (1956).

34. K.J. Laidler and B.W. Wojciechowski, Proc. Roy. Soc. A259, 257 (1960).

35. J.E. Hobbs and C.N. Hinshelwood, Proc. Roy. Soc., A167, 447 (1938).

36. K.U. Ingold, F.J. Stubbs and C.N. Hinshelwood, Proc. Roy. Soc., A203, 486 (1950).

37. E.W.R. Steacie, Chem. Rev., 22, 311 (1938).

38. W.M. Jackson and J.R. McNesby, J. Am. Chem. Soc., 83, 4891 (1961).

39. P. Goldfinger, M. Letort and M. Niclause, Volume Commémoratif Victor Henri: Contribution à l'Etude de la Structure Moléculaire, Liège, Desoer, 1948, p. 283.

40. L. Küchler and H. Theile, Z. physik. Chem., B42, 359 (1939).

41. K.J. Laidler and B.W. Wojciechowski, Proc. Roy. Soc. A260, 91 (1961).

42. E.K. Gill and K.J. Laidler, Proc. Roy. Soc., A250, 121 (1959).

43. B.W. Wojciechowski and K.J. Laidler, Chem. Soc. Spec., Publ. no. 17, in press.

44. O.K. Rice and H.C. Ramsperger, J. Am. Chem. Soc., 49, 1617 (1927).

45. L.S. Kassel, J. Phys. Chem., 32, 1065 (1928).

46. A.F. Trotman-Dickenson, Gas Kinetics, Butterworth Scientific Publications, London. 1955 p. 125.

47. S. Bywater and E.W.R. Steacie, J. Chem. Phys., 19, 319 (1951); ibid., idem. 172, 326.

48. E.W.R. Steacie, Atomic and Free-Radical Reactions, Reinhold, New York 1954.

49. W.R. Trost and E.W.R. Steacie, J. Chem. Phys., 16, 361 (1948).

50. J.A. Kerr and J.G. Calvert, J. Am. Chem. Soc., 83, 3391 (1961).

51. J.A. Kerr and A.F. Trotman-Dickenson, Chemistry and Industry, 125 (1959).

52. J.A. Kerr and A.F. Trotman-Dickenson, Trans. Faraday Soc., 55, 572 (1959).

53. J.G. Calvert and W.C. Sleppy, J. Am. Chem. Soc., 81, 1544 (1959).

54. N.N. Semenov. Some Problems in Chemical Kinetics and Reactivity, Vol. I, Pergamon Press, London. 1959.

55. R.E. Dodd and E.W.R. Steacie, Proc. Roy. Soc., A223, 238 (1951).

56. B.W. Wojciechowski and K.J. Laidler, Can. J. Chem., 38, 1027 (1960).

57. K.J. Laidler and B.W. Wojciechowski, Proc. Roy. Soc., A260, 103 (1961).

58. L.A.K. Staveley, Proc. Roy. Soc. A162, 557 (1937).

59. F.O. Rice and O.L. Polly, J. Chem. Phys., 6, 273 (1938).

60. V.E. Goldansky, Uspekhi Khim., 15, 63 (1946).

61. P.J. Stubbs and C.N. Hinshelwood, Proc. Roy. Soc., A200, 458 (1950).

62. P.J. Stubbs and C.N. Hinshelwood, Proc. Roy. Soc., A201, 18 (1950).

63. P.J. Stubbs, K.U. Ingold, B.C. Spall, C.J. Danby and C.N. Hinshelwood, Proc. Roy. Soc., A214, 20 (1952).

64. J. Jach and C.N. Hinshelwood, Proc. Roy. Soc., A231, 145 (1955).

65. D.P. Stevenson, C.D. Wagner, O. Beeck and J.W. Otvos, J. Chem. Phys., 20, 192 (1952).

66. V.A. Poltorak and V.V. Voevodsky, Doklady Akad. Nauk. S.S.S.R. 91, 589 (1953).

67. M.A.A. Clyne and B.A. Thrush, Trans. Faraday Soc., 57, 1305 (1961).

68. M.J.Y. Clement and D.A. Ramsay, Can. J. Phys. 39, 205 (1961).

69. C.D. Hurd and L.U. Spence, J. Am. Chem. Soc. 51, 3353 (1929).

70. A. Cambron, Can. J. Research, 7, 646 (1932).

71. L.F. Marek and M. Neuhaus, Ind. Eng. Chem., 24, 400 (1932).

72. L.F. Marek and M. Neuhaus, Ind. Eng. Chem., 25, 516 (1933).

73. E.W.R. Steacie and I.E. Puddington, Can. J. Research, B16 176 (1938).

74. L.S. Echols and R.N. Pease, J. Am. Chem. Soc., 61, 208 (1939).

75. F.O. Rice and K.K. Rice, The Aliphatic Free Radicals, John Hopkins Press, Baltimore, 1935.

76. S.W. Benson, The Foundations of Chemical Kinetics, McGraw-Hill, New York, 1960. pp. 343-363.

77. A.J.B. Robertson, Proc. Roy. Soc., A199, 394 (1949).

78. C.D. Hurd and J.L. Azorlosa, J. Am. Chem. Soc., 73, 33 (1951).

79. W.W. Heckert and E. Mack, J. Am. Chem. Soc., 51, 2706 (1929).

80. F.E. Frey, Ind. Eng. Chem., 26, 198 (1934).

81. Z.K. Maizus, V.G. Markovich and M.B. Neiman, Zhur. Fiz. Khim., 23, 1189 (1949).

82. W.A. Bryce and D.J. Ruzicka, Can. J. Chem., 38, 835 (1960).

83. V.A. Crawford and E.W.R. Steacie, Can. J. Chem., 31, 937 (1953).

84. J. Engel, A. Combe, M. Letort and M. Niclause, Compt. rend., 244, 453 (1957).

85. J. Engel, A. Combe, M. Letort and M. Niclause, Rev. Inst. franç. Pétrole, 12, 627 (1957).

86. J.H. Purnell and C.P. Quinn, J. Chem. Soc., 4128 (1961).

87. A.D. Stepukhovich, R.V. Kosyreva and V.I. Petrosyan, Rus. J. Phys. Chem., 35, 653 (1961).

88. A. Kuppermann and J.G. Larson, Long abstracts of papers presented at American Chemical Society meeting, Washington, D.C. 21-24 March, 1962.

89. E.W.R. Steacie and H.O. Folkins, Can. J. Research, B18, 1 (1940).

90. P.J. Boddy and E.W.R. Steacie, Can. J. Chem., 38, 1576 (1960).

91. J.T. Gruver and J.G. Calvert, J. Am. Chem. Soc., 78, 5208 (1956).

92. J.A. Kerr and A.F. Trotman-Dickenson, J. Chem. Soc., 1602 (1960).

93. M.H. Jones and E.W.R. Steacie, Can. J. Chem., 31, 505 (1953).

94. H.I. Schiff and E.W.R. Steacie, Can. J. Chem., 29, 1 (1951).

95. K.J. Ivin and E.W.R. Steacie, Proc. Roy. Soc., A208, 25 (1951).

96. J.G. Calvert, Chem. Rev., 59, 568 (1959).

97. E.L. Metcalfe and A.F. Trotman-Dickenson, J. Chem. Soc., 5072 (1960).

98. J.R. Mellesby, J. Phys. Chem., 64, 1671 (1960).

99. A.S. Gordon and J.R. McNesby, J. Chem. Phys., 33, 1882 (1960).

100. J. Jach and C.N. Hinshelwood, Proc. Roy. Soc., A229, 143 (1955).

101. R.K. Brinton and E.W.R. Steacie, Can. J. Chem., 33, 1840 (1955).

102. T.L. Cottrell, The Strengths of Chemical Bonds, Butterworth Scientific Publications, London. 1958. pp. 270-275.

103. M.I. Temkin, Zhur. Fiz. Khim., 15, 296 (1941).

104. P.E.M. Allen, H.W. Melville and J.C. Robb, Proc. Roy. Soc., A218, 311 (1953).

105. L.S. Echols and R.N. Pease, J. Am. Chem. Soc., 59, 766 (1937).

106. L.S. Echols and R.N. Pease, J. Am. Chem. Soc., 60, 1701 (1938).

107. L.S. Echols and R.N. Pease, J. Am. Chem. Soc., 61, 1024 (1939).

108. P. Goldfinger, Discussions Faraday Soc., 2, 149 (1947).

109. E.W.R. Steacie and H.O. Folkins, Can. J. Research, B17, 105 (1939).

110. R.G. Partington and C.J. Danby, J. Chem. Soc., 2226 (1948).

111. K.U. Ingold, F.J. Stubbs and C.N. Hinshelwood, Proc. Roy. Soc., A208, 285 (1951).

112. J.H. Purnell and C.P. Quinn, Nature, 189, 656 (1961).

113. A. Kuppermann and J.G. Larson, J. Chem. Phys., 33, 1264 (1960).

114. D.J. McKenney, B.W. Wojciechowski and K.J. Laidler, Can. J. Chem., submitted for publication.

115. B.G. Gowenlock, J. Trotman and L. Batt, Chem. Soc. Spec. Publ., No. 10, 75 (1957).

116. W.A. Bryce and K.U. Ingold, J. Chem. Phys., 23, 1968 (1955).